Dissertation

Construction of Interpolating and Orthonormal Multigenerators and Multiwavelets on the Interval

Mojdeh Hematidaryoni

2022

Construction of Interpolating and Orthonormal Multigenerators and Multiwavelets on the Interval

Dissertation

zur
Erlangung des akademischen Grades
Doktor der Naturwissenschaften
(Dr. rer. nat.)

vorgelegt
dem Fachbereich Mathematik und Informatik
der
Philipps–Universität Marburg

von

Mojdeh Hematidaryoni

Aus Schiras (Iran)

Marburg April 2022

Vom Fachbereich Mathematik und Informatik
der Philipps-Universität Marburg (Hochschulkennziffer: 1180)
als Dissertation angenommen am: 27. April 2022

Erstgutachter: **Prof. Dr. Stephan Dahlke**, Philipps-Universität Marburg

Zweitgutachter: **Prof. Dr. Christian Rieger**, Philipps-Universität Marburg

Tag der mündlichen Prüfung: 29. Juli 2022

Mathematics knows no races or geographic boundaries; for mathematics, the cultural world is one country.

David Hilbert(1862-1943)

Dedicated to my family.

Acknowledgement

Foremost, I would like to express my sincere gratitude to my advisor, Prof. Dr. Stephan Dahlke for the continuous support of my PhD study, for his patience, motivation, enthusiasm, and immense knowledge. His guidance helped me in all the time of research and writing of this thesis. I am grateful to him for giving me the chance to attend various conferences as well as summer school in Genoa, which I enjoyed very much.

Besides my advisor, I would like to thank my colleagues from the Workgroup Numerics at Philipps-Universität Marburg for helping me whenever needed, particularly, during the last year. My special thanks go to Sven and Dorian for their help in programming and Anne for her comments and reading very carefully my thesis.

At this point, I am also thankful to Marita for her encouragement during my stay in Marburg. Financial support by Philipps-Universität Marburg and DAAD during the COVID-19 pandemic is gratefully acknowledged.

Finally, I would like to thank my family, in particular, my parents for encouraging and supporting me throughout my life. Last but not the least, I want to thank Behrouz, for his love, his patience and very precious moments after mathematics.

Contents

List of Figures

Chapter 1

Introduction

In recent years, wavelets have become a very powerful tool in applied mathematics. In general, a wavelet basis is a system of functions that is generated by scaling, translating and dilating a finite set of functions, the so-called mother wavelets. A mother wavelet is a function $\psi \in L_2(\mathbb{R})$ such that for some parameters $a > 1$ and $b > 0$, the collection

$$\{a^{\frac{j}{2}}\psi(a^j x - bk)|j,k \in \mathbb{Z}\}$$

is an orthonormal basis of $L_2(\mathbb{R})$. Wavelets have been very successfully applied in image/signal analysis, e.g., for denoising and compression purposes. In contrast to traditional Fourier- or Gabor transforms, wavelet methods are useful for analyzing local and non-stationary structures on different scales. This is accomplished by multi-scale decompositions, e.g., a signal or image is mapped to a phase space parametrized by a time/space- and a scale/size/resolution parameter. We refer to the monograph [51] for details. Another important field of applications is the analysis and the numerical treatment of operator equations [19]. In particular, it has been possible to design adaptive numerical algorithms based on wavelets for a huge class of operator equations including operators of negative order [15, 16]. The success of wavelet algorithms is an ultimative consequence of the following facts:

- Weighted sequence norms of wavelet expansion coefficients are equivalent in a certain range (depending on the regularity of the wavelets) to smoothness norms such as Besov or Sobolev norms.
- For a wide class of operators their representation in wavelet coordinates is nearly diagonal.
- The vanishing moments of wavelets remove the smooth part of a function and give rise to very efficient compression strategies.

These facts can, e.g., be used to construct adaptive numerical strategies that are guaranteed to converge with optimal order, in the sense that these algorithms realize the convergence order of best N-term approximation schemes. The most far-reaching results have been obtained for linear, symmetric elliptic operator equations. Generalization to nonlinear elliptic equations also exist [17]. However, then one is faced with a serious bottleneck: every numerical algorithm for these equations requires the evaluation of a nonlinear functional applied to a wavelet series. Although some very sophisticated algorithms exist [22],

they turn out to perform quite slowly in practice. In recent studies, it has been shown that this problem can be ameliorated by means of so-called interpolants [61]. However, then the problem occurs that most of the known bases of interpolants do not form stable bases in $L_2[a, b]$.

In this work, we provide a significant contribution to this problem and construct new families of interpolants on bounded domains that are not only interpolating, but also stable in $L_2[a, b]$. Since this is hard to achieve (or maybe even impossible) with just one generator, we will work with *multigenerators* and *multiwavelets*, that is, vectors $(\psi_0, \ldots, \psi_{r-1})^\top,\ r > 0$ of $L_2(\mathbb{R})$, for which the collection

$$\{\psi_{i,j,k}(x) := 2^{\frac{j}{2}}\psi_i(2^j x - k) | j, k \in \mathbb{Z},\ 0 \leq i < r\}$$

constitutes a (Riesz) basis of $L_2(\mathbb{R})$. One can obtain multiwavelets from multigenerators or scaling vectors $(\phi_0, \ldots, \phi_{r-1})^\top,\ r > 0$ of $L_2(\mathbb{R})$, which are the solutions of a matrix refinement equation. Details are given in Section 3.2.1.

The use of a multigenerator appears to be more attractive since their component functions have relatively small support and in many cases have more favorable properties. Indeed, in the papers [42, 43, 45] it has been shown that, in the setting of multiwavelets, it is possible to construct orthogonal and biorthogonal bases that are in addition interpolating, at least on the real line. It is the aim of this project to adapt the constructions in [42] to an interval. In the first step, we want to restrict ourselves to the interpolation property. Strictly inside the interval, we will use the interpolating wavelets from [42]. However, to preserve the approximation properties of the underlying multiresolution analysis, some modifications at the boundary are necessary in the sense that the polynomial exactness is maintained. These modifications have to be performed in such a way that the interpolation property is not destroyed. To some extend, we will follow the approach in [4, 5]. The analysis in these papers has only been carried out for a single generator, so it has to be generalized to several generators.

After this is done, the next step is the construction of boundary vectors to preserve the orthogonality. For the case of one generator, several approaches for the construction of biorthogonal and orthonormal bases on intervals already exist [18, 21, 58]. But the scalar orthogonal wavelets can not passes the nice features such as compact support, approximation order and smoothness at the same time. Furthermore, the published works so far study a particular case of orthogonal wavelets on the interval. To overcome these restrictions, We construct orthogonal multigenerators and multiwavelets which preserve all the nice properties. Motivated by the results in [2, 3, 41], we propose an approach to adapt the Discrete Multiwavelets Transform (DMWT) on the interval. The DMWT is applied for denoising and compression of infinitely signals and images. In many applications, we deal with finite signal and need to modify the DMWT near the boundaries. Again we utilize the construction of Karsten Koch in [42] and try to find the appropriate boundary functions at the edges.

This thesis is proceeded as follows. In Chapter 2 we introduce the necessary notations and definitions for our work. We start with the function spaces and specially in Subsection 2.1.1 we give an introduction to the Sobolev spaces. Then we present some definitions which are needed throughout this thesis. The next chapter is devoted to the wavelets and multiwavelets setting. In section 3.1 we briefly recall some basic concepts of wavelets. Moreover, we introduce the scaling vectors and their properties in Section

3.2. Then we define the Discrete Multiwavelets Transform and multiwavlets. Particularly, we focus on the construction of Karsten Koch in [42]. In Chapter 4 we adapt this construction to a bounded domain. In Section 4.1 we propose a method for constructing the interpolating scaling vectors on the interval $[0, 1]$. In the next section we will verify, if they are as well refinable. This is particularly important to construction a new multiresolution analysis on the interval. Section 4.3 is devoted to the approximation order of boundary scaling vectors. First we investigate the ability of boundary scaling vectors to reproduce the polynomials. Then we look over, if the interpolation operator verifies the error estimate in $L_2(\mathbb{R})$ and $L_2[0, 1]$. This is the main and difficult part of this chapter. In the next section we visualize our construction with some examples. Finally, in Section 4.5 we construct the multiwavelets corresponding to interpolating boundary scaling vectors and give some examples. In Chapter 5 we develop an approach for the construction of orthogonal boundary scaling vectors which have short support and the same regularity as those on the line. First of all we investigate the necessary and sufficient conditions for our construction. Then in Section 5.2 we modify the DMWT to find appropriate functions near the boundaries. Moreover, we compute the necessary numbers of boundary scaling functions at each edge. The next section is concerned with the the necessary and sufficient conditions for the approximation order of orthogonal boundary vectors. In Section 5.4.1 we introduce the general algorithm of our construction and then present some examples. The last section is devoted to the construction of orthogonal multiwavelets corresponding to orthogonal boundary vectors and as well visualization of them. Finally, in Chapter 6 we summarize our result and discuss the future researchs. Furthermore, a list of notations can be found starting on page 97.

Chapter 2

Preliminaries

In this chapter we present some concepts and notations that are required throughout this dissertation. In the first section we give an introduction to the function spaces. We start with the general notations and then define some important spaces and their corresponding norms. In Section 2.1.1 we focus on the Sobolev spaces and some of their properties and results, which are crucial for our purpose. Finally in Section 2.2 we introduce the important definations needed by our work. The results in this chapter stem from [1,7,30,37,41,53,60].

2.1 Function Spaces

In this section we introduce some function spaces and their basic properties. First of all, we fix some notations used in this thesis. By $\mathbb{N}$, $\mathbb{Z}$, $\mathbb{R}$ and $\mathbb{C}$, we denote the set of all natural, integer, real and complex numbers, respectively. Furthermore, suppose that $\mathbb{N}_0 = \mathbb{N} \cup \{0\}$ and $\mathbb{R}^n$ be Euclidean n-space, where $n \in \mathbb{N}$. The vector $\alpha = (\alpha_1, \ldots, \alpha_n) \in \mathbb{N}_0^n$ with absolute value $|\alpha| = \sum_{j=1}^n \alpha_j$ is called *multiindex*. For $x = (x_1, \ldots, x_n) \in \mathbb{R}^n$ we put

$$x^\alpha = x_1^\alpha \ldots x_n^\alpha.$$

Then we define partial derivatives as

$$D^\alpha f := \frac{\partial^{|\alpha|}}{\partial x_1^{\alpha_1} \cdots \partial x_n^{\alpha_n}} f,$$

where f is a sufficient smooth real valued function.

Definition 2.1. ($C^m(\Omega)$ spaces). Let $\Omega \subseteq \mathbb{R}^n$ be a *domain*, i.e. an open, bounded and connected subset in $\mathbb{R}^n$. By $C^m(\Omega)$, $m \in \mathbb{N}_0$, we denote the space of functions which are bounded and m times continuously differentiable in Ω. Moreover, for $f \in C^m(\Omega)$ the associated norm

$$\|f\|_{C^m(\Omega)} := \sum_{|\alpha| \leq m} \sup_{x \in \Omega} |D^\alpha f(x)|,$$

is finite.

We denote the *support* of a function f, defined for $x \in \Omega$, with

$$\text{supp} f := \overline{\{x \in \Omega : f(x) \neq 0\}}.$$

Then we determine the space of *test functions* with

$$C_0^\infty(\Omega) := \{f \in C^\infty(\Omega) : \mathrm{supp} f \subset \Omega\},$$

where $C^\infty(\Omega)$ is the space of functions which are bounded and infinitely continuously differentiable. We define also the space of Hölder continuous functions denoted by $C^{m,k}(\Omega)$, $m \in \mathbb{N}_0$ and $0 < k < 1$ with the norm

$$\|f\|_{C^{m,k}(\Omega)} := \|f\|_{C^m(\Omega)} + \sum_{|\alpha|=m} \sup_{x,y\in\Omega, x\neq y} \frac{|D^\alpha f(x) - D^\alpha f(y)|}{|x-y|^k}.$$

Definition 2.2. **($L_p(\Omega)$ spaces)**. By $L_p(\Omega)$ we denote the space of all equivalence classes of measurable functions on Ω whose powers of order p are integrable. The corresponding norm is

$$\|f\|_{L_p(\Omega)} := \begin{cases} \left(\int_\Omega |f|^p \mathrm{d}x\right)^{1/p}, & 1 \le p < \infty, \\ \operatorname{ess\,sup}_{x\in\Omega} |f(x)|, & p = \infty. \end{cases}$$

The spaces $L_p(\Omega)$ are Banach space with respect to the norm $\|\cdot\|_{L_p(\Omega)}$ and the spaces $L_2(\Omega)$ are Hilbert space. Moreover, for $f, g \in L_2(\Omega)$ we can define the *inner product*

$$\langle f, g\rangle := \int_\Omega f(x)g(x)\mathrm{d}x,$$

and *Cauchy–Schwarz inequality* with

$$\int_\Omega |f(x)g(x)|\mathrm{d}x \le \|f\|_{L_2(\Omega)} \|g\|_{L_2(\Omega)}.$$

Moreover, the inner product for the vectors $f = (f_1, \ldots, f_n)$ and $g = (g_1, \ldots, g_n)$ is defined by

$$\langle f, g\rangle := \begin{pmatrix} \langle f_1, g_1\rangle & \ldots & \langle f_1, g_n\rangle \\ \vdots & \ddots & \vdots \\ \langle f_n, g_1\rangle & \ldots & \langle f_n, g_n\rangle \end{pmatrix}.$$

Definition 2.3. **($\ell_p(\mathbb{Z})$ spaces)**. For $1 \le p < \infty$, we can define

$$\ell_p := \{(c_n) : c_n \in \mathbb{R}, \ \sum_{n=1}^{\infty} |c_n|^p < \infty\},$$

and corresponding ℓ_p-norm for $\{c_k\}_{k\in\mathbb{Z}}$ as

$$\|c\|_{\ell_p} := \left(\sum_{k\in\mathbb{Z}} |c_k|^p\right)^{1/p}.$$

2.1.1 Sobolev Spaces and their Properties

In this subsection we recall some definitions and results from sobolev spaces which are required for the approximation order of boundary scaling vectors. To discuss about Sobolev spaces we may start with some basic notations and definitions that are necessary for introducing these spaces.

Definition 2.4. Suppose that $x \in \mathbb{R}^n$, A_1 an open ball with center in x and A_2 an open ball not containing x. The set

$$C_x = A_1 \cap \{x + \lambda(y - x) : y \in A_2, \lambda > 0\},$$

is called *finite cone* in $\mathbb{R}^n$ having vertex at x.

Definition 2.5. Domain $\Omega \subseteq \mathbb{R}^n$ has the *cone property* if there exists a finite cone C such that each point $x \in \Omega$ is the vertex of a finite cone C_x contained in Ω and congruent to C. That means, C_x is obtained from C by a rigid motion.

Definition 2.6. The boundary $\partial\Omega$ of an open set $\Omega \subseteq \mathbb{R}^n$ is locally Lipschitz, if each point $x \in \partial\Omega$ has a neighborhood A_x such that $\Omega \cap A_x$ is the graph of a Lipschitz continuous function. In this case Ω is called a *Lipschitz domain*.

We define the space of locally integrable functions $L_1^{loc}(\Omega)$ by

$$L_1^{loc}(\Omega) := \{f : f \in L_1(K) \text{ for all closed bounded } K \subset \Omega\}.$$

Definition 2.7. Let $\Omega \subseteq \mathbb{R}^n$ be a domain and α a multiindex. A function $f \in L_1^{loc}(\Omega)$ has an *α-th weak derivative*, if there exists a function $g \in L_1^{loc}(\Omega)$ satisfying

$$\langle g, \varphi\rangle = (-1)^{|\alpha|}\langle f, D^\alpha\varphi\rangle, \quad \text{for all } \varphi \in C_0^\infty(\Omega).$$

Moreover we denote the α-th weak derivative by $D^\alpha f := g$.

In the following, we introduce the space of functions with weak derivatives, Sobolev Spaces.

Definition 2.8. (Sobolev spaces). For $m \in \mathbb{N}_0$ and $1 \le p \le \infty$, we define the Sobolev spaces as

$$W_p^m(\Omega) := \{f \in L_p(\Omega) : D^\alpha f \in L_p(\Omega), 0 \le |\alpha| \le m\},$$

and the corresponding norm with

$$\|f\|_{W_p^m(\Omega)} := \begin{cases} \left(\sum\limits_{|\alpha|\le m} \|D^\alpha f\|^p_{L_p(\Omega)}\right)^{1/p}, & 1 \le p < \infty, \\ \max\limits_{|\alpha|\le m} ||D^\alpha f||_{L_p(\Omega)}, & p = \infty. \end{cases}$$

Clearly $W_p^0(\Omega) = L_p(\Omega)$ and for $1 \le p < \infty$, $W_p^m(\Omega) \subset L_p(\Omega)$.
Consequently, Sobolev spaces can be defined for any arbitrary $s \in \mathbb{R}$. Suppose that $m \in \mathbb{N}_0$ and $0 < s \in \mathbb{R}$ with $s = m + k$, $0 < k < 1$, then we can introduce the Sobolev norms $\|\cdot\|_{W_p^s(\Omega)}$ as

$$\|f\|_{W_p^s(\Omega)} := \left\{\|f\|^p_{W_p^m(\Omega)} + |f|^p_{k,p,\Omega}\right\}^{1/p},$$

where

$$|f|^p_{k,p,\Omega} := \sum_{|\alpha|=m} \int_\Omega \int_\Omega \frac{|D^\alpha f(x) - D^\alpha f(y)|^p}{|x-y|^{n+pk}} \, \mathrm{d}x \, \mathrm{d}y.$$

Furthermore, for $p = 2$, Sobolev spaces form a Hilbert space and and have the special notation $H^s(\Omega) := W^s_2(\Omega)$. In this case, for $s = m \in \mathbb{N}_0$ we can define the inner product as

$$\langle f, g \rangle_{H^m(\Omega)} := \sum_{|\alpha|\leq m} \int_\Omega D^\alpha f(x) D^\alpha g(x) \mathrm{d}x,$$

and for $s = m + k$, $0 < k < 1$, we have

$$\begin{aligned}\langle f, g \rangle_{H^s(\Omega)} :=& \langle f, g \rangle_{H^m(\Omega)} \\ &+ \sum_{|\alpha|=m} \int_\Omega \int_\Omega \frac{|D^\alpha f(x) - D^\alpha f(y)||D^\alpha g(x) - D^\alpha g(y)|}{|x-y|^{n+2k}} \, \mathrm{d}x \, \mathrm{d}y.\end{aligned}$$

For $s < 0$ and $1 < p < \infty$ the Sobolev space $W^s_p(\Omega)$ is defined as the dual space of $\mathring{W}^{-s}_q(\Omega)$, which is the closure of $C^\infty_0(\Omega)$ with respect to the norm $\| \cdot \|_{W^{-s}_q(\Omega)}$. Moreover, the corresponding norm is defined as

$$\|f\|_{W^s_p(\Omega)} := \sup_{0 \neq g \in \mathring{W}^{-s}_q(\Omega)} \frac{|\langle f, g \rangle|_\Omega}{\|g\|_{W^{-s}_q(\Omega)}},$$

where $1/q + 1/p = 1$. Consequently, $\mathring{W}^s_p(\Omega)$ is the dual space of $W^{-s}_q(\Omega)$.

Now we want to state some properties of Sobolev spaces, which are required later in Chapter 4. One of the important properties is called *extention property* which is described in the following.

Definition 2.9. Let $\Omega \subseteq \mathbb{R}^n$ be a domain. For given m and p, a linear operator $E : W^m_p(\Omega) \to W^m_p(\mathbb{R}^n)$ is called an (m, p)-extension operator for Ω if there exist a constant C such that for every $f \in W^m_p(\Omega)$, the following conditions hold:

$$\begin{cases} Ef(x) = f(x) \quad \text{a.e. in } \Omega, \\ \|Ef\|_{m,p,\mathbb{R}^n} \leq C \|f\|_{m,p,\Omega}. \end{cases}$$

Another importance of Sobolev spaces is related to in their connections with the spaces of continuous and uniformly continuous functions. This is indicated in embedding theorems:

Theorem 2.10. *Let $\Omega \subseteq \mathbb{R}^n$ be a bounded domain with Lipschitz boundary $\partial\Omega$ and let*

$$n \leq s \quad \textit{for } p = 1, \quad n/p < s \quad \textit{for } p > 1.$$

For $f \in W^s_p(\Omega)$ and a constant C, we obtain

$$\|Ef\|_{L_\infty(\Omega)} \leq C \|f\|_{W^s_p(\Omega)}, \quad \textit{for all } f \in W^s_p(\Omega).$$

The proof is given in [7, 53].

Theorem 2.11. *Let Ω be a domain having the cone property in $\mathbb{R}^n$. Let $s > 0$ and $1 < p < n$.*

(a) if $n > sp$, then we get the embadding $W_p^s(\Omega) \hookrightarrow L_r(\Omega)$ for $p \le r \le np/(n-sp)$.

(b) if $n = sp$, then we get the embadding $W_p^s(\Omega) \hookrightarrow L_r(\Omega)$ for $p \le r < \infty$.

For the proof, see [1].

Theorem 2.12. *Let Ω be a bounded domain having the cone property in $\mathbb{R}^n$. Then the following embedding is compact:*

$$W_p^{m+j}(\Omega) \subset W_q^m(\Omega) \text{ if } n - jp > 0 \text{ and } m + j - n/p \ge m - n/p.$$

We refer to [1] for the proof.

Another concept that is related with Sobolev spaces, is distributions. This motivates the following definitions and results.

Definition 2.13. A continuous linear functional $T : C_0^\infty(\Omega) \to \mathbb{C}$ is called a *distribution*. T is continuous on $C_0^\infty(\Omega)$, if $\varphi_k \to \varphi$ in $C_0^\infty(\Omega)$ always implies $T(\varphi_k) \to T(\varphi)$. The set of all distributions on $C_0^\infty(\Omega)$ is denoted by $(C_0^\infty(\Omega))'$.

Example 2.14. Let $f \in L_1^{loc}(\Omega)$. Then a distribution is defined by

$$T_f(\varphi) := \int_\Omega f(x)\varphi(x)\mathrm{d}x, \quad \text{for } \varphi \in C_0^\infty(\Omega).$$

This type of distributions are called *regular distribution*. Otherwise they are called singular.

Moreover, the higher order derivatives of a distribution $T_f \in C_0^\infty(\Omega)$ is defined by

$$(D^\alpha T_f)(\varphi) := (-1)^{|\alpha|} T_f(D^\alpha \varphi), \quad \text{for } \varphi \in C_0^\infty(\Omega).$$

To conclude this section, we introduce another definition of the Sobolev spaces $H^s(\mathbb{R}^n),\ s \in \mathbb{R}$ which is based on the Fourier transform of distributions. We start with the definition of the Schwartz spaces $\mathcal{S}(\mathbb{R}^n)$.

Definition 2.15. Let $\varphi \in C^\infty(\mathbb{R}^n)$ satisfy

$$\|\varphi\|_{k,m} := \sup_{x \in \mathbb{R}^n} (|x|^k + 1) \sum_{|\alpha| \le m} |D^\alpha \varphi(x)| < \infty, \quad \text{for all } \ k, m \in \mathbb{N}_0.$$

Then $\mathcal{S}(\mathbb{R}^n)$ is the space of functions φ. Moreover, with $\mathcal{S}'(\mathbb{R}^n)$ we denote the space of temperate distributions as the space of all complex valued linear functional T over $\mathcal{S}(\mathbb{R}^n)$.

Consequently, for a function $\varphi \in \mathcal{S}(\mathbb{R}^n)$, one can be defined the Fourier transform $\hat{\varphi} \in \mathcal{S}(\mathbb{R}^n)$ as

$$\hat{\varphi}(\omega) := (\mathcal{F}\varphi)(\omega) = (2\pi)^{-\frac{n}{2}} \int_{\mathbb{R}^n} \varphi(x) e^{-i\langle x, \omega \rangle} \mathrm{d}x, \quad \text{for } \omega \in \mathbb{R}^n.$$

The mapping $\mathcal{F} : \mathcal{S}(\mathbb{R}^n) \to \mathcal{S}(\mathbb{R}^n)$ is invertible and the inverse Fourier transform is given by

$$(\mathcal{F}^{-1}\hat{\varphi})(x) = (2\pi)^{-\frac{n}{2}} \int_{\mathbb{R}^n} \hat{\varphi}(\omega) e^{i\langle x, \omega \rangle}\ \mathrm{d}\omega, \quad x \in \mathbb{R}^n.$$

Definition 2.16. For $s \in \mathbb{R}$ and $f \in \mathcal{S}(\mathbb{R}^n)$, we define the bounded linear operator $\mathcal{J}^s : \mathcal{S}(\mathbb{R}^n) \to \mathcal{S}(\mathbb{R}^n)$, called the *Bessel potential* of order s, by

$$\mathcal{J}^s f(x) := (2\pi)^{-\frac{n}{2}} \int_{\mathbb{R}^n} (1 + |\omega|^2)^{s/2} \hat{f}(\omega) e^{i\langle x,\omega\rangle} \, \mathrm{d}\omega, \quad x \in \mathbb{R}^n.$$

Regarding this definition and as an application of the Fourier transform we have

$$(\mathcal{F}\mathcal{J}^s f)(\omega) = (1 + |\omega|^2)^{s/2} \hat{f}(\omega).$$

Now for $T \in \mathcal{S}'(\mathbb{R}^n)$, we define the bounded linear operator $\mathcal{J}^s : \mathcal{S}'(\mathbb{R}^n) \to \mathcal{S}'(\mathbb{R}^n)$ on the space of temperate distributions as

$$(\mathcal{J}^s T)(\varphi) := T(\mathcal{J}^s \varphi), \quad \text{for all } \varphi \in \mathcal{S}(\mathbb{R}^n).$$

Ultimately, we define the Sobolev spaces $H^s(\mathbb{R}^n),\ s \in \mathbb{R}$ by

$$H^s(\mathbb{R}^n) := \{ f \in \mathcal{S}'(\mathbb{R}^n) : \mathcal{J}^s f \in L_2(\mathbb{R}^n) \}.$$

and for all $f, g \in \mathcal{S}'(\mathbb{R}^n)$ we equip this space with the inner product

$$\langle f, g \rangle_{H^s(\mathbb{R}^n)} := \langle \mathcal{J}^s f, \mathcal{J}^s g \rangle_{L_2(\mathbb{R}^n)},$$

which implies the norm

$$\|f\|^2_{H^s(\mathbb{R}^n)} := \|\mathcal{J}^s f\|^2_{L_2(\mathbb{R}^n)} = \int_{\mathbb{R}^n} (1 + |\omega|^2)^s |\hat{f}(\omega)|^2 \, \mathrm{d}\omega.$$

2.2 Some Definitions

In this section we present some definitions which are needed later. We refer to [30, 37, 41] for more details.

Definition 2.17. (Laurent Polynomials). In a formal variable z, Laurent polynomial is an expression of the form

$$p(z) = \sum_{k \in \mathbb{Z}} p_k z^k,$$

where $p_k \in \mathbb{C}$, and only finitely many of the p_k are nonzero. The Laurent polynomials treat as the regular polynomials except that the negative powers for z are allowed.

Similarly, vector or matrix Laurent polynomial has the form

$$P(z) = \sum_{k \in \mathbb{Z}} P_k z^k,$$

where the coefficients are vectors or matrices. In other words, they are vectors or matrices with polynomials entries.

Now for $\omega \in \mathbb{R}$, we can define the trigonometric polynomial as

$$p(\omega) = \sum_{k \in \mathbb{Z}} p_k e^{-ik\omega}.$$

All trigonometric polynomials are 2π-periodic and infinitely often differentiable. Analogously, for vector or matrix trigonometric polynomial, we have

$$P(\omega) = \sum_{k\in\mathbb{Z}} P_k e^{-ik\omega},$$

with the coefficients of vectors or matrices. In many situations, it is easier to work with if we use the z-notation as

$$P(z) = \sum_{k\in\mathbb{Z}} P_k z^k, \quad z \in \mathbb{T},$$

where $\mathbb{T}$ denotes the complex unit circle,

$$\mathbb{T} = \left\{ z \in \mathbb{C} \,\middle|\, z = e^{-i\omega} \quad , \omega \in \mathbb{R} \right\}.$$

In the end, we introduce one of the useful tools in linear algebra that is called *Singular Value Decomposition (SVD).*

Theorem 2.18. *If A is a real matrix of size $m \times n$, then there exist orthogonal matrices $U \in \mathbb{R}^{m\times m}$ and $V \in \mathbb{R}^{n\times n}$, such that*

$$U^\top A V = \Sigma,$$

where

$$\Sigma = diag(\sigma_1, \ldots, \sigma_k) \in \mathbb{R}^{m\times n}, \quad k = \min\{m, n\},$$

is a diagonal matrix, in which $\Sigma_{ii} = \sigma_i$ for $i = 1, 2, \ldots, k$, and $\Sigma_{ij} = 0$ for $i \neq j$. Moreover, we have

$$\sigma_1 \geq \sigma_2 \geq \ldots \geq \sigma_k \geq 0.$$

The proof is given in [30].

The SVD is more written as a factorization of A,

$$A = U\Sigma V^\top.$$

The diagonal entries of Σ are the *singular values* of A. The columns of U are the *left singular vectors*, and the columns of V are the *right singular vectors*.

Example 2.19. The matrix

$$A = \begin{pmatrix} 0.96 & 1.72 \\ 2.28 & 0.96 \end{pmatrix}$$

has the following SVD:

$$U = \begin{pmatrix} 0.6 & -0.8 \\ 0.8 & 0.6 \end{pmatrix}, \quad \Sigma = \begin{pmatrix} 3 & 0 \\ 0 & 1 \end{pmatrix}, \quad V = \begin{pmatrix} 0.8 & 0.6 \\ 0.6 & -0.8 \end{pmatrix}.$$

As a consequence of the SVD, the singular values and vectors satisfy the relations

$$\begin{aligned} &Av_i = \sigma_i u_i, \\ &A^\top u_i = \sigma_i v_i, \quad i = 1, 2, \ldots, \min\{m, n\}. \end{aligned}$$

The SVD reveals useful informations about the structure of a matrix. Let r be the number of nonzero singular values. Then r is the rank of A, and

$$\begin{aligned}\text{range}(A) &= \text{span}\{u_1, \ldots, u_r\},\\ \text{null}(A) &= \text{span}\{v_{r+1}, \ldots, v_k\}.\end{aligned}$$

That means, the SVD yields orthonormal bases of the range and null space of A. Consequently, we have

$$A = \sum_{i=1}^{r} \sigma_i u_i v_i^\top,$$

which is called the *SVD expansion* of A.

Chapter 3

Wavelets and Multiwavelets

In this thesis, we are working mainly with multiwavelets, but to better comprehension of their concept, we give a brief intruduction to the classical univariate wavelet setting in the first section. We begin with the definition of wavelets and multiresolution analysis. Then we describe some properties of wavelets, which are very desirable for application purposes. The second section deals with multiwavelet theory in $L_2(\mathbb{R})$. In particular, we consider multiwavelets which were constructed by Karsten Koch [43, 45] and have really nice features for our work and practical applications.

3.1 Wavelets

As stated before, the interest in wavelets has grown enormously during the last years. In the most general sense, wavelet bases are discrete families of functions obtained by dilations and translations of a finite number of well chosen mother functions. The most famous ones are certainly dyadic orthonormal bases of $L_2(\mathbb{R})$, of the type

$$\psi_{j,k}(x) = 2^{\frac{j}{2}}\psi(2^j x - k), \quad j,k \in \mathbb{Z}. \tag{3.1}$$

These bases have found many interesting applications, both in mathematics because they form Riesz bases for many functional spaces and in signal processing because wavelet expansions are more appropriate than Fourier series to represent the abrupt changes in non-stationary signals. Several examples have been given by [54] and [23], generalizing the classic Haar basis in [33], where the *mother wavelet* $\psi := \chi_{[0,\frac{1}{2})} - \chi_{[\frac{1}{2},1]}$ suffers from a lack of regularity since it is not even continuous. In late 1986, Mallat and Meyer recognized that construction of different wavelet bases can be realized by the concept of multiresolution, see [52, 54].
A *multiresolution analysis (MRA)* is a sequence $(V_j)_{j\in\mathbb{Z}}$ of closed subspaces of $L_2(\mathbb{R})$ which satisfies:

(a) $V_j \subset V_{j+1}$ for each $j \in \mathbb{Z}$,

(b) $\bigcap\limits_{j\in\mathbb{Z}} V_j = \{0\}$,

(c) $\bigcup\limits_{j\in\mathbb{Z}} V_j$ is dense in $L_2(\mathbb{R})$,

(d) $f(x) \in V_j$ if and only if $f(2x) \in V_{j+1}$ for each $j \in \mathbb{Z}$,

(e) there exist $\phi \in L_2(\mathbb{R})$ such that $\{\phi(x-k)\,|k \in \mathbb{Z}\}$ is an orthonormal basis in V_0.

The function ϕ in (e) is called the *scaling function* or *father wavelet*. Furthermore, since that V_0 is the closed subspace generated by the integer translates of a single function ϕ, we say that ϕ generates the MRA. It follows from Condition (d), which is the main property of the MRA, that for each $j \in \mathbb{Z}$ the set $\{\phi_{jk} = 2^{\frac{j}{2}}\phi(2^j x - k)\,|k \in \mathbb{Z}\}$ is an orthonormal basis for V_j. Also, regarding condition (a), we have $V_0 \subset V_1$ and ϕ has to satisfy the *refinement equation*

$$\phi(x) = \sum_{k\in\mathbb{Z}} a_k \phi(2x-k) \qquad \text{for almost all } x \in \mathbb{R}, \tag{3.2}$$

where the *mask* $(a_k)_{k\in\mathbb{Z}}$ is determined by the relation $a_k = 2\langle\phi, \phi(2\cdot - k)\rangle$. Here, and in the following, $\langle\cdot,\cdot\rangle$ denotes the usual L_2 inner product.
Figure 3.1 shows two different examples of a father and a mother wavelet.

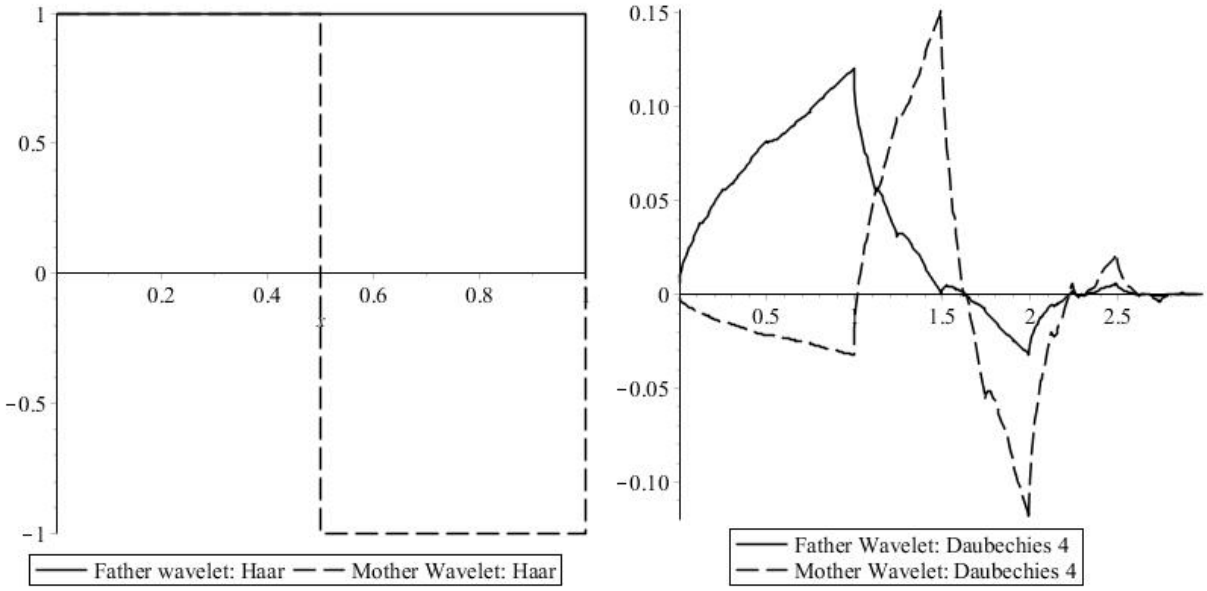

Figure 3.1: Haar and Daubechies wavelets

Conditions (b) and (c) can be expressed in terms of the orthogonal projections P_j of an arbitrary function $f \in L_2(\mathbb{R})$ onto V_j and we can result the following lemma.

Lemma 3.1. *For any $f \in L_2(\mathbb{R})$, $P_j f \to f$ in $L_2(\mathbb{R})$ as $j \to \infty$.*

The projection $P_j f$ can be considered as an *approximation* of f at the *resolution* or *scale* 2^{-j}. Therefore, the successive approximations of a given function $f \in L_2(\mathbb{R})$ are defined as the orthogonal projections P_j onto the space V_j by

$$P_j f = \sum_{k\in\mathbb{Z}} c_{jk}\phi_{jk},$$

where $c_{jk} = \langle f, \phi_{jk}\rangle$ and the basis functions ϕ_{jk} are shifted in steps of 2^{-j} as k varies, thus $P_j f$ cannot represent any detail on a scale smaller than that.

The real power of the multiresolution analysis arises from considering the differences between approximations at different levels. The difference between the approximations at resolution 2^{-j} and 2^{-j-1} is called the *fine detail at resolution* 2^{-j}:

$$Q_j f(x) = P_{j+1} f(x) - P_j f(x),$$

and Q_j is as well an orthogonal projection. Since $V_j \subset V_{j+1}$, we define W_j as the orthogonal complement of V_j in V_{j+1} for every $j \in \mathbb{Z}$ so that we have

$$V_{j+1} = V_j \oplus W_j.$$

Moreover, the sequence $(W_j)_{j\in\mathbb{Z}}$ satisfies conditions similar to MRA conditions. Thus, given an orthogonal MRA with scaling function ϕ, we have

(1) $W_j \perp W_{j'}$ if $j \neq j'$,

(2) $L_2(\mathbb{R}) = \bigoplus_{j\in\mathbb{Z}} W_j$,

(3) $f \in W_j$ if and only if $f(2\cdot) \in W_{j+1}$,

(4) if we find a function $\psi \in W_0$ such that $\{\psi(\cdot - k) \,|k \in \mathbb{Z}\}$ is an orthonormal basis of W_0, then for each $j \in \mathbb{Z}$ the set $\{\psi_{j,k} = 2^{\frac{j}{2}}\psi(2^j \cdot -k) \,|k \in \mathbb{Z}\}$ constitutes an orthonormal basis for W_j,

(5) Since $\psi \in W_0$ and $W_0 \subset V_1$, there has to exist a sequence $(b_k)_{k\in\mathbb{Z}}$ such that

$$\psi(x) = \sum_{k\in\mathbb{Z}} b_k \phi(2x - k) \qquad \text{for almost all } x \in \mathbb{R}. \tag{3.3}$$

Consequently, using the following theorem, we can find the sequence $(b_k)_{k\in\mathbb{Z}}$. More details can be found in [45].

Theorem 3.2. *Let $(V_j)_{j\in\mathbb{Z}}$ be an MRA, and let ϕ be the corresponding scaling function with mask $(a_k)_{k\in\mathbb{Z}}$. For any odd number N*

$$b_k = (-1)^k a_{N-k}, \qquad k \in \mathbb{Z},$$

and then equation (3.3) defines a wavelet ψ associated to $(V_j)_{j\in\mathbb{Z}}$.

Note that ψ is defined in terms of ϕ, not in terms of itself and therefore it is not a refinable function.

We now come to an important concept, the *discrete wavelet transform (DWT)*, with decent properties which allows the effortless computation of the wavelet coefficients. Given a function $f \in L_2(\mathbb{R})$, one can define the projection Q_j in terms of the wavelet function as

$$Q_j f = \sum_k d_{jk} \psi_{jk},$$

with $d_{jk} = \langle f, \psi_{jk} \rangle$. Then we can represent f as

$$f = \sum_{j=-\infty}^{\infty} Q_j f, \tag{3.4}$$

which complete decomposition in terms of detail at all levels. Although, in practical applications one is needed to find a finite approximation of f. To achieve this purpose, most of the wavelet coefficients have to vanish or be very small in modulus. In other words, the representation (3.4) is desired to be *sparse*. Also to compute or approximate the coefficients d_{jk}, the wavelet function ψ should decay reasonably fast. Thus, a compactly supported wavelet ψ is more desirable. Furthermore, if the function f possesses as well a compactly support, then for each fixed scale j we obtain a finite number of coefficients $d_{jk} \neq 0$. Hence, the only thing that remains to be control, is the behavior of the d_{jk} when $j \to \pm\infty$. For $j \to -\infty$, we can start at any level j' and use the approximation at resolution $2^{-j'}$ plus all the detail at finer resolution:

$$f = P_{j'} f + \sum_{j=j'}^{\infty} Q_j f. \tag{3.5}$$

For application purposes, we need to earn a finite representation of the form (3.5). The key property of a wavelet which enables the obtainment of sparse representations of functions as well as sparse representations of some operators is a high order of *vanishing moments*, i.e., there exists an integer $m \geq 1$ such that

$$\int_{\mathbb{R}} x^n \psi(x) dx = 0 \quad \text{for} \quad n = 0, \ldots, m-1.$$

A high number of vanishing moments for a wavelet leads to a high compressibility since the fine scale wavelet coefficients of a function are essentially zero where the function is smooth enough, see [15, 16].

Practically, the vanishing moments of a wavelet may be not sufficient to obtain control over the d_{jk} for $j \to \infty$. This problem can be bypassed by reducing the representation (3.5), i.e., by introducing a finest scale J. Suppose that $f \in V_J$ for some $J > j'$. Then

$$f = P_J f = P_{j'} f + \sum_{j=j'}^{J-1} Q_j f. \tag{3.6}$$

It means that the original function or signal f is decomposed into a coarse approximation $P_{j'} f$, and fine detail at several resolutions. Therefor, the DWT can be described by equation (3.6).

We refer to the following section for more details in a general setting.

3.2 Multiwavelets

As we have seen in the preceding section, wavelets have nice features such as interpolation, smoothness and orthogonality which are very useful for practical purposes like image/signal analysis as well as in numerical analysis, geophysics and in many other fields. A scalar wavelet setting is based on a single scaling function and mother wavelet. Particularly we are interested to use interpolating scaling functions and it has turned out that this setting can not provide enough flexibility and is somewhat restricted. A very simple example of interpolating function in the univariate setting is the Haar function, i.e.,

the characteristic function of the unit interval. This function is the only compactly supported scalar generator of a multiresolution analysis which is orthonormal, interpolating and symmetric. Therefore, with the wavelet setting we can not have desirable properties at the same time.

One approach to provide more flexibility, is to use the biorthogonal wavelets. In this case, we have two refinable functions ϕ and $\widetilde{\phi}$ which satisfy the condition

$$\langle \phi(x), \widetilde{\phi}(x-k) \rangle = \delta_{0,k}, \quad \text{for all } k \in \mathbb{Z}.$$

Here $\widetilde{\phi}$ is called the dual of ϕ. In other words, we use a dual pair of wavelet bases instead of one orthogonal basis. This causes the better results but as it is stated in [44], there exists some restrictions. Another possibility is to utilize the frames. Frames are stable, redundant generating systems in Hilbert spaces but they do not establish an orthonormal basis. They represent an alternative approach for decomposition of elements in $L_2(\mathbb{R})$. However, they have nice properties in applications but also bear some limitations. For more details, refer to [11]. Finally, we will discuss a preferable approach to overcome the restrictions. We use a generalization of scalar wavelets which is called multiwavelets. The concept of multiwavelet goes back to the early 1990s. Recently, multiwavelets have been introduced as a powerful multiscale analysis tool, see [25, 29, 32, 35]. In this approach, we replace the scaling function by a function vector. This makes it possible to have several nice properties such as symmetry, orthogonality, short support and a higher number of vanishing moments simultaneously. Furthermore, an interpolating and continuous scaling vectors with compact support have been constructed in [59]. Therefore, with the vector setting we can bypass most of the restrictions of using scalar wavelets. However, there exist as well some disadvantages and most of the approaches do not provide all the nice properties, like interpolation, compact support and orthonormality, at the same time. Moreover, there are some problems in construction of multiwavelets corresponding to interpolating scaling vectors. In [44], Karsten Koch, tackled these problems and constructed interpolating scaling vectors and multiwavelets, which are optimal ones in the vector approaches with really nice properties.

In this section we intend to introduce the scaling vectors and multiwavelets constructed by Karsten Koch in [44]. Furthermore, we discuss their nice properties and vector multiresolution analysis. Finally, we present some examples of orthonormal and interpolating scaling vectors and corresponding multiwavelets.

3.2.1 Refinable Scaling Vectors

As it was stated in Section 3.1 the refinability of scaling functions is an important feature for the construction of wavelets. Therefore, we start this subsection with introducing the scaling vectors which satisfy a refinement equation similar to (3.2).

Let $\Phi := (\phi_0, \ldots, \phi_{r-1})^\top,\ r > 0$, be a vector of $L_2(\mathbb{R})$-functions and satisfies a *matrix refinement equation*

$$\Phi(x) = \sum_{k \in \mathbb{Z}} A_k \Phi(2x - k), \tag{3.7}$$

with the mask $\mathbf{A} = (A_k)_{k\in\mathbb{Z}}$ of real $r \times r$ matrices. Then Φ is called a refinable *r-scaling vector*. Furthermore, the mask entries are denoted by

$$A_k = \begin{pmatrix} a_k^{(0,0)} & \dots & a_k^{(0,r-1)} \\ \vdots & \ddots & \vdots \\ a_k^{(r-1,0)} & \dots & a_k^{(r-1,r-1)} \end{pmatrix}. \tag{3.8}$$

We apply the Fourier transform component-wise to equation (3.7) and get

$$\widehat{\Phi}(\omega) = \frac{1}{2}\mathbf{A}(e^{-i\frac{\omega}{2}})\widehat{\Phi}(\frac{\omega}{2}), \quad \omega \in \mathbb{R} \tag{3.9}$$

with the symbol

$$\mathbf{A}(z) = \sum_{k\in\mathbb{Z}} A_k z^k, \quad z \in \mathbb{T}, \tag{3.10}$$

where $\mathbb{T}$ denotes the complex unit circle,

$$\mathbb{T} = \left\{ z \in \mathbb{C} \,\middle|\, z = e^{-i\omega} \quad , \omega \in \mathbb{R} \right\}.$$

Consequently, with iterating (3.9) we obtain

$$\widehat{\Phi}(\omega) = \prod_{j=1}^{\infty} \frac{1}{2}\mathbf{A}(e^{-i\,\frac{\omega}{2^j}})\widehat{\Phi}(0) =: P(\omega)\widehat{\Phi}(0),$$

and if the infinite product $P(\omega)$ converges then the scaling vector Φ can be determined by its symbol or mask. However, the Fourier transform of refinement equation (3.9) implies that $\widehat{\Phi}(0) = \frac{1}{2}\mathbf{A}(1)\widehat{\Phi}(0)$. Therefore, either $\widehat{\Phi}(0)$ is an 2–eigenvector of $\mathbf{A}(1)$ or we have $\widehat{\Phi}(0) = 0$ which is not desirable case.

The following theorem, stated in [9], supply the sufficient condition for the existence of a compactly supported solution for refinement equation (3.7). Let $\ell_0(\mathbb{Z})^{r\times r}$ denote the sequence space corresponding to the masks with finite number of non-vanishing coefficients.

Theorem 3.3. *For a mask $A \in \ell_0(\mathbb{Z})^{r\times r}$ let $\boldsymbol{A}(1)$ have the eigenvalues $\lambda_1 = 2, |\lambda_2|, \dots, |\lambda_r| < 2$, then the following statements hold:*

(i) The infinite matrix product $P(\omega)$ converges uniformly on compact sets.

(ii) Any 2–eigenvector υ of $\boldsymbol{A}(1)$ defines a compactly supported distributional solution Φ of (3.7) via $\widehat{\Phi}(\omega) =: P(\omega)\upsilon$.

(iii) If Φ is a nontrivial compactly supported distributional solution of (3.7) then $\widehat{\Phi}(0)$ is an 2–eigenvector of $\boldsymbol{A}(1)$.

Another approach to get approximate point values of $\Phi(x)$ is the *cascade algorithm* or *subdivision scheme*, which is a fixed point iteration applied to the refinement equation. We choose a suitable starting vector $\Phi^{(0)}$, and define

$$\Phi^{(n)}(x) = \sum_{k\in\mathbb{Z}} A_k \Phi^{(n-1)}(2x - k).$$

In many cases, this will converge to a vector of $L_2(\mathbb{R})$-functions. For more details see [12].

3.2.2 Desirable Properties

As stated before, we are interested in the scaling vector with nice properties such as interpolating, compact support and orthogonality. In this subsection we investigate the fundamental properties of 2-scaling vectors ($r = 2$) and multiwavelets constructed in [44]. First of all, we introduce some definitions needed in this subsection.

We define the ith *subsymbol* $\mathbf{A}_i(z)$ of $\mathbf{A}(z)$ by

$$\mathbf{A}_i(z) := \sum_{k\in\mathbb{Z}} A_{2k+i} z^k, \quad z \in \mathbb{T}, \quad i = 0, 1,$$

such that we have the decomposition

$$\mathbf{A}(z) = \mathbf{A}_0(z^2) + z\mathbf{A}_1(z^2).$$

Definition 3.4. For a matrix M or an operator M defined on a finite dimensional linear space, we say that M satisfies *Condition E* if M has a simple eigenvalue of 1, and all other eigenvalues are smaller than 1 in modulus.

Definition 3.5. The *transition operator* or *transfer operator* for the symbol $\mathbf{A}(z)$ is defined by

$$\mathbf{T}_{\mathbf{A}}\mathbf{C}(z) = \frac{1}{4}\left(\mathbf{A}(\sqrt{z})\mathbf{C}(\sqrt{z})\overline{\mathbf{A}(\sqrt{z})}^{\top} + \mathbf{A}(-\sqrt{z})\mathbf{C}(-\sqrt{z})\overline{\mathbf{A}(-\sqrt{z})}^{\top}\right), \quad z \in \mathbb{T},$$

for all 2×2 matrices of Laurent polynomials $\mathbf{C}(z)$.

If the transition operator satisfies Condition E, the cascade algorithm converges for any starting vector $\Phi^{(0)}$. Consequently, the spectral properties of the transition operator plays an important role in the stability and regularity of scaling vectors. Moreover, $\mathbf{T}_{\mathbf{A}} : \mathbb{H} \longrightarrow \mathbb{H}$ is a linear operator which the certain finite dimension space $\mathbb{H}$ is invariant under $\mathbf{T}_{\mathbf{A}}$ and can be represented by the matrix $\mathcal{T} \in \ell_0(\mathbb{Z})^{4\times 4}$:

$$\mathcal{T} := \frac{1}{2}(\Gamma_{2k-\alpha})_{k,\alpha\in K},$$

with

$$\Gamma_\alpha := \sum_{\beta\in\mathbb{Z}} A_{\beta-\alpha} \otimes \overline{A_\beta}, \quad \alpha \in \mathbb{Z},$$

where $P \otimes Q$ stands for the *Kronecker product* of arbitrary matrices P and Q. The index set K is given by

$$K := \left(\sum_{n=1}^{\infty} 2^{-n}\text{supp }(\mathcal{T})\right) \cap \mathbb{Z}.$$

Definition 3.6. A scaling vector Φ is said to be L_2-stable if there are constants $0 < A \leq B < \infty$, such that

$$A\sum_{\rho=0}^{1} \|c_\rho\|_{\ell_2}^2 \leq \left\|\sum_{\rho=0}^{1}\sum_{k\in\mathbb{Z}} \overline{c_{\rho,k}}\phi_\rho(\cdot - k)\right\|_{L_2}^2 \leq B\sum_{\rho=0}^{1} \|c_\rho\|_{\ell_2}^2 \tag{3.11}$$

holds for any sequences $c_\rho = (c_{\rho,k})_{k\in\mathbb{Z}} \in \ell_2(\mathbb{Z}), \rho = 0, 1$.

Many properties of scaling vectors can be determined by their symbols. Particularly, the following condition from [57] are related to our purpose.

Lemma 3.7. *If Φ is a compactly supported, L_2-stable solution vector of (3.7), then $\boldsymbol{A}(1)$ has a simple eigenvalue 2 and the moduli of all its other eigenvalues are less than 2.*

Note that Lemma 3.7 together with Theorem 3.3 imply that a compactly supported L_2-stable scaling vector Φ with finite mask satisfies $\widehat{\Phi}(0) \neq 0$.

As we have already mentioned, scaling vectors satisfying interpolation requirements have become of increasing interest and in many applications are very beneficial. For the case 2-scaling vector an interpolation property similar to the scalar case can be defined. A continuous 2-scaling vector Φ is called *interpolating* if for $\rho \in \{0, 1\}$, the components of Φ satisfy

$$\phi_\rho(\frac{n}{2}) = \delta_{\rho,n} = \begin{cases} 0, & \text{if } \ n \in \mathbb{Z} \setminus \{\rho\} \\ 1, & \text{if } \ n = \rho. \end{cases} \tag{3.12}$$

One advantage of interpolating scaling vectors is that they give rise to a Shannon–like sampling theorem as follows. For a compactly supported function vector Φ and for $k, l \in \mathbb{Z}$, we define

$$S(\Phi) := \left\{ \sum_{k\in\mathbb{Z}} \upsilon_k \Phi(\cdot - k) \mid \upsilon \in \ell(\mathbb{Z})^{1\times 2} \right\}. \tag{3.13}$$

Since Φ has compact support, $S(\Phi)$ is well defined, for more details see [44]. Then for any function $f \in S(\Phi)$ the equation

$$f(x) = \sum_{k\in\mathbf{Z}} f(k)\phi_0(x-k) + f(k+\frac{1}{2})\phi_1(x-k), \tag{3.14}$$

holds. Consequently, for compactly supported Φ the interpolation property yields (algebraically) *linearly independent translates*, i. e., for $(\upsilon_k)_{k\in\mathbb{Z}} := ((c_k, d_k))_{k\in\mathbb{Z}}$ with $c_k, d_k \in \mathbb{C}$, we have

$$\sum_{k\in\mathbb{Z}} \upsilon_k \Phi(x-k) = 0 \quad \Longrightarrow \quad \upsilon_k = \mathbf{0} \text{ for all } k \in \mathbb{Z}.$$

Another advantage of interpolating scaling vectors is that their masks have a simple structure. Inserting the refinement equation (3.7) into the interpolation condition (3.12) and using the coefficient matrices A_k in (3.8) for 2-scaling vectors leads to

$$a_k^{\rho 0} = \delta_{\rho,k}.$$

Consequently, for the symbol $\mathbf{A}(z)$ we obtain

$$\mathbf{A}(z) = \begin{pmatrix} 1 & a_0(z) \\ z & a_1(z) \end{pmatrix}, \quad z \in \mathbb{T}, \tag{3.15}$$

with entries

$$a_\rho(z) := \sum_{k\in\mathbb{Z}} a_k^{\rho 1} z^k, \quad \rho \in \{0, 1\}.$$

This form of symbols will simplify remarkably the construction of scaling vectors.

Another desirable property of scaling vectors is orthonormality. A scaling vector Φ is called orthonormal, if its integer translates are orthonormal, i.e.,

$$\langle \phi_\rho, \phi_\mu(\cdot - k)\rangle = \delta_{0,k}\delta_{\rho,\mu}, \qquad 0 \le \rho, \mu < 2, \quad k \in \mathbb{Z}. \tag{3.16}$$

A necessary condition for Φ to be orthonormal is that its symbol has to satisfy

$$\mathbf{I}_2 = \frac{1}{4}\left(\mathbf{A}(z)\overline{\mathbf{A}(z)}^\top + \mathbf{A}(-z)\overline{\mathbf{A}(-z)}^\top\right), \quad z \in \mathbb{T}, \tag{3.17}$$

where I_2 denotes the 2-dimensional unit matrix.

It was shown in [40] that this condition is also sufficient as follows.

Theorem 3.8. *Let Φ be 2-scaling vector with finitely supported mask $A \in \ell_0(\mathbb{Z})^{2\times 2}$. Φ is orthonormal if and only if the following statements hold:*

(i) $\boldsymbol{A}(z)$ *satisfy (3.17),*

(ii) $1 \in spec(\boldsymbol{A}_i(1)^\top)$ *for $i = 0, 1$, where spec denotes the spectrum of an operator or a matrix,*

(iii) $\boldsymbol{A}(1)$ *has a simple eigenvalue 2 and the moduli of all its other eigenvalues are smaller than 2 in modulus, and*

(iv) $\boldsymbol{T_A}$ *satisfies Condition E.*

In the following, a scaling vector satisfying (3.12) and (3.16) is called an orthonormal interpolating scaling vector.

3.2.3 Multiresolution Analysis and Multiwavelets

In this subsection we want to introduce the multiwavelet corresponding to the scaling vactor in Subsection 3.2.1. As in the scalar case, the multiwavelet is constructed by a multiresolution analysis (MRA). The definition of MRA for the vector case are the same as in Section 3.1, but has to be modify to the multifunction setting, see [31, 39] for more details.

A multiresolution analysis (MRA) is a sequence $(V_j)_{j\in\mathbb{Z}}$ of closed subspaces of $L_2(\mathbb{R})$ which satisfies:

(1) $V_j \subset V_{j+1}$ for each $j \in \mathbb{Z}$,

(2) $g(x) \in V_j$ if and only if $g(2x) \in V_{j+1}$ for each $j \in \mathbb{Z}$,

(3) $\bigcap_{j\in\mathbb{Z}} V_j = \{0\}$,

(4) $\bigcup_{j\in\mathbb{Z}} V_j$ is dense in $L_2(\mathbb{R})$, and

(5) there exist an L_2-stable $\Phi \in L_2(\mathbb{R})^r$ such that

$$V_0 = \overline{\operatorname{span}\{\phi_i(x-k),\ k \in \mathbb{Z},\ 0 \le i < r\}}.$$

To construct some multiwavelets, we first have to check all these conditions to find a suitable MRA. For a detailed discussion see, e.g., [23, 32, 44]. In the following, we explain an approach to obtain a multiwavelet basis.

Suppose that W_0 denotes an algebraic complement of V_0 in V_1 and define $W_j := \{g(2^j\cdot)\,|g \in W_0\}$. Then, we obtain $V_{j+1} = V_j \oplus W_j$ and as a consequence of conditions (3) and (4), we get

$$L_2(\mathbb{R}) = \bigoplus_{j\in\mathbb{Z}} W_j.$$

Now we can find the r-multiwavelet, i.e., the function vectors $\Psi = (\psi_0, \ldots, \psi_{r-1})^\top \in L_2(\mathbb{R})^r$, such that the integer translates of its components is a stable basis of W_0. Consequently, after dilation of components, we obtain a (Riesz) basis of $L_2(\mathbb{R})$ as

$$\left\{\psi_0(2^j\cdot -k), \ldots, \psi_{r-1}(2^j\cdot -k)|j,k \in \mathbb{Z}\right\}.$$

Moreover, since $W_0 \subset V_1$, we represent each Ψ as

$$\Psi(x) = \sum_{k\in\mathbb{Z}} B_k \Phi(2x-k) \tag{3.18}$$

with real $r \times r$ matrices B_k. By applying the Fourier transform to this equation we obtain

$$\widehat{\Psi}(\omega) = \frac{1}{2}\mathbf{B}(e^{-i\frac{\omega}{2}})\widehat{\Phi}(\frac{\omega}{2}), \quad \omega \in \mathbb{R},$$

with the symbol

$$\mathbf{B}(z) = \sum_{k\in\mathbb{Z}} B_k z^k, \qquad z \in \mathbb{T}.$$

Thus instead of finding a stable multiwavelet basis, we can construct the symbols $\mathbf{B}(z)$. Furthermore many fundamental properties of the solution of the matrix refinement equation (3.7) can be characterized in terms of the symbol.

3.2.4 Discrete Multiwavelet Transform

Similar to the traditional wavelets, we can define the *Discrete Multiwavelet Transform (DMWT)* based on the decomposition

$$V_j = V_{\acute{j}} \oplus W_{\acute{j}} \oplus W_{\acute{j}+1} \oplus \ldots \oplus W_{j-1}.$$

It means that the DMWT takes a function $f \in V_j$ for some j and decomposes it into a coarser approximation at level $\acute{j} < j$, plus the fine detail at the intermediate levels:

$$f = P_j f = P_{\acute{j}} f + \sum_{k=\acute{j}}^{j-1} Q_k f.$$

Now suppose that we have a function $f \in V_j$ represented by its coefficient sequence $\{f_{jk}^\top\}$ as

$$f = \sum_k f_{jk}^\top \Phi_{jk}.$$

One can decompose f into its components in V_{j-1} and W_{j-1}:

$$f = P_{j-1}f + Q_{j-1}f = \sum_n f_{j-1,n}^\top \Phi_{j-1,n} + \sum_n g_{j-1,n}^\top \Psi_{j-1,n},$$

where $\left\{f_{j-1,n}^\top\right\} = \{\langle f, \Phi_{j-1,n}\rangle\}$ and $\left\{g_{j-1,n}^\top\right\} = \{\langle f, \Psi_{j-1,n}\rangle\}$.
For the masks A_k in (3.7) and B_k in (3.18), the DMWT is defined by

$$\begin{aligned} f_{j-1,n} &= \sum_k A_{k-2n} f_{jk}, \\ g_{j-1,n} &= \sum_k B_{k-2n} f_{jk}. \end{aligned} \tag{3.19}$$

Furthermore, the inverse DMWT is given by

$$f_{jk} = \sum_n A_{k-2n}^\top f_{j-1,n} + \sum_n B_{k-2n}^\top g_{j-1,n}.$$

To become the notation nicer, we interleave the coefficients $f_{j-1,n}$ and $g_{j-1,n}$ in (3.19) and obtain the following matrix formulation:

$$\begin{pmatrix} \vdots \\ (fg)_{j-1,-1} \\ (fg)_{j-1,0} \\ (fg)_{j-1,1} \\ \vdots \end{pmatrix} = \begin{pmatrix} \cdots & \cdots & \cdots & & & & \\ \cdots & S_{-1} & S_0 & S_1 & \cdots & & \\ & \cdots & S_{-1} & S_0 & S_1 & \cdots & \\ & & \cdots & S_{-1} & S_0 & S_1 & \cdots \\ & & & & \cdots & \cdots & \cdots \end{pmatrix} = \begin{pmatrix} \vdots \\ f_{j,-1} \\ f_{j,0} \\ f_{j,1} \\ \vdots \end{pmatrix},$$

where

$$S_k = \begin{pmatrix} A_{2k} & A_{2k+1} \\ B_{2k} & B_{2k+1} \end{pmatrix}, \quad k \in \mathbb{Z}. \tag{3.20}$$

Therefore the DMWT can be represented as

$$(fg)_{j-1} = S\ f_j, \tag{3.21}$$

where $S = (S_k)_{k\in\mathbb{Z}}$ and

$$(fg)_{j-1} = \begin{pmatrix} \vdots \\ f_{j-1,0} \\ g_{j-1,0} \\ f_{j-1,1} \\ g_{j-1,1} \\ \vdots \end{pmatrix},$$

Similarly, the inverse DMWT can be written as

$$f_j = S^\top (fg)_{j-1}.$$

Note that the infinite matrix S is orthogonal. For more details, you can refer to [41].

3.2.5 Biorthogonality

As we have seen in the last subsections, Φ is a L_2-stable scaling vector and generates a multiresolution analysis. Moreover, it is possible to orthonormalize an existing scaling vector with stable shifts, but then it does not usually have strong properties any more. This makes it less desirable for practical applications.Therefore, to provide more flexibility such as symmetric, good approximation and regularity properties, it is often beneficial to switch to the biorthogonal case.
r-scaling vectors Φ, $\widetilde{\Phi}$ are biorthogonal or duals of each other if the integer translates of all component functions are mutually orthogonal, i.e.,

$$\langle \phi_\rho, \widetilde{\phi}_\mu(\cdot - k)\rangle = c\ \delta_{0,k}\delta_{\rho,\mu}, \qquad 0 \le \rho, \mu < r, \tag{3.22}$$

holds for all $k \in \mathbb{Z}$ and a constant $c > 0$.
A necessary condition for Φ, $\widetilde{\Phi}$ to be biorthogonal is that their symbols $\mathbf{A}(z)$ and $\widetilde{\mathbf{A}}(z)$ satisfy

$$\mathbf{A}(z)\overline{\widetilde{\mathbf{A}}(z)}^{\top} + \mathbf{A}(-z)\overline{\widetilde{\mathbf{A}}(-z)}^{\top} = 4\mathbf{I}_r.$$

It was shown in [12] that these conditions are sufficient to ensure biorthogonality if the cascade algorithm for both Φ and $\widetilde{\Phi}$ converges.

Unfortunately it is not possible for a scaling vector Φ to be interpolating and strictly orthonormal at the same time. However, regarding the following theorem, we can switch between these properties via multiplying Φ by $\sqrt{r}$ and $1/\sqrt{r}$ respectively.

Theorem 3.9. *Let $\Phi = (\phi_0, \ldots, \phi_{r-1})^\top$ be a compactly supported interpolating r–scaling vector with finite mask that satisfies (3.16) with $\widetilde{\Phi} = \Phi$. Then we have*

$$\|\phi_i\|_{L_2}^2 = \int_{\mathbb{R}} \phi_i(x)\ dx = \frac{1}{r},$$

for $i \in \{0, \ldots, r-1\}$.

The proof is given in [44].

Now, let $\Phi, \widetilde{\Phi} \in L_2(\mathbb{R})^r$ and $A, \widetilde{A} \in \ell_0(\mathbb{Z})^{r\times r}$, then the biorthogonality condition (3.22) implies that Φ and $\widetilde{\Phi}$ are L_2-stable, see [13, 14]. Moreover, Theorem 3.3 yields that both, Φ as well as $\widetilde{\Phi}$, are compactly supported. Consequently, each scaling vector generates an MRA. Now assume that we have two MRAs V_j and $\widetilde{V}_j$, generated by biorthogonal scaling vectors Φ and $\widetilde{\Phi}$. The projections P_j and $\widetilde{P}_j$ from $L_2(\mathbb{R})$ into V_j and $\widetilde{V}_j$ respectively, are given by

$$P_j f = \sum_{k\in\mathbb{Z}} \sum_{i=0}^{r-1} \langle f, \widetilde{\phi}_{i,j,k}\rangle \phi_{i,j,k}(x),$$
$$\widetilde{P}_j f = \sum_{k\in\mathbb{Z}} \sum_{i=0}^{r-1} \langle f, \phi_{i,j,k}\rangle \widetilde{\phi}_{i,j,k}(x).$$

These are now nonorthogonal projections. If there exist some multiwavelets associated to these MRAs, then the task of finding these multiwavelets can be reduced to finding the corresponding symbols.

3.2.6 Approximation Order of Scaling Vector

One of the important properties of a scaling vector is its ability to reproduce polynomials. In this subsection we want to give a brief introduction to this property and approximation order of scaling vectors. We begin with some definitions and notations.

Definition 3.10. Suppose that π_m denotes the space of all polynomials of total degree less or equal than m in $\mathbb{R}$. A function vector Φ with compact support is said to provide *accuracy order* $m+1$, if $\pi_m \subset S(\Phi)$.

Definition 3.11. A compactly supported function vector $\Phi \in L_2(\mathbb{R})$ is said to provide *approximation order* $m > 0$ if the *Jackson-type inequality*

$$\inf_{g \in V_j} \left\{ \|f - g\|_{L_2} \right\} \leq C 2^{-jm} \|f\|_{H^m}, \tag{3.23}$$

holds for all f contained in the Sobolev space $H^m(\mathbb{R})$ with $C > 0$ and

$$V_j = \overline{\operatorname{span}\{\phi_i(2^j \cdot -k),\ k \in \mathbb{Z},\ 0 \leq i < r\}}.$$

The approximation order plays a crucial role in the regularity or smoothness of a scaling vector. Moreover, the regularity leads to a certain minimum approximation order, see [41].

Note that if a compactly supported scaling vector Φ has linearly independent integer translates or is at least stable, then the order of accuracy is equivalent to the approximation order provided by Φ. For more details, see [38].
Following theorem from [55] shows that the approximation order of scaling vectors is connected with a specific factorization of the symbol.

Theorem 3.12. ***(Plonka).*** *Let Φ be a compactly supported r–scaling vector, and let $\{\phi_\rho(\cdot - n) : n \in \mathbb{Z}, \rho = 0, \ldots, r-1\}$ form a (algebraically) linearly independent basis of their closed linear span. Then Φ provides approximation order m if and only if the symbol $\boldsymbol{A}(z)$ of Φ satisfies the following conditions:*
The elements of $\boldsymbol{A}(z)$ are Laurent polynomials, and there are vectors $y_k \in \mathbb{R}^r, y_0 \neq \boldsymbol{0}, k = 0, \ldots, m-1$, such that for $n = 0, \ldots, m-1$

$$\begin{aligned} \sum_{k=0}^{n} \binom{n}{k} (y_k)^\top (2i)^{k-n} \left(D^{n-k} \boldsymbol{A}\right)(1) &= 2^{1-n} (y_n)^\top, \\ \sum_{k=0}^{n} \binom{n}{k} (y_k)^\top (2i)^{k-n} \left(D^{n-k} \boldsymbol{A}\right)(-1) &= \boldsymbol{0}^\top, \end{aligned} \tag{3.24}$$

holds. Furthermore there exist matrices $\boldsymbol{C}_k, k = 0, \ldots, m-1$, such that $\boldsymbol{A}(z)$ factorizes like

$$\boldsymbol{A}(z) = \frac{1}{2^{m-1}} \boldsymbol{C}_0(z^2) \ldots \boldsymbol{C}_{m-1}(z^2) \boldsymbol{A}_m(z) \boldsymbol{C}_{m-1}^{-1}(z) \boldsymbol{C}_0^{-1}(z),$$

where $\boldsymbol{A}_m(z)$ is a suitable matrix with Laurent polynomials as entries.

Here D denotes the differential operator with respect to ω in terms of $z = e^{-i\omega}$, i. e., $D\mathbf{A}(e^{-i\omega}) := \left(\frac{d}{d\omega}\mathbf{A}(e^{-i\omega})\right)(\omega)$.

The equations (3.24) are called *sum rules of order m* and were also obtained by Heil et al. in [34].

Remark 3.13. Note that condition (ii) in Theorem 3.8 is equivalent to the mask A satisfying the sum rules of order 1. Furthermore, conditions (iv) in Theorem 3.8 and (3.24) are the necessary and sufficient conditions for the convergence of cascade algorithm. For more details, see [12, 41].

Beside that compactly supported scaling vector Φ provides accuracy of order m, if the mask of Φ satisfies the sum rules of order m. The proof is given in [8, 40]. If additionally, Φ is stable, then Φ reproduces polynomials of total degree less than m. Moreover, since Φ provides accuracy of order m, it holds that $x^n \in S(\Phi)$ for $|n| < m$, and, due to the sampling property (3.14), we have

$$x^n = \sum_{k\in\mathbb{Z}} \sum_{i=0}^{r-1} (k + \frac{1}{2}\rho_i)^n \phi_i(x-k), \tag{3.25}$$

where $\{\rho_i\}_{i=0}^{r-1}$ denote a complete set of representatives of $\mathbb{Z}/2\mathbb{Z}$. For the case $r = 2$, we choose $\rho_0 = 0$ and $\rho_1 = 1$.
The ability of scaling vector for the reproduction of polynomials are very important for the properties of multiwavelets. As in the scalar case, a function vector $\Psi \in L_2(\mathbb{R})^r$ is said to have *vanishing moments of order* m, if

$$\langle x^n, \Psi(x)\rangle := (\langle x^n, \psi_0(x)\rangle, \ldots, \langle x^n, \psi_{r-1}(x)\rangle) = 0$$

for all $n \in \mathbb{Z}^+$ with $|n| < m$.
Similar to the univariate scalar setting, vanishing moments play a key role in many applications. For example in signal/image processing, the coefficients in the wavelet expansion become very small with the high order of vanishing moments and this leads to a compressed signal or image. See Chapter 7 from [44] for more details.

3.2.7 Construction of Scaling Vectors and Multiwavelets

In this subsection we intend to assemble all the results in the previous subsections to construct the orthonormal interpolating 2-scaling vectors. Karsten Koch in [43] transformed the interpolating and orthonormality conditions into an applicable version. This has shown in the following theorem.

Theorem 3.14. *Let Φ be a compactly supported interpolating 2-scaling vector with symbol*

$$\boldsymbol{A}(z) = \begin{pmatrix} 1 & a_0(z) \\ z & a_1(z) \end{pmatrix}, \quad a_0(z) \neq z^\nu,\ \nu \in \mathbb{Z}.$$

If Φ is also orthonormal, then the symbol entries $a_0(z)$ and $a_1(z)$ have to satisfy

$$2 = |a_0(z)|^2 + |a_0(-z)|^2$$

and

$$a_1(z) = \pm z^{2\kappa+1}\overline{a_0(-z)}, \quad \kappa \in \mathbb{Z},$$

with

$$a_0(z) = \sum_{k=M}^{N} a_k z^k, \quad M, N \in \mathbb{Z}, \quad N - M \text{ odd}.$$

Corollary 3.15. *With the notations and conditions of Theorem 3.14 the 2-scaling vector* Φ *provides approximation order* m *iff for* $n = 0, \ldots, m-1$ *the mask coefficients of the symbol entry* $a_0(z)$ *satisfy*

$$2^{-n} = \sum_k (-2k)^n a_{2k} - \sum_k (2(k-\kappa)+1)^n a_{2k+1},$$
$$2^{-n} = \sum_k (-2k-1)^n a_{2k+1} - \sum_k (2(k-\kappa))^n a_{2k}.$$

Based on Theorem 3.14 and Corollary 3.15, one can be constructed orthonormal interpolating 2-scaling vector.

In the following, we present two examples from [42], which are interpolating and orthonormal 2-scaling vector with the highest regularity.

Example 3.16. In Figure 3.2, we plot a one-parameter set of 2-scaling vectors Φ supported on the interval $[-1, 2]$ with symbols

$$\mathbf{A}(z) = \begin{pmatrix} 1 & 0.2208z^{-1} + 0.9486 - 0.2208z + 0.0514z^2 \\ z & 0.0514z^{-1} + 0.2208 + 0.9486z - 0.2208z^2 \end{pmatrix}, \quad z \in \mathbb{T}. \tag{3.26}$$

In this case, one turns out an interpolating and orthonormal 2-scaling vector which provides approximation order 1.

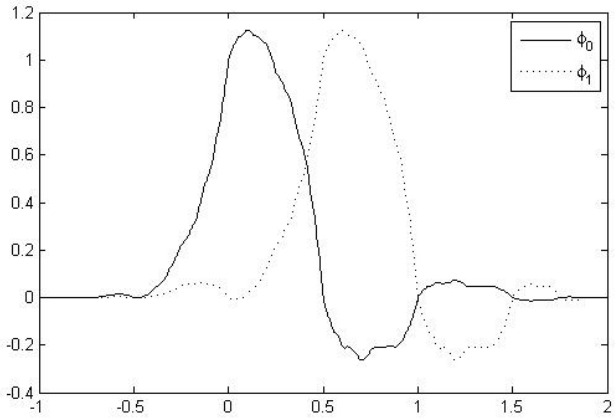

Figure 3.2: Interpolating and orthonormal 2-scaling vector, approximation order 1

Example 3.17. For 2-scaling vector Φ supported on the interval $[-2, 3]$, one obtains the symbols

$$\mathbf{A}(z) = \begin{pmatrix} 1 & a_0(z) \\ z & a_1(z) \end{pmatrix}, \quad z \in \mathbb{T},$$

where

$$a_0(z) = 0.0313z^{-2} + 0.2460z^{-1} + 0.9375 - 0.2421z + 0.0313z^2 - 0.0040z^3$$

and

$$a_1(z) = 0.0040z^{-2} + 0.0313z^{-1} + 0.2421 + 0.9375z - 0.2460z^2 + 0.0313z^3.$$

This construction leads to an interpolating and orthonormal solution which provides approximation order 2 and is shown in Figure 3.3.

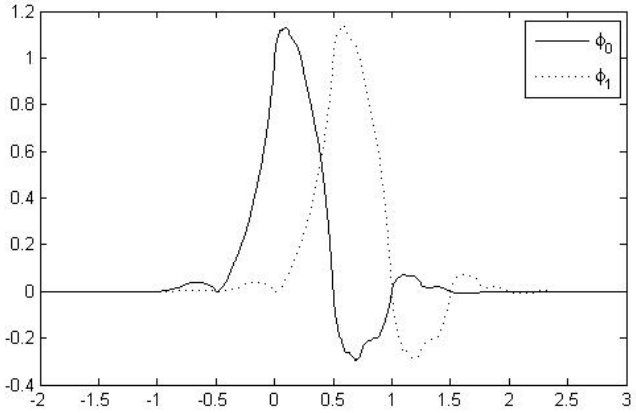

Figure 3.3: Interpolating and orthonormal 2-scaling vector, approximation order 2

Now we intend to construct a 2-multiwavelet corresponding to the interpolating and orthonormal 2-scaling vector Φ. As it was already mentioned, for the construction of multiwavelets, we need to compute the symbol $\mathbf{B}(z)$ of Ψ. It was shown in [31,32] that to construct the orthonormal multiwavelets, the symbol has to satisfy

$$\mathbf{B}(z) := \mathbf{B}_0(z^2) + z\mathbf{B}_1(z^2), \qquad z \in \mathbb{T},$$

where $\mathbf{B}_0(z)$ and $\mathbf{B}_1(z)$ are submatrices of an quadratic matrix $\mathbf{Q}(z)$, i. e.,

$$\mathbf{Q}(z) = \frac{1}{\sqrt{2}} \begin{pmatrix} \mathbf{A}_0(z) & \mathbf{A}_1(z) \\ \mathbf{B}_0(z) & \mathbf{B}_1(z) \end{pmatrix}.$$

It would be desirable, that Ψ is also interpolating, i. e.,

$$\Psi(\frac{n}{2}) = \begin{pmatrix} \delta_{0,n} \\ \delta_{1,n} \end{pmatrix}, \quad n \in \mathbb{Z}.$$

In this case, the symbol $\mathbf{B}(z)$ is completely determined by the symbol $\mathbf{A}(z)$ in (3.15) and satisfies

$$\mathbf{B}(z) = \begin{pmatrix} 1 & -a_0(z) \\ z & -a_1(z) \end{pmatrix}, \quad z \in \mathbb{T}.$$

For more details, see [43, 59].

Figure 3.4 and 3.5 show two orthonormal and interpolating 2-multiwavelets corresponding to the scaling vectors in 3.2, 3.3 respectively.

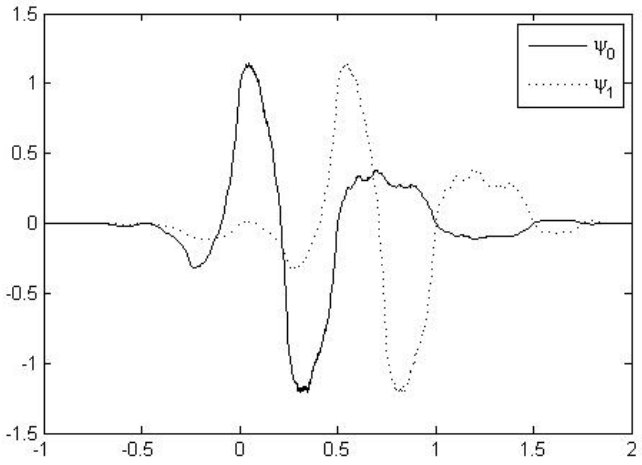

Figure 3.4: Interpolating 2-multiwavelets supported on $[-1, 2]$

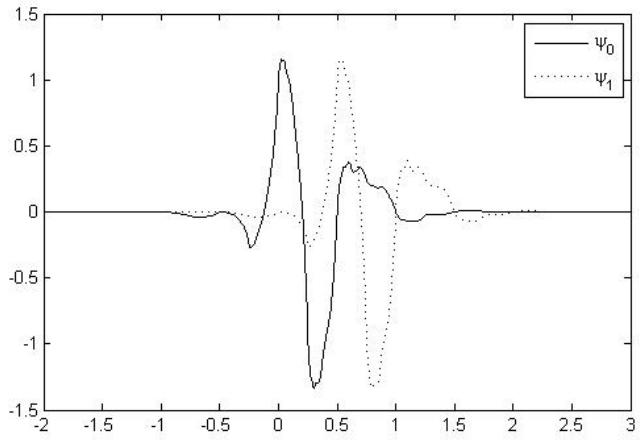

Figure 3.5: Interpolating 2-multiwavelets supported on $[-2, 3]$

Chapter 4

Interpolating Scaling Vectors and Multiwavelets on the Interval $[0, 1]$

The methods based on wavelets have been recently studied in the analysis and the numerical treatment of operator equations [19, 20]. The advantage of such methods is that they provide a good localization both in space and frequency. Thanks to wavelet properties, it is possible to predict the behavior of the solution at a certain time-step from the previous time-step. Moreover some methods based on the wavelet transform can be used to accelerate the numerical schemes [6]. Wavelet bases are usually constructed via multiresolution analysis on $\mathbb{R}$, which make them very attractive in pure and applied mathematics. However in many applications, we are interested in problems confined on the interval. Examples are solutions to the partial differential equations with boundary conditions at the edges of the interval, image analysis: where the domain of interest is the Cartesian product of two intervals.
Unfortunately, there exist some difficulties when applying such methods to problems in bounded domain. Classical wavelets cause some instability problems, since that they are originally a basis on the whole line. Moreover, in the methods for solving a boundary value problem, one is needed to compute the nonlinear terms in the physical space and then projecting them back to the wavelet coefficient space through some quadrature formula. This technique reduces the efficiency of procedure and slows the computations.
In this chapter, we want to overcome these problems in a satisfactory way. We construct new families of interpolating scaling vectors with short support and more favorable properties. First of all, we use the multigenerators from [42] and the approach in [4] for adapting them to a bounded interval in a general way. The interpolating nature of these multigenerators appears to be a powerful tool for obtaining multiresolution analyses on more complex geometries. Consequently, we have to introduce new multiresolution analysis (MRA) on the interval. Then we have to check out that the approximation properties are preserved. Finally, we will construct corresponding multiwavelets on the interval and give some examples for our results. To fix notations, let us assume that the interval is $[0, 1]$.

4.1 Construction of Interpolating Multigenerators on the Interval

In this section we intend to modify a given interpolating r-scaling vector which generates a multiresolution analysis for $L_2(\mathbb{R})$, so that it generates a multiresolution analysis for $L_2([0,1])$ with desired properties. For simplicity of calculations, we suppose that $r = 2$ and begin with the 2-scaling vector which have the following properties:

- $\Phi = (\phi_0, \phi_1)^\top$ is a vector of $L_2(\mathbb{R})$-functions which satisfies a matrix refinement equation (3.7) and the support of Φ is contained in the interval $[-N, N+1]$, $N \in \mathbb{N}$. Therefore the number of refinement terms is finite and there is a minimal positive integer M such that
$$\Phi(x) = \sum_{t=-M}^{M} A_t \Phi(2x - t), \tag{4.1}$$
with $A_t = 0$ for $t < -M$ or $t > M$.

- The 2-scaling vector Φ is continuous and interpolating, i.e., for $\rho \in \{0, 1\}$, Φ satisfies
$$\phi_\rho(\frac{n}{2}) = \delta_{\rho,n} = \begin{cases} 0, & \text{if } n \in \mathbb{Z} \setminus \{\rho\} \\ 1, & \text{if } n = \rho. \end{cases} \tag{4.2}$$

- Φ satisfies a shannon-like sampling theorem, i.e., for any function $f \in S(\Phi)$ the equation (3.14) holds. Since Φ provides accuracy of order m, it holds that $x^n \in S(\Phi)$ for $|n| < m$, and due to this property, we have
$$x^n = \sum_{k\in\mathbb{Z}} \sum_{i=0}^{1} (k + \frac{1}{2}i)^n \phi_i(x - k). \tag{4.3}$$

- Φ is $L_2 - \textit{stable}$ and satisfies the inequality (3.11).

- Φ provides approximation order $m > 0$ and satisfies the Jackson-type inequality (3.23).

Now we define an interpolation operator $I_j : H^m(\mathbb{R}) \to V_j$, $m > 0$, by means of
$$I_j f(x) = \sum_{k\in\mathbb{Z}} \sum_{i=0}^{1} f(\frac{k + \frac{1}{2}i}{2^j}) \phi_i(2^j x - k), \tag{4.4}$$
where f is defined on $\mathbb{R}$. Since that $S(\Phi)$ in (3.13) is well defined and Φ is a compactly supported interpolating 2-scaling vector, it is clear that (4.4) is well defined. Moreover, we are interested in approximating $I_j f\,\big|_{[0,1]}$.
Let us now suppose that we know the values of f only in $[0, 1]$, at the dyadic points $x_{i,k} = (\frac{k+\frac{1}{2}i}{2^j})$, $i \in \{0, 1\}$. Since the support of Φ is contained in the interval $[-M, M]$, we require to compute the values of f at the points $x_{i,n}$ for $n = -M, \ldots, -1$ and $n = 2^j + 1, \ldots, 2^j + M$. For $2^j > 2m + 2$ (j has to be large enough for non-interacting the

boundaries on the left and right side), where $m > 0$ is the approximation order of Φ, we define *extrapolating polynomials* P^L and P^R of degree m that interpolate f at the dyadic points internal to the interval $[0, 1]$ by

$$\begin{aligned} P^L(\frac{k+\frac{1}{2}i}{2^j}) &= f(\frac{k+\frac{1}{2}i}{2^j}), \qquad k = 0, \dots, m, \\ P^R(\frac{k+\frac{1}{2}i}{2^j}) &= f(\frac{k+\frac{1}{2}i}{2^j}), \qquad k = 2^j - m, \dots, 2^j. \end{aligned}$$

and at the external dyadic points by

$$\begin{aligned} P^L(\frac{n+\frac{1}{2}i}{2^j}) &= \sum_{k=0}^{m} c_{i,k,n} f(\frac{k+\frac{1}{2}i}{2^j}), \qquad n = -M, \dots, -1, \\ P^R(\frac{n+\frac{1}{2}i}{2^j}) &= \sum_{k=2^j-m}^{2^j} d_{i,k,n} f(\frac{k+\frac{1}{2}i}{2^j}), \qquad n = 2^j + 1, \dots, 2^j + M, \end{aligned} \tag{4.5}$$

with

$$\begin{aligned} c_{i,k,n} &= \ell^L_{i,k}(x_{i,n}), \\ d_{i,k,n} &= \ell^R_{i,k}(x_{i,n}), \end{aligned} \tag{4.6}$$

where $\ell^L_{i,k}$ and $\ell^R_{i,k}$ are the *Lagrange polynomials* relative to the interpolation points:

$$\begin{aligned} \ell^L_{i,k}(x) &= \prod_{\substack{s=0 \\ s\neq k}}^{m} \frac{x - x_{i,s}}{x_{i,k} - x_{i,s}}, \qquad k = 0, \dots, m, \\ \ell^R_{i,k}(x) &= \prod_{\substack{s=2^j-m \\ s\neq k}}^{2^j} \frac{x - x_{i,s}}{x_{i,k} - x_{i,s}}, \qquad k = 2^j - m, \dots, 2^j, \end{aligned}$$

with $x_{i,s} = (\frac{s+\frac{1}{2}i}{2^j})$ and $i \in \{0, 1\}$. Using such polynomials will enable us to preserve the interpolation property and same accuracy.
Now we can define $I_j f\,\big|_{[0,1]}$, denoted by $\mathcal{I}_j f$ as following:

$$\begin{aligned} \mathcal{I}_j f(x) = &\sum_{n=-M}^{-1} \sum_{i=0}^{1} P^L(\frac{n+\frac{1}{2}i}{2^j}) \phi_i(2^j x - n) \\ &+ \sum_{k=0}^{2^j} \sum_{i=0}^{1} f(\frac{k+\frac{1}{2}i}{2^j}) \phi_i(2^j x - k) \\ &+ \sum_{n=2^j+1}^{2^j+M} \sum_{i=0}^{1} P^R(\frac{n+\frac{1}{2}i}{2^j}) \phi_i(2^j x - n). \end{aligned} \tag{4.7}$$

By combining equations (4.5) and (4.7), we have

$$\begin{aligned}\mathcal{I}_j f(x) = \sum_{k=0}^{m}\sum_{i=0}^{1} f(\tfrac{k+\frac{1}{2}i}{2^j})\left(\phi_i(2^jx-k)+\sum_{n=-M}^{-1} c_{i,k,n}\phi_i(2^jx-n)\right)\\ +\sum_{k=m+1}^{2^j-m-1}\sum_{i=0}^{1} f(\tfrac{k+\frac{1}{2}i}{2^j})\phi_i(2^jx-k)\\ +\sum_{k=2^j-m}^{2^j}\sum_{i=0}^{1} f(\tfrac{k+\frac{1}{2}i}{2^j})\left(\phi_i(2^jx-k)+\sum_{n=2^j+1}^{2^j+M} d_{i,k,n}\phi_i(2^jx-n)\right).\end{aligned}$$

With this new definition of $I_j f$, we can introduce the *boundary interpolating vectors* $\Phi^L = (\phi_0^L, \phi_1^L)^\top$ and $\Phi^R = (\phi_0^R, \phi_1^R)^\top$ by means of

$$\begin{aligned}\phi_i^L(2^jx-k) &= \phi_i(2^jx-k)+\sum_{n=-M}^{-1} c_{i,k,n}\phi_i(2^jx-n), \qquad k=0,\dots,m,\\ \phi_i^R(2^jx-k) &= \phi_i(2^jx-k)+\sum_{n=2^j+1}^{2^j+M} d_{i,k,n}\phi_i(2^jx-n), \qquad k=2^j-m,\dots,2^j.\end{aligned} \tag{4.8}$$

where $i=0,1$, and for $n=k$, we have $c_{i,k,n}=d_{i,k,n}=1$. Furthermore we set $\phi_{i,j,k}(x) := 2^{\frac{j}{2}}\phi_i(2^jx-k)$ and obtain

$$\begin{aligned}\phi_{i,j,k}^L(x) &= \sum_{n=-M}^{m} c_{i,k,n}\phi_{i,j,n}(x), \qquad k=0,\dots,m, \quad i=0,1,\\ \phi_{i,j,k}^R(x) &= \sum_{n=2^j-m}^{2^j+M} d_{i,k,n}\phi_{i,j,n}(x), \qquad k=2^j-m,\dots,2^j, \quad i=0,1.\end{aligned}$$

Consequently, for $\Phi_{j,k}^L = (\phi_{0,j,k}^L, \phi_{1,j,k}^L)^\top$ and $\Phi_{j,k}^R = (\phi_{0,j,k}^R, \phi_{1,j,k}^R)^\top$, we have the following matrix equations

$$\begin{aligned}\Phi_{j,k}^L(x) &= \sum_{n=-M}^{m} C_{k,n}\Phi_{j,n}(x), \qquad k=0,\dots,m,\\ \Phi_{j,k}^R(x) &= \sum_{n=2^j-m}^{2^j+M} D_{k,n}\Phi_{j,n}(x), \qquad k=2^j-m,\dots,2^j,\end{aligned} \tag{4.9}$$

where $C_{k,n}$ and $D_{k,n}$ are diagonal matrixes with the entries $c_{i,k,n}$ and $d_{i,k,n}$ respectively. In conclusion, with using the scaling vectors inside to interval and polynomials P^L and P^R, we defined boundary vectors on the left and right side of the interval $[0,1]$. But the main point is that these vectors still satisfy the interpolation property, which we will prove in the following.

Lemma 4.1. *Boundary scaling functions ϕ_i^L and ϕ_i^R in (4.8) still verify the interpolation property and for $\ell, k = 0,\dots,2^j$ and $s,i=0,1$, we have*

$$\begin{aligned}\phi_{i,j,k}^L(\tfrac{\ell+\frac{1}{2}s}{2^j}) &= 2^{\frac{j}{2}}\delta_{\ell k}\delta_{si},\\ \phi_{i,j,k}^R(\tfrac{\ell+\frac{1}{2}s}{2^j}) &= 2^{\frac{j}{2}}\delta_{\ell k}\delta_{si}.\end{aligned} \tag{4.10}$$

Proof. For $\ell = k$ and $s = i$ on the left edge functions we have

$$\phi^L_{i,j,k}(\frac{k+\frac{1}{2}i}{2^j}) = 2^{\frac{j}{2}}\phi^L_i(2^j(\frac{k+\frac{1}{2}i}{2^j})-k) = 2^{\frac{j}{2}}\phi_i(2^j(\frac{k+\frac{1}{2}i}{2^j})-k)+2^{\frac{j}{2}}\sum_{n=-M}^{-1} c_{i,k,n}\phi_i(2^j(\frac{k+\frac{1}{2}i}{2^j})-n).$$

Since the scaling functions ϕ_i are interpolating and $k \neq n$, we obtain

$$\phi^L_i(2^j(\frac{k+\frac{1}{2}i}{2^j}) - k) = \phi^L_i(\frac{1}{2}i) = \phi_i(\frac{1}{2}i) + \sum_{n=-M}^{-1} c_{i,k,n}\phi_i(\frac{1}{2}i + k - n) = 1,$$

and therefore we have

$$\phi^L_{i,j,k}(\frac{k+\frac{1}{2}i}{2^j}) = 2^{\frac{j}{2}}.$$

In every other case, we obtain

$$\phi^L_{i,j,k}(\frac{\ell+\frac{1}{2}s}{2^j}) = 0.$$

Analogously, the equality (4.10) can be proved in the same manner for the right edge functions. □

4.2 Refinability of Boundary Scaling Vectors

In this section we intend to construct a multiresolution analysis on the interval. For constructing the spaces V_j on the interval $[0,1]$ and then a multiresolution analysis of $L_2[0,1]$, one has to check the refinability of the boundary scaling vectors. It signifies that the spaces $V_j[0,1]$ have to satisfy:

$$V_j[0,1] \subset V_{j+1}[0,1] \subset L_2[0,1],\ j \in \mathbb{Z}.$$

In the following Theorem, we intend to prove that Φ^L and Φ^R are refinable.

Theorem 4.2. *For $x \in [0,1]$, assume that Φ is a vector of $L_2(\mathbb{R})$-functions and satisfies a matrix refinement equation (3.7). The boundary vectors $\Phi^L_{j,k}$, $k = 0,\dots,m$ and $\Phi^R_{j,k}$, $k = 2^j - m,\dots,2^j$ from (4.9) are refinable and satisfy the equations*

$$\Phi^L_{j,k}(x) = 2^{-\frac{1}{2}}\sum_{\ell=0}^{m} E^L_{k,\ell}\Phi^L_{j+1,\ell}(x) + 2^{-\frac{1}{2}}\sum_{t=m+1}^{M+2m} F^L_{k,t}\Phi_{j+1,t}(x), \tag{4.11}$$

and

$$\Phi^R_{j,k}(x) = 2^{-\frac{1}{2}}\sum_{t=2^{j+1}-M-2m}^{2^{j+1}-m-1} F^R_{k,t}\Phi_{j+1,t}(x) + 2^{-\frac{1}{2}}\sum_{\ell=2^{j+1}-m}^{2^{j+1}} E^R_{k,\ell}\Phi^R_{j+1,\ell}(x) \tag{4.12}$$

where there exist matrices $E^L = (E^L_{k,\ell})$ and $E^R = (E^R_{k,\ell})$ of size $2(m+1) \times 2(m+1)$, $F^L = (F^L_{k,t})$ and $F^R = (F^R_{k,t})$ of size $2(m+1) \times 2(m+M)$.

Proof. We will call $\Phi^L_{j,k}$ refinable if it satisfies the relation (4.11) and for that, we have to find matrices E^L and F^L. First of all, regarding (4.1), for $n \in \mathbb{Z}$ we have

$$\begin{aligned}\Phi(2^j x - n) &= \sum_{t=-M}^{M} A_t \Phi(2(2^j x - n) - t) \\ &= \sum_{t=-M+2n}^{M+2n} A_{t-2n} \Phi(2^{j+1} x - t).\end{aligned} \tag{4.13}$$

Using (4.13), for the left boundary vectors $\Phi^L_{j,k}$, $k = 0, \ldots, m$ and $0 \le x \le 1$, we deduce that

$$\begin{aligned}\Phi^L_{j,k}(x) &= \sum_{n=-M}^{m} C_{k,n} \Phi_{j,n} \\ &= \sum_{n=-M}^{m} C_{k,n} \left[2^{-\frac{1}{2}} \sum_{t=-M+2n}^{M+2n} A_{t-2n} \Phi_{j+1,t}(x) \right] \\ &= 2^{-\frac{1}{2}} \sum_{t=-3M}^{M+2m} \left[\sum_{n=-M}^{m} C_{k,n} A_{t-2n} \right] \Phi_{j+1,t}(x).\end{aligned} \tag{4.14}$$

By regarding the restriction $x \ge 0$ we obtain

$$\Phi^L_{j,k}(x) = 2^{-\frac{1}{2}} \sum_{t=-M}^{M+2m} \left[\sum_{n=-M}^{m} C_{k,n} A_{t-2n} \right] \Phi_{j+1,t}(x). \tag{4.15}$$

If we substitute (4.9) into (4.11), we get

$$\Phi^L_{j,k}(x) = 2^{-\frac{1}{2}} \sum_{\ell=0}^{m} E^L_{k,\ell} \sum_{t=-M}^{m} C_{\ell,t} \Phi_{j+1,t}(x) + 2^{-\frac{1}{2}} \sum_{t=m+1}^{M+2m} F^L_{k,t} \Phi_{j+1,t}(x).$$

Therefore, we have

$$\Phi^L_{j,k}(x) = 2^{-\frac{1}{2}} \sum_{t=-M}^{m} \left(\sum_{\ell=0}^{m} E^L_{k,\ell} C_{\ell,t} \right) \Phi_{j+1,t}(x) + 2^{-\frac{1}{2}} \sum_{t=m+1}^{M+2m} F^L_{k,t} \Phi_{j+1,t}(x). \tag{4.16}$$

Comparing (4.15) and (4.16) we obtain the following identities,

$$\begin{aligned}\sum_{n=-M}^{m} C_{k,n} A_{t-2n} &= \sum_{\ell=0}^{m} E^L_{k,\ell} C_{\ell,t}, \qquad t = -M, \ldots, m, \\ \sum_{n=-M}^{m} C_{k,n} A_{t-2n} &= F^L_{k,t}, \qquad t = m+1, \ldots, M+2m.\end{aligned}$$

If Φ^L is refinable, the coefficients have to be related by

$$\begin{aligned}CV &= E^L C, \\ CW &= F^L,\end{aligned} \tag{4.17}$$

where

$$C = \begin{pmatrix} C_{0,-M} & C_{0,-M+1} & \dots & C_{0,-1} & I & 0 & \dots & 0 \\ C_{1,-M} & C_{1,-M+1} & \dots & C_{1,-1} & 0 & I & \ddots & \vdots \\ \vdots & \vdots & \ddots & \vdots & \vdots & \ddots & \ddots & 0 \\ C_{m,-M} & C_{m,-M+1} & \dots & C_{m,-1} & 0 & \dots & 0 & I \end{pmatrix},$$

is of size $2(m+1)\times 2(m+M+1)$, $E^L = (E^L_{k,0}, \cdots, E^L_{k,m})$ and $F^L = (F^L_{k,m+1}, \cdots, F^L_{k,M+2m})$. Furthermore, $V = (A_{t-2n})_{n,t}$, $n, t = -M, \dots, m$, is of size $2(m+M+1) \times 2(m+M+1)$ and $W = (A_{t-2n})_{n,t}$, $n = -M, \dots, m$, $t = m+1, \dots, M+2m$ is of size $2(m+M+1) \times 2(m+M)$. Now we can find matrices E^L and F^L from (4.17). It is clear that C has linearly independent rows and consequently, $C^\top$ has linearly independent columns. Thus $C^\top$ may be decomposed as $C^\top = QR$, where Q is a matrix with orthonormal columns and R is an upper triangular matrix. Then $C = R^\top Q^\top$ satisfies $CC^\top = I$ and $E^L = CVC^\top$. This completes the proof of refinability for the left boundary vectors $\Phi^L_{j,k}$.

The refinability of the right edge functions $\Phi^R_{j,k}$ are derived in a similar manner. Using (4.9) and (4.13), we find that

$$\begin{aligned} \Phi^R_{j,k}(x) &= \sum_{n=2^j-m}^{2^j+M} D_{k,n}\Phi_{j,n}(x) \\ &= \sum_{n=2^j-m}^{2^j+M} D_{k,n}\left[2^{-\frac{1}{2}} \sum_{t=-M+2n}^{M+2n} A_{t-2n}\Phi_{j+1,t}(x)\right] \\ &= 2^{-\frac{1}{2}} \sum_{t=2^{j+1}-M-2m}^{2^{j+1}+3M} \left[\sum_{n=2^j-m}^{2^j+M} D_{k,n}A_{t-2n}\right] \Phi_{j+1,t}(x). \end{aligned}$$

By taking the restriction $0 \le x \le 1$ into consideration, we obtain

$$\Phi^R_{j,k}(x) = 2^{-\frac{1}{2}} \sum_{t=2^{j+1}-M-2m}^{2^{j+1}+M} \left[\sum_{n=2^j-m}^{2^j+M} D_{k,n}A_{t-2n}\right] \Phi_{j+1,t}(x). \tag{4.18}$$

If we substitute (4.9) into (4.12), we get

$$\begin{aligned} \Phi^R_{j,k}(x) = 2^{-\frac{1}{2}} &\sum_{t=2^{j+1}-M-2m}^{2^{j+1}-m-1} F^R_{k,t}\Phi_{j+1,t}(x) \\ &+ 2^{-\frac{1}{2}} \sum_{\ell=2^{j+1}-m}^{2^{j+1}} E^R_{k,\ell} \sum_{t=2^{j+1}-m}^{2^{j+1}+M} D_{\ell,t}\Phi_{j+1,t}(x). \end{aligned}$$

Then we have

$$\begin{aligned} \Phi^R_{j,k}(x) = 2^{-\frac{1}{2}} &\sum_{t=2^{j+1}-M-2m}^{2^{j+1}-m-1} F^R_{k,t}\Phi_{j+1,t}(x) \\ &+ 2^{-\frac{1}{2}} \sum_{t=2^{j+1}-m}^{2^{j+1}+M} \left(\sum_{\ell=2^{j+1}-m}^{2^{j+1}} E^R_{k,\ell}D_{\ell,t}\right) \Phi_{j+1,t}(x). \end{aligned} \tag{4.19}$$

By comparing (4.18) and (4.19), we obtain the following identities

$$\sum_{n=2^j-m}^{2^j+M} D_{k,n}A_{t-2n} = F^R_{k,t} \qquad t = 2^{j+1}-M-2m,\dots,2^{j+1}-m-1,$$

$$\sum_{n=2^j-m}^{2^j+M} D_{k,n}A_{t-2n} = \sum_{\ell=2^{j+1}-m}^{2^{j+1}} E^R_{k,\ell}D_{\ell,t} \qquad t = 2^{j+1}-m,\dots,2^{j+1}+M.$$

In the same way as the left edge functions we can find matrices E^R and F^R. Consequently, the scaling vectors on the right are refinable as well. □

Now we can construct our space $V_j[0,1]$ as $V_j[0,1] = \text{span}\left\{\Phi^{[\,]}_{j,k}\right\}$ where

$$\Phi^{[\,]}_{j,k}(x) = \begin{cases} \Phi^L_{j,k}(x), & \text{if } \ 0 \le k \le m, \\ \Phi_{j,k}(x)|_{[0,1]}, & \text{if } \ m+1 \le k \le 2^j-m-1, \\ \Phi^R_{j,k}(x), & \text{if } \ 2^j-m \le k \le 2^j. \end{cases} \tag{4.20}$$

The refinability of interior scaling vectors $\Phi_{j,k}(x)$ is clear and since Φ^L and Φ^R are refinable as well, we can write $\Phi^{[\,]}_{j,k}$ as

$$\Phi^{[\,]}_{jk}(x) = 2^{-\frac{1}{2}}\sum_{t=0}^{2^{j+1}} A^{[\,]}_{k,t}\Phi^{[\,]}_{j+1,t}(x), \tag{4.21}$$

where

$$A^{[\,]}_{k,t} = \begin{cases} E^L_{k,t}, F^L_{k,t}, & \text{if } \ 0 \le k \le m, \\ A_{k,t}, & \text{if } \ m+1 \le k \le 2^j-m-1, \\ F^R_{k,t}, E^R_{k,t}, & \text{if } \ 2^j-m \le k \le 2^j. \end{cases} \tag{4.22}$$

Therefore we have $V_j[0,1] \subset V_{j+1}[0,1]$.

4.3 Error Estimate of Interpolation Operator

In Section 4.1, we defined the interpolation operator $\mathcal{I}_j f$ to construct the boundary vectors. The main goal of this section is to investigate that this operator gives us an approximation of f with the same approximation order as we had on the line. That is, we will show that the operator $\mathcal{I}_j$ verifies the *error estimate* in $L_2[0,1]$. Moreover, we want to indicate that the boundary vectors can be able to reproduce polynomials.

As we mentioned, the approximation properties of a scaling vector are closely related to its ability to reproduce polynomials. Furthermore, we have seen that interior scaling vectors have approximation order m and satisfy (4.3). For the left edge and $x \ge 0$, we have

$$\begin{aligned} x^n|_{[0,+\infty)} &= \sum_{t=-M}^{\infty}\sum_{i=0}^{1}(t+\frac{1}{2}i)^n\phi_i(x-t) \\ &= \sum_{t=-M}^{m}\sum_{i=0}^{1}(t+\frac{1}{2}i)^n\phi_i(x-t) + \sum_{t=m+1}^{\infty}\sum_{i=0}^{1}(t+\frac{1}{2}i)^n\phi_i(x-t), \end{aligned} \tag{4.23}$$

where $|n| < m$. On the other hand, the left boundary vectors can reproduce polynomials of degree m, if they satisfy

$$x^n|_{[0,+\infty)} = \sum_{k=0}^{m}\sum_{i=0}^{1} \upsilon_{i,k}\phi_i^L(x-k) + \sum_{k=m+1}^{\infty}\sum_{i=0}^{1}(k+\frac{1}{2}i)^n\phi_i(x-k),$$

for some unknowns $\upsilon_{i,k}$. Using the definition of $\phi_i^L(x-k)$ in (4.8) for $j=0$, we get

$$\begin{aligned} x^n|_{[0,+\infty)} &= \sum_{k=0}^{m}\sum_{i=0}^{1} \upsilon_{i,k}\left[\phi_i(x-k) + \sum_{t=-M}^{-1} c_{i,k,t}\phi_i(x-t)\right] + \sum_{k=m+1}^{\infty}\sum_{i=0}^{1}(k+\frac{1}{2}i)^n\phi_i(x-k) \\ &= \sum_{k=0}^{m}\sum_{i=0}^{1} \upsilon_{i,k}\phi_i(x-k) + \sum_{t=-M}^{-1}\sum_{k=0}^{m} \upsilon_{i,k}c_{i,k,t}\phi_i(x-t) + \sum_{k=m+1}^{\infty}\sum_{i=0}^{1}(k+\frac{1}{2}i)^n\phi_i(x-k), \end{aligned}$$

or

$$x^n|_{[0,+\infty)} = \sum_{t=-M}^{-1}\sum_{k=0}^{m} \upsilon_{i,k}c_{i,k,t}\phi_i(x-t) + \sum_{t=0}^{m}\sum_{i=0}^{1} \upsilon_{i,t}\phi_i(x-t) + \sum_{t=m+1}^{\infty}\sum_{i=0}^{1}(t+\frac{1}{2}i)^n\phi_i(x-t). \tag{4.24}$$

Now with comparing (4.23) and (4.24), we obtain

$$\begin{aligned} \sum_{k=0}^{m} \upsilon_{i,k}c_{i,k,t} &= (t+\frac{1}{2}i)^n, \quad t=-M,\dots,-1, \\ \upsilon_{i,t} &= (t+\frac{1}{2}i)^n, \quad t=0,\dots,m, \end{aligned} \tag{4.25}$$

where $i = 0, 1$. Therefore, $\upsilon_{i,k}$ can be computed from the second equation in (4.25). Moreover, substituting this equation into the first equation, we get

$$\sum_{k=0}^{m}(k+\frac{1}{2}i)^n c_{i,k,t} = (t+\frac{1}{2}i)^n, \quad t=-M,\dots,-1.$$

Regarding the definition of $c_{i,k,n}$ as the Lagrange polynomials and interpolation theorem in [49], this is satisfied.

For the boundary vectors on the right side, this can be proven in the same way.

Now, we want to give an estimate of the interpolation error on the interval. Before that, we have to prove the error estimate of interpolation operator $I_j f$ in L_∞ and $L_2(\mathbb{R})$.

Theorem 4.3. *Suppose that $\Phi = (\phi_0, \phi_1)^\top$ is a compactly supported interpolating 2-scaling vector and provides approximation order m. Fix m and suppose that $\lambda \in \mathbb{R}$ and $\lambda > m+1$. For $f \in H^{m+\frac{1}{2}}$ and $I_j f$ in (4.4), there is a constant C such that*

$$\|f - I_j f\|_{L_\infty} \le C 2^{-mj} \|f\|_{H^{m+\frac{1}{2}}}.$$

Proof. For $S(\Phi)$ in (3.13), suppose $p \in S(\Phi)$. By (4.4), we obtain

$$p(x) = \sum_{k\in\mathbb{Z}}\sum_{i=0}^{1} p(\frac{k+\frac{1}{2}i}{2^j})\phi_i(2^j x - k).$$

Hence for polynomials $p \in \pi_m(\mathbb{R})$, $m \in \mathbb{Z}$ we have $I_j p = p$. Since that Φ provides approximation order m, it holds that $x^\alpha \in S(\Phi)$ for $|\alpha| < m$ and we have

$$\frac{x^\alpha}{\alpha!} = \sum_{k\in\mathbb{Z}} \sum_{i=0}^{1} \frac{1}{\alpha!} (\frac{k+\frac{1}{2}i}{2^j})^\alpha \phi_i(2^j x - k).$$

For more details refer to [44]. Now fix an $x \in \mathbb{R}$ and let p be the Taylor polynomial of degree $m-1$ for f at x. If r is the remainder in Taylor's Theorem, then $f = p + r$ and

$$r(y) = \sum_{|\alpha|=m} (D^\alpha f)(\xi_{\alpha y}) \frac{(y-x)^\alpha}{\alpha!}, \quad x, y, \xi \in \mathbb{R}.$$

Hence,

$$\begin{aligned}
\|(f - I_j f)(x)\|_{L_\infty} &= \|p(x) - I_j f(x)\|_{L_\infty} \\
&= \|I_j p(x) - I_j f(x)\|_{L_\infty} \\
&= \|I_j r(x)\|_{L_\infty} \\
&= \left\| \sum_{k\in\mathbb{Z}} \sum_{i=0}^{1} r(\frac{k+\frac{1}{2}i}{2^j}) \phi_i(2^j x - k) \right\|_{L_\infty} \\
&= \left\| \sum_{k\in\mathbb{Z}} \langle \Phi(2^j x - k), R_j(k) \rangle \right\|_{L_\infty},
\end{aligned}$$

where $\langle \cdot, \cdot \rangle$ is the standard scalar product and $R_j(k) = (r(\frac{k}{2^j}), r(\frac{k+\frac{1}{2}}{2^j}))^\top$.
Now let $V_\alpha(x) = (\frac{x^\alpha}{\alpha!}, \frac{(x-\frac{1}{2})^\alpha}{\alpha!})^\top$. Using the Cauchy–Schwarz inequality it holds that

$$\begin{aligned}
\sum_{k\in\mathbb{Z}} \langle \Phi(2^j x - k), R_j(k) \rangle &\le \sum_{k\in\mathbb{Z}} \left\| \Phi(2^j x - k) \right\|_2 \|R_j(k)\|_2 \\
&\le \sum_{k\in\mathbb{Z}} \left\| \Phi(2^j x - k) \right\|_2 \sqrt{r^2(\frac{k}{2^j}) + r^2(\frac{k+\frac{1}{2}}{2^j})} \\
&= \sum_{k\in\mathbb{Z}} \left\| \Phi(2^j x - k) \right\|_2 \sqrt{\left[\sum_{|\alpha|=m} (D^\alpha f)(\xi_{\alpha \frac{k}{2^j}}) \frac{(\frac{k}{2^j} - x)^\alpha}{\alpha!} \right]^2 + \left[\sum_{|\alpha|=m} (D^\alpha f)(\xi_{\alpha \frac{k+\frac{1}{2}}{2^j}}) \frac{(\frac{k+\frac{1}{2}}{2^j} - x)^\alpha}{\alpha!} \right]^2} \\
&\le \sum_{k\in\mathbb{Z}} \left\| \Phi(2^j x - k) \right\|_2 \left(\max_{|\alpha|\le m} \|D^\alpha f\|_{L_\infty} \right) \left(2^{-mj} \sum_{|\alpha|=m} \left\| V_\alpha(2^j x - k) \right\|_2 \right) \\
&= 2^{-mj} \|f\|_{W_\infty^m} \sum_{|\alpha|=m} \sum_{k\in\mathbb{Z}} \left\| \Phi(2^j x - k) \right\|_2 \left\| V_\alpha(2^j x - k) \right\|_2.
\end{aligned}$$

Considering that Φ has compact support, we assume that

$$M = \sup_{x\in\mathbb{R}} \|\Phi(x)\|_2 \|V_\alpha(x)\|_2 (1 + |x|)^\lambda e^{|x|} < \infty.$$

Now we set $y = 2^j x$ and get

$$\begin{aligned}
\sum_{k\in\mathbb{Z}} \|\Phi(y-k)\|_2 \|V_\alpha(y-k)\|_2 &\le \sum_{k\in\mathbb{Z}} M(1+|y-k|)^{-\lambda} e^{-|k-y|} \\
&\le \sum_{|k|\neq 0,1} M(1+|y-k|)^{-\lambda} e^{|y|} e^{-|k|} \\
&\le e^{|y|} \sum_{|k|\neq 0,1} \frac{Me^{-|k|}|k|^{2\lambda}}{(|k|^2+|y-k|)^\lambda} \\
&\le e^{|y|} \sum_{|k|\neq 0,1} \frac{Me^{-|k|}|k|^{2\lambda}}{(|k|^2+|y|-|k|)^\lambda} \\
&\le e^{|y|} \sum_{|k|\neq 0,1} \frac{Me^{-|k|}|k|^{2\lambda}}{(1+|y|)^\lambda} \\
&\le \frac{Me^{|y|}}{(1+|y|)^\lambda} \sum_{|k|\neq 0,1} |k|^{2\lambda} e^{-|k|}.
\end{aligned}$$

Since the last summation is convergent, we obtain

$$\sum_{k\in\mathbb{Z}} \|\Phi(y-k)\|_2 \|V_\alpha(y-k)\|_2 \le C_1 \frac{Me^{|y|}}{(1+|y|)^\lambda} < \infty,$$

for $C_1 > 0$. Thus

$$\sum_{|\alpha|=m} \sum_{k\in\mathbb{Z}} \|\Phi(y-k)\|_2 \|V_\alpha(y-k)\|_2 \le C,$$

for $C > 0$. Therefore we obtain

$$\|f - I_j f\|_{L_\infty} \le C 2^{-mj} \|f\|_{W_\infty^m}.$$

Finally the desired result follows from the embedding theorem 2.12 as

$$\|f\|_{W_\infty^m} \le C \|f\|_{H^{m+\frac{1}{2}}}.$$

□

Now it is enough to compute the error estimate in $L_2(\mathbb{R})$.

Theorem 4.4. *Suppose that $\Phi = (\phi_0, \phi_1)^\top$ is a compactly supported interpolating and biorthogonal 2-scaling vector and provides approximation order m. For $f \in H^m$ and $I_j f$ in (4.4), there is a constant C such that*

$$\|f - I_j f\|_{L_2} \le C 2^{-jm} \|f\|_{H^m}.$$

Proof. Suppose that $P_j f : L_2(\mathbb{R}) \to V_j$ is the biorthogonal projection where

$$P_j f(x) = \sum_{k\in\mathbb{Z}} \sum_{i=0}^{1} \langle f, \widetilde{\phi}_{i,j,k} \rangle \phi_{i,j,k}(x).$$

First we prove that $P_j f$ is uniformly bounded. With the substitution $2^j x = y$, $dx = 2^{-j} dy$, we have

$$\begin{aligned}\langle f, \widetilde{\phi}_{i,j,k} \rangle &= \int_{\mathbb{R}} f(x) 2^{\frac{j}{2}} \widetilde{\phi}_i(2^j x - k) dx \\ &= 2^{\frac{-j}{2}} \int_{\mathbb{R}} f(2^{-j} y) \widetilde{\phi}_i(y - k) dy,\end{aligned}$$

and therefore for $C_1 > 0$:

$$\begin{aligned}\|P_j f(x)\|_{L_2}^2 &= \left\| \sum_{k\in\mathbb{Z}} \sum_{i=0}^{1} \langle f, \widetilde{\phi}_{i,j,k} \rangle \phi_{i,j,k}(x) \right\|_{L_2}^2 \\ &= \left\| \sum_{k\in\mathbb{Z}} \sum_{i=0}^{1} 2^{\frac{-j}{2}} \langle f(2^{-j}\cdot), \widetilde{\phi}_i(\cdot - k) \rangle 2^{\frac{j}{2}} \phi_i(2^j x - k) \right\|_{L_2}^2 \\ &= \left\| \sum_{k\in\mathbb{Z}} \sum_{i=0}^{1} \langle f(2^{-j}\cdot), \widetilde{\phi}_i(\cdot - k) \rangle 2^{-j} \phi_i(\cdot - k) \right\|_{L_2}^2 \\ &= \left\| 2^{-j} P_0(f(2^{-j}\cdot)) \right\|_{L_2}^2 \\ &\leq \|P_0\|_{L_2}^2 \left\| 2^{-j} f(2^{-j}\cdot) \right\|_{L_2}^2 \\ &= \|P_0\|_{L_2}^2 \|f\|_{L_2}^2 \\ &\leq C_1 \|f\|_{L_2}^2 .\end{aligned}$$

Beside that, we have

$$\begin{aligned}\|f - I_j f\|_{L_2} &= \|f - P_j f + P_j f - I_j f\|_{L_2} \\ &\leq \|f - P_j f\|_{L_2} + \|P_j f - I_j f\|_{L_2} .\end{aligned}$$

By (3.23), we obtain for $g \in V_j$ and $C_2, C_3 > 0$:

$$\begin{aligned}\|f - P_j f\|_{L_2} &= \|f - g + g - P_j f\|_{L_2} \\ &\leq \|f - g\|_{L_2} + \|P_j g - P_j f\|_{L_2} \\ &\leq \|f - g\|_{L_2} + \|P_j\|_{L_2} \|g - f\|_{L_2} \\ &\leq (1 + \|P_j\|_{L_2}) \|f - g\|_{L_2} \\ &\leq (1 + C_2) \inf_{g\in V_j} \|f - g\|_{L_2} \\ &\leq C_3 2^{-jm} \|f\|_{H^m} .\end{aligned}$$

Now we need to find an upper bound $\|P_j f - I_j f\|_{L_2}$. Let us assume that $\chi_{I_{j,k}}$ is the characteristic function of $I_{j,k} = \operatorname{supp} \widetilde{\phi}_{i,j,k}$. It was shown in [44] that for a compactly supported interpolating scaling vector Φ we have

$$\sum_{k\in\mathbb{Z}} \sum_{i=0}^{1} \phi_i(x - k) = 1.$$

Since Φ reproduces all polynomials of degree less than m, the following holds for $f \in S(\Phi)$,

$$f(x) = \sum_{k\in\mathbb{Z}} \sum_{i=0}^{1} f(k + \frac{1}{2}i)\phi_i(x-k).$$

Then we get

$$\begin{aligned}
\int \widetilde{\phi}_0(x)dx &= \int 1\ \widetilde{\phi}_0(x)dx \\
&= \int (\sum_{k\in\mathbb{Z}} \sum_{i=0}^{1} \phi_i(x-k))\widetilde{\phi}_0(x)dx \\
&= \sum_{k\in\mathbb{Z}} \Big[\langle \phi_0(x-k), \widetilde{\phi}_0(x)\rangle + \langle \phi_1(x-k), \widetilde{\phi}_0(x)\rangle\Big] \\
&= 1.
\end{aligned}$$

Analogously, we can show that $\int \widetilde{\phi}_1(x)dx = 1$. Now with the substitution $2^j x - k = y$, $dx = 2^{-j}dy$ we have

$$\begin{aligned}
\langle f(\frac{k+\frac{1}{2}i}{2^j})\chi_{I_{j,k}}, \widetilde{\phi}_{i,j,k}\rangle &= \int_{I_{j,k}} f(\frac{k+\frac{1}{2}i}{2^j})\widetilde{\phi}_{i,j,k}(x)dx \\
&= \int_{I_{j,k}} f(\frac{k+\frac{1}{2}i}{2^j})2^{\frac{j}{2}}\widetilde{\phi}_i(2^j x - k)dx \\
&= \int_{I_{0,0}} f(\frac{k+\frac{1}{2}i}{2^j})2^{\frac{-j}{2}}\widetilde{\phi}_i(y)dy \\
&= 2^{\frac{-j}{2}} f(\frac{k+\frac{1}{2}i}{2^j}).
\end{aligned}$$

Therefore

$$2^{\frac{j}{2}}\langle f(\frac{k+\frac{1}{2}i}{2^j})\chi_{I_{j,k}}, \widetilde{\phi}_{i,j,k}\rangle = f(\frac{k+\frac{1}{2}i}{2^j}).$$

Since

$$I_j f(x) = 2^{\frac{-j}{2}} \sum_{k\in\mathbb{Z}} \sum_{i=0}^{1} f(\frac{k+\frac{1}{2}i}{2^j})\phi_{i,j,k}(x),$$

we obtain

$$\begin{aligned}
&\|P_j f(x) - I_j f(x)\|_{L_2}^2 \\
&= \left\| \sum_{k\in\mathbb{Z}} \sum_{i=0}^{1} \langle f, \widetilde{\phi}_{i,j,k}\rangle \phi_{j,k}^i(x) - 2^{\frac{-j}{2}} \sum_{k\in\mathbb{Z}} \sum_{i=0}^{1} f(\frac{k+\frac{1}{2}i}{2^j})\phi_{i,j,k}(x) \right\|_{L_2}^2 \\
&= \left\| \sum_{k\in\mathbb{Z}} \sum_{i=0}^{1} \left(\langle f, \widetilde{\phi}_{i,j,k}\rangle \phi_{i,j,k}(x) - \langle f(\frac{k+\frac{1}{2}i}{2^j})\chi_{I_{j,k}}, \widetilde{\phi}_{i,j,k}\rangle \phi_{i,j,k}(x) \right) \right\|_{L_2}^2 \\
&= \left\| \sum_{k\in\mathbb{Z}} \sum_{i=0}^{1} \langle f - f(\frac{k+\frac{1}{2}i}{2^j})\chi_{I_{j,k}}, \widetilde{\phi}_{i,j,k}\rangle \phi_{i,j,k}(x) \right\|_{L_2}^2 .
\end{aligned}$$

The stability of the scaling vectors implies that

$$\|P_j f - I_j f\|_{L_2}^2 \leq C_4 \sum_{k\in\mathbb{Z}} \sum_{i=0}^{1} \left| \langle f - f(\frac{k+\frac{1}{2}i}{2^j})\chi_{I_{j,k}}, \widetilde{\phi}_{i,j,k} \rangle \right|^2,$$

where $C_4 > 0$. If we consider $\alpha_{ki} = \left| \langle f - f(\frac{k+\frac{1}{2}i}{2^j})\chi_{I_{j,k}}, \widetilde{\phi}_{i,j,k} \rangle \right|$, then

$$\begin{aligned}\alpha_{ki} &= \left| \int_{I_{j,k}} (f - f(\frac{k+\frac{1}{2}i}{2^j}))\widetilde{\phi}_{i,j,k}(x)dx \right| \\ &\leq \int_{I_{j,k}} \left| f - f(\frac{k+\frac{1}{2}i}{2^j}) \right| \left| \widetilde{\phi}_{i,j,k}(x) \right| dx.\end{aligned}$$

By the mean value theorem, we get

$$\begin{aligned}\left| f(x) - f(\frac{k+\frac{1}{2}i}{2^j}) \right| &= |f'(\xi)||x - \frac{k+\frac{1}{2}i}{2^j}| \\ &\leq \|f\|_{w_\infty^1} 2^{-j}.\end{aligned}$$

Consequently for $\widetilde{C} > 0$:

$$\begin{aligned}\alpha_{ki} &\leq \|f\|_{w_\infty^1} 2^{-j} 2^{-\frac{j}{2}} \int_{I_{0,0}} |\widetilde{\phi}_i(x)|dx \\ &\leq \widetilde{C} \|f\|_{w_\infty^1} 2^{-j} 2^{-\frac{j}{2}}.\end{aligned}$$

Therefore we obtain

$$\|P_j f - I_j f\|_{L_2}^2 \leq C_4 \widetilde{C}^2 \|f\|_{w_\infty^1}^2 \left(\sum_{k\in\mathbb{Z}} \sum_{i=0}^{1} 2^{-3j} \right).$$

Now it is clear that on the unbounded domain the last sum is not finite. However, for our purpose it should be enough to assume that $\mathrm{supp} f$ is compact, i.e., for $A > 0$, $\mathrm{supp} f \subseteq [-A, A]$. Then

$$\begin{aligned}\|P_j f - I_j f\|_{L_2}^2 &\leq C^2 \|f\|_{w_\infty^1}^2 \left(2^j 2^{-3j}\right) \\ &\leq C^2 \|f\|_{w_\infty^1}^2 2^{-2j},\end{aligned}$$

and consequently using the embedding theorem 2.12, we have

$$\begin{aligned}\|P_j f - I_j f\|_{L_2} &\leq C 2^{-j} \|f\|_{w_\infty^1} \\ &\leq C 2^{-j} \|f\|_{H^{\frac{3}{2}}}.\end{aligned}$$

where $C > 0$. □

Finally, we prove the following error estimate for the operator $\mathcal{I}_j f$ on the interval $[0,1]$.

Lemma 4.5. *The operator $\mathcal{I}_j f$ in (4.7) for function $f \in H^s[0,1]$, $s > \frac{1}{2}$ satisfies the following error estimate:*

$$\|f - \mathcal{I}_j f\|_{L_2[0,1]} \leq C 2^{-sj} \|f\|_{H^s[0,1]}.$$

Proof. It was shown in [27] that for any continuously differentiable f, there is a continuous linear extension $E : H^s[0,1] \to H^s(\mathbb{R})$, $s > \frac{1}{2}$ verifying

$$Ef|_{[0,1]} = \begin{cases} f(x) & \text{if } \ x \geq 0, \\ 3f(-x) - 2f(-2x) & \text{if } \ x < 0. \end{cases}$$

With using this extension, we have

$$\|f - \mathcal{I}_j f\|_{L_2[0,1]} \leq \|f - I_j Ef\|_{L_2[0,1]} + \|I_j Ef - \mathcal{I}_j f\|_{L_2[0,1]}.$$

We remark that

$$\begin{aligned} \|f - I_j Ef\|_{L_2[0,1]} &= \|Ef - I_j Ef\|_{L_2[0,1]} \\ &\leq C2^{-sj} \|Ef\|_{H^s(\mathbb{R})} \\ &\leq C2^{-sj} \|f\|_{H^s[0,1]}. \end{aligned}$$

where the last inequality obtains from Proposition 6.10. in [27].

Next, we want to find an upper bound for $\|I_j Ef - \mathcal{I}_j f\|_{L_2[0,1]}$. Using the definitions of $I_j f$ and $\mathcal{I}_j f$, we have

$$\begin{aligned} &\|I_j Ef - \mathcal{I}_j f\|_{L_2[0,1]} \\ &= \|2^{-\frac{j}{2}} \left(\sum_{\ell=-M}^{-1} + \sum_{\ell=0}^{m} + \sum_{\ell=m+1}^{2^j-m-1} + \sum_{\ell=2^j-m}^{2^j} + \sum_{\ell=2^j+1}^{2^j+M} \right) \sum_{i=0}^{1} Ef(\frac{\ell+\frac{1}{2}i}{2^j})\phi_{i,j,\ell} \\ &\quad - 2^{-\frac{j}{2}} \sum_{i=0}^{1} (\sum_{\ell=-M}^{-1} \sum_{k=0}^{m} f(\frac{k+\frac{1}{2}i}{2^j}) c_{i,k,\ell} \phi_{i,j,\ell} + \sum_{\ell=0}^{m} f(\frac{\ell+\frac{1}{2}i}{2^j})\phi_{i,j,\ell} \\ &\quad + \sum_{\ell=m+1}^{2^j-m-1} f(\frac{\ell+\frac{1}{2}i}{2^j})\phi_{i,j,\ell} + \sum_{\ell=2^j-m}^{2^j} f(\frac{\ell+\frac{1}{2}i}{2^j})\phi_{i,j,\ell} \\ &\quad + \sum_{\ell=2^j+1}^{2^j+M} \sum_{k=2^j-m}^{2^j} f(\frac{k+\frac{1}{2}i}{2^j}) d_{i,k,\ell}\phi_{i,j,\ell}) \|_{L_2[0,1]} \\ &= \|2^{-\frac{j}{2}} \sum_{\ell=-M}^{-1} \sum_{i=0}^{1} \left(Ef(\frac{\ell+\frac{1}{2}i}{2^j}) - \sum_{k=0}^{m} f(\frac{k+\frac{1}{2}i}{2^j}) c_{i,k,\ell} \right) \phi_{i,j,\ell} \\ &\quad + 2^{-\frac{j}{2}} \sum_{\ell=2^j+1}^{2^j+M} \sum_{i=0}^{1} \left(Ef(\frac{\ell+\frac{1}{2}i}{2^j}) - \sum_{k=2^j-m}^{2^j} f(\frac{k+\frac{1}{2}i}{2^j}) d_{i,k,\ell} \right) \phi_{i,j,\ell} \|_{L_2[0,1]}. \end{aligned}$$

Let us find an upper bound for the first sum. Since the scaling vectors ϕ^i are L_2-stable, for constant $0 < B < \infty$, we have

$$\begin{aligned} &\left\| 2^{-\frac{j}{2}} \sum_{\ell=-M}^{-1} \sum_{i=0}^{1} \left(Ef(\frac{\ell+\frac{1}{2}i}{2^j}) - \sum_{k=0}^{m} f(\frac{k+\frac{1}{2}i}{2^j}) c_{i,k,\ell} \right) \phi_{i,j,\ell} \right\|_{L_2[0,1]} \\ &\leq 2^{-\frac{j}{2}} B \sqrt{ \sum_{\ell=-M}^{-1} \sum_{i=0}^{1} \left| Ef(\frac{\ell+\frac{1}{2}i}{2^j}) - \sum_{k=0}^{m} f(\frac{k+\frac{1}{2}i}{2^j}) c_{i,k,\ell} \right|^2 }. \end{aligned}$$

By (4.5), we know that

$$P^L(x_{i,j,\ell}) = \sum_{k=0}^{m} c_{i,k,\ell} f(x_{i,j,k}),$$

as $c_{i,k,\ell}$, $\ell = -M, \dots, -1$ is defined in (4.6) and $x_{i,j,k} = (\frac{k+\frac{1}{2}i}{2^j})$. Beside that the Lagrange polynomial approximation theorem tells us

$$f(x) = P^L(x) + R(x),$$

where $R(x)$ is the error term of the form hC with constant $C > 0$ and $h = (x_{i,j,\ell} - x_{i,j,0})(x_{i,j,\ell} - x_{i,j,1}) \dots (x_{i,j,\ell} - x_{i,j,m})$. By the embedding of $H^{\frac{3}{2}+\epsilon}[0,1]$ in $W^{1,\infty}$ we deduce

$$\begin{aligned}
&\left| Ef(\frac{\ell+\frac{1}{2}i}{2^j}) - \sum_{k=0}^{m} f(\frac{k+\frac{1}{2}i}{2^j}) c_{i,k,\ell} \right| \\
&= |3f(-x_{i,j,\ell}) - 2f(-2x_{i,j,\ell}) - f(x_{i,j,\ell}) + R(x_{i,j,\ell})| \\
&= |3f(-x_{i,j,\ell}) - 3f(-2x_{i,j,\ell}) + f(-2x_{i,j,\ell}) - f(x_{i,j,\ell}) + R(x_{i,j,\ell})| \\
&\leq |f'(\xi_1)|| - x_{i,j,\ell}| + 3|f'(\xi_2)|| - 3x_{i,j,\ell}| + |R(x_{i,j,\ell})| \\
&\leq |f|_{1,\infty,\mathbb{R}} |x_{i,j,\ell}| + 3|f|_{1,\infty,\mathbb{R}} |3x_{i,j,\ell}| + |hC| \\
&\leq C 2^{-j} |f|_{H^{\frac{3}{2}+\epsilon}[0,1]}.
\end{aligned}$$

This implies

$$\begin{aligned}
&\left\| 2^{-\frac{j}{2}} \sum_{\ell=-M}^{-1} \sum_{i=0}^{1} \left(Ef(\frac{\ell+\frac{1}{2}i}{2^j}) - \sum_{k=0}^{m} f(\frac{k+\frac{1}{2}i}{2^j}) c_{i,k,\ell} \right) \phi_{i,j,\ell} \right\|_{L_2[0,1]} \\
&\leq 2^{-\frac{3}{2}j} |f|_{H^{\frac{3}{2}+\epsilon}[0,1]}.
\end{aligned}$$

With bounding the second sum in the same way, we obtain

$$\|I_j Ef - \mathcal{I}_j f\|_{L_2[0,1]} \leq C 2^{-\frac{3}{2}j} |f|_{H^{\frac{3}{2}+\epsilon}[0,1]}$$

□

4.4 Examples

In this section we present some examples of our results for interpolating boundary vectors on the interval. For our purpose, we use the scaling vectors from [44], which are interpolating and orthonormal. Especially we are interested in those solutions which possess the highest regularity.

Example 4.6. First, we consider the interpolating and orthonormal scaling vectors in Example 3.16, which are supported on the interval $[-1,2]$ and possess the approximation order 1. We compute the masks A_k from the symbols $\mathbf{A}(z)$ in (3.26) as

$$\begin{aligned}
A_{-1} &= \begin{pmatrix} 0 & 0.2208 \\ 0 & 0.0514 \end{pmatrix}, \quad A_0 = \begin{pmatrix} 1 & 0.9486 \\ 0 & 0.2208 \end{pmatrix}, \\
A_1 &= \begin{pmatrix} 0 & -0.2208 \\ 1 & 0.9486 \end{pmatrix}, \quad A_2 = \begin{pmatrix} 0 & 0.0514 \\ 0 & -0.2208 \end{pmatrix}.
\end{aligned}$$

Using (4.1) and (4.9), we can obtain the scaling vector $\Phi(x)$ and then the corresponding left scaling vector $\Phi^L = (\phi_0^L, \phi_1^L)^\top$. Figure 4.1 shows the left scaling functions ϕ_0^L and ϕ_1^L.

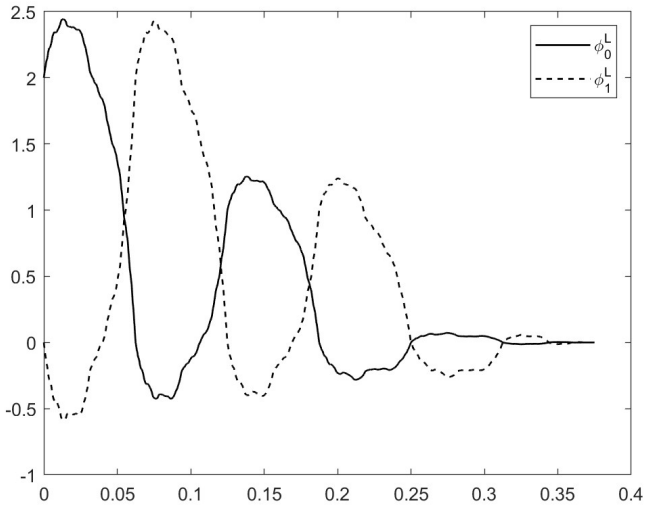

Figure 4.1: Interpolating left scaling vector on the interval $[0, 1]$

Also similar to the left edge, we can plot the scaling vector for the right side. Figure 4.2 shows the right scaling vector $\Phi^R = (\phi_0^R, \phi_1^R)^\top$.

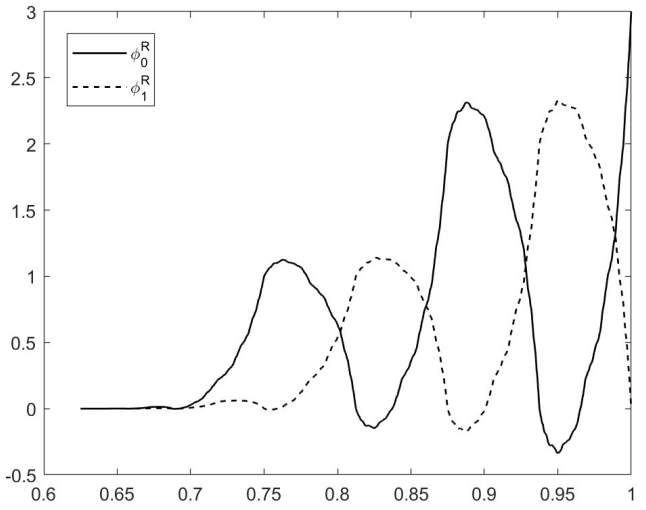

Figure 4.2: Interpolating right scaling vector on the interval $[0, 1]$

Example 4.7. In this example, we use the interpolating scaling vectors in Example 3.17, which are supported on the interval $[-2, 3]$ and have the approximation order 2. Again

we compute the symbols A_k from $\mathbf{A}(z)$ as

$$A_{-2} = \begin{pmatrix} 0 & 0.0313 \\ 0 & 0.0040 \end{pmatrix}, \quad A_{-1} = \begin{pmatrix} 0 & 0.2460 \\ 0 & 0.0313 \end{pmatrix}, \quad A_0 = \begin{pmatrix} 1 & 0.9375 \\ 0 & 0.2421 \end{pmatrix},$$
$$A_1 = \begin{pmatrix} 0 & -0.2421 \\ 1 & 0.9375 \end{pmatrix}, \quad A_2 = \begin{pmatrix} 0 & 0.0313 \\ 0 & -0.2460 \end{pmatrix}, \quad A_3 = \begin{pmatrix} 0 & -0.0040 \\ 0 & 0.0313 \end{pmatrix}.$$

Using these symbols and computing the coefficients $c_{i,k,n}$ in (4.5), we can plot the boundary scaling functions. Figures 4.3 and 4.4 shows respectively the scaling vectors Φ^L on the left and Φ^R on the right.

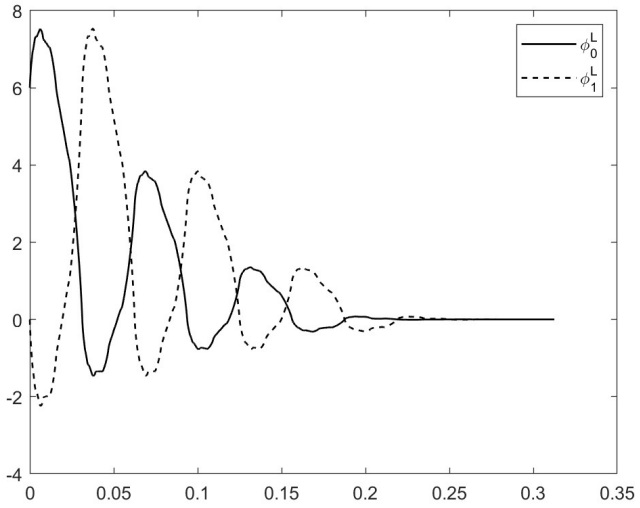

Figure 4.3: Interpolating left scaling vector on the interval $[0,1]$

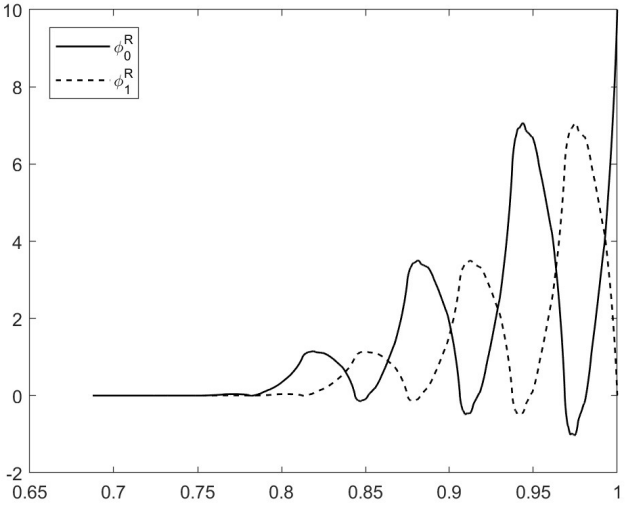

Figure 4.4: Interpolating right scaling vector on the interval $[0,1]$

4.5 Construction of multiwavelets on the interval

In this section, we intend to construct the multiwavelets corresponding to the interpolating scaling vectors on the interval. So far such constructions have been introduced for wavelets like those in [21, 28]. Compared to the classical wavelets on the interval, our construction will possess more flexibility for the practical purposes. In Section 4.1, we introduced an MRA on the interval, which can be utilized for computing the boundary multiwavelets.

First of all, we define $Q_j^{[0,1]} = \mathcal{I}_{j+1}^{[0,1]} - \mathcal{I}_j^{[0,1]}$ and set $W_j[0,1] = \text{Range}(Q_j^{[0,1]})$. We now seek an accessible representation for the elements of $W_j[0,1]$. We know that

$$W_j[0,1] = (\mathcal{I}_{j+1} - \mathcal{I}_j)(V_{j+1})_{[0,1]}.$$

On the other hand

$$\begin{aligned} V_{j+1}[0,1] &= \mathcal{I}_{j+1}(V_{j+1})_{[0,1]} \\ &= (\mathcal{I}_{j+1} - \mathcal{I}_j)(V_{j+1})_{[0,1]} + \mathcal{I}_j(V_{j+1})_{[0,1]} \\ &= W_j[0,1] + V_j[0,1]. \end{aligned}$$

Using this interpretation, we can construct the multiwavelets on the interval. Similar to the multiwavelets on the line, we have to show that there is a representation of multiwavelets on the interval in terms of the scaling vector in the larger scale. We define $\Psi_{j,k}^{[\,]}(x) = (\psi_{0,j,k}^{[\,]}(x), \psi_{1,j,k}^{[\,]}(x))^\top$ and it can be written as

$$\Psi_{j,k}^{[\,]}(x) = (\mathcal{I}_{j+1} - \mathcal{I}_j)\Phi_{j+1,k}^{[\,]}(x)$$

First of all, we start with the construction on the left edge. For $i = 0, 1$ and $k = 0, \cdots, m$ we can write:

$$\begin{aligned} \psi_{i,j,k}^L(x) &= (\mathcal{I}_{j+1} - \mathcal{I}_j)\phi_{i,j+1,k}^L(x) \\ &= \phi_{i,j+1,k}^L(x) - \left(\sum_{\ell=0}^{m} \sum_{s=0}^{1} \phi_{i,j+1,k}^L(\frac{\ell + \frac{1}{2}s}{2^j}) \phi_{s,j,\ell}^L(x) \right). \end{aligned} \tag{4.26}$$

If we define the 2×2 matrix $B_{j+1,k,\ell}^L$ as

$$B_{j+1,k,\ell}^L = \begin{pmatrix} \phi_{0,j+1,k}^L(\frac{\ell}{2^j}) & \phi_{0,j+1,k}^L(\frac{\ell+\frac{1}{2}}{2^j}) \\ \phi_{1,j+1,k}^L(\frac{\ell}{2^j}) & \phi_{1,j+1,k}^L(\frac{\ell+\frac{1}{2}}{2^j}) \end{pmatrix},$$

and use the refinability relation (4.11), then for $\Psi_{j,k}^L(x) = (\psi_{0,j,k}^L(x), \psi_{1,j,k}^L(x))^T$, we have

$$\begin{aligned} \Psi_{j,k}^L(x) &= \Phi_{j+1,k}^L(x) - 2^{-\frac{1}{2}} \sum_{\ell=0}^{m} B_{j+1,k,\ell}^L \left(\sum_{t=0}^{m} E_{\ell,t}^L \Phi_{j+1,t}^L(x) + \sum_{t=m+1}^{M+2m} F_{\ell,t}^L \Phi_{j+1,t}(x) \right) \\ &= \Phi_{j+1,k}^L(x) - 2^{-\frac{1}{2}} \sum_{t=0}^{m} \sum_{\ell=0}^{m} B_{j+1,k,\ell}^L E_{\ell,t}^L \Phi_{j+1,t}^L(x) \\ &- 2^{-\frac{1}{2}} \sum_{t=m+1}^{M+2m} \sum_{\ell=0}^{m} B_{j+1,k,\ell}^L F_{\ell,t}^L \Phi_{j+1,t}(x). \end{aligned} \tag{4.27}$$

The equation (4.27) describes left multiwavelets on the interval in terms of the left scaling vectors on the interval plus the interior scaling vector. Furthermore we can construct the right boundary multiwavelets from their corresponding boundary scaling vectors as

$$\begin{aligned}\psi^R_{i,j,k}(x) &= (\mathcal{I}_{j+1} - \mathcal{I}_j)\phi^R_{i,j+1,k}(x) \\ &= \phi^R_{i,j+1,k}(x) - \left(\sum_{\ell=2^j-m}^{2^j} \sum_{s=0}^{1} \phi^R_{i,j+1,k}(\frac{\ell + \frac{1}{2}s}{2^j}) \phi^R_{s,j,\ell}(x) \right). \end{aligned} \tag{4.28}$$

Using the refinability relation (4.12), for $\Psi^R_{j,k}(x) = (\psi^R_{0,j,k}(x), \psi^R_{1,j,k}(x))^T$, we obtain

$$\begin{aligned}\Psi^R_{j,k}(x) &= \Phi^R_{j+1,k}(x) - 2^{-\frac{1}{2}} \sum_{\ell=2^j-m}^{2^j} B^R_{j+1,k,\ell} \left(\sum_{t=2^{j+1}-M-2m}^{2^{j+1}-m-1} F^R_{\ell,t} \Phi_{j+1,t}(x) + \sum_{t=2^{j+1}-m}^{2^{j+1}} E^R_{\ell,t} \Phi^R_{j+1,t}(x) \right) \\ &= \Phi^R_{j+1,k}(x) - 2^{-\frac{1}{2}} \sum_{t=2^{j+1}-M-2m}^{2^{j+1}-m-1} \sum_{\ell=2^j-m}^{2^j} B^R_{j+1,k,\ell} F^R_{\ell,t} \Phi_{j+1,t}(x) \\ &- 2^{-\frac{1}{2}} \sum_{t=2^{j+1}-m}^{2^{j+1}} \sum_{\ell=2^j-m}^{2^j} B^R_{j+1,k,\ell} E^R_{\ell,t} \Phi^R_{j+1,t}(x),\end{aligned}$$

where

$$B^R_{j+1,k,\ell} = \begin{pmatrix} \phi^R_{0,j+1,k}(\frac{\ell}{2^j}) & \phi^R_{0,j+1,k}(\frac{\ell+\frac{1}{2}}{2^j}) \\ \phi^R_{1,j+1,k}(\frac{\ell}{2^j}) & \phi^R_{1,j+1,k}(\frac{\ell+\frac{1}{2}}{2^j}) \end{pmatrix}.$$

Now we define the multiwavelets on the interval as follows:

$$\Psi^{[\,]}_{j,k}(x) := \begin{cases} \Psi^L_{j,k}(x), & if \;\; 0 \le k \le m, \\ \Psi_{j,k}(x)|_{[0,1]}, & if \;\; m+1 \le k \le 2^j - m - 1, \\ \Psi^R_{j,k}(x), & if \;\; 2^j - m \le k \le 2^j, \end{cases}$$

where $\Psi_{j,k}(x)|_{[0,1]}$ are the interior scaling vectors from [42].

The following Lemma is a result from the above discussion.

Lemma 4.8. *A function f in $V_{j+1}[0,1]$, $j \in \mathbb{Z}$, has got the representation*

$$f(x) = 2^{-\frac{j}{2}} \sum_{k=0}^{2^j} \sum_{i=0}^{1} c_{i,j,k} \phi^{[\,]}_{i,j,k}(x) + 2^{-\frac{j}{2}} \sum_{k=0}^{2^j} \sum_{i=0}^{1} d_{i,j,k} \psi^{[\,]}_{i,j,k}(x),$$

where

$$c_{i,j,k} = \sum_{\ell=0}^{2^j} \sum_{s=0}^{1} f(\frac{\ell + \frac{1}{2}s}{2^j}) \phi^{[\,]}_{s,j+1,\ell}(\frac{k + \frac{1}{2}i}{2^j}),$$

$$d_{i,j,k} = f(\frac{k + \frac{1}{2}i}{2^j}).$$

Furthermore, the first sum is in the space $V_j[0,1]$ and the second one in the space $W_j[0,1]$.

Proof. Every $f \in V_{j+1}[0,1]$ can be written as

$$f(x) = \mathcal{I}_{j+1}f(x) = (\mathcal{I}_{j+1} - \mathcal{I}_j + \mathcal{I}_j)f(x) = (\mathcal{I}_{j+1} - \mathcal{I}_j)f(x) + \mathcal{I}_j f(x),$$

and since $(\mathcal{I}_{j+1} - \mathcal{I}_j)f(x) \in W_j[0,1]$, we have:

$$\begin{aligned}
f(x) &= 2^{-\frac{j}{2}} \sum_{k=0}^{2^j} \sum_{i=0}^{1} f(\frac{k+\frac{1}{2}i}{2^j})(\mathcal{I}_{j+1} - \mathcal{I}_j)(\phi^{[\,]}_{i,j+1,k}(x)) \\
&+ 2^{-\frac{j}{2}} \sum_{\ell=0}^{2^j} \sum_{s=0}^{1} f(\frac{\ell+\frac{1}{2}s}{2^j})\mathcal{I}_j(\phi^{[\,]}_{s,j+1,\ell}(x)) \\
&= 2^{-\frac{j}{2}} \sum_{k=0}^{2^j} \sum_{i=0}^{1} f(\frac{k+\frac{1}{2}i}{2^j})\psi^{[\,]}_{i,j,k}(x) \\
&+ 2^{-\frac{j}{2}} \sum_{\ell=0}^{2^j} \sum_{s=0}^{1} f(\frac{\ell+\frac{1}{2}s}{2^j}) \left(\sum_{k=0}^{2^j} \sum_{i=0}^{1} \phi^{[\,]}_{s,j+1,\ell}(\frac{k+\frac{1}{2}i}{2^j})\phi^{[\,]}_{i,j,k}(x) \right) \\
&= 2^{-\frac{j}{2}} \sum_{k=0}^{2^j} \sum_{i=0}^{1} f(\frac{k+\frac{1}{2}i}{2^j})\psi^{[\,]}_{i,j,k}(x) \\
&+ 2^{-\frac{j}{2}} \sum_{k=0}^{2^j} \sum_{\ell=0}^{2^j} \sum_{i,s=0}^{1} f(\frac{\ell+\frac{1}{2}s}{2^j})\phi^{[\,]}_{s,j+1,\ell}(\frac{k+\frac{1}{2}i}{2^j})\phi^{[\,]}_{i,j,k}(x).
\end{aligned}$$

□

Finally, we will present some examples of left and right multiwavelets on the interval. To plot the boundary multiwavelets, we used the relations (4.26) and (4.28). Figures 4.5 and 4.6 present the left and right boundary multiwavelets corresponding to the left and right scaling vectors in Example 4.6.

Moreover, the boundary multiwavelets corresponding to the boundary scaling vectors in Example 4.7 are shown in Figures 4.7 and 4.8.

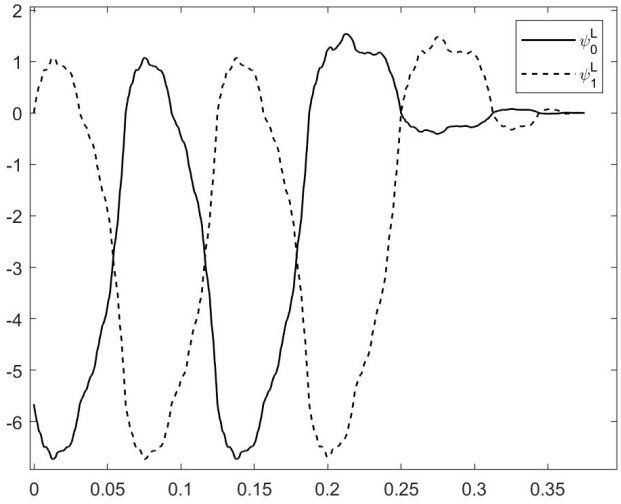

Figure 4.5: Left multiwavelet on the interval $[0, 1]$

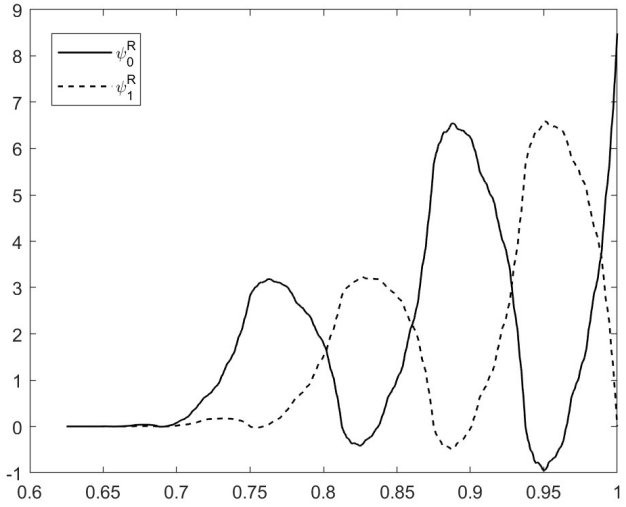

Figure 4.6: Right multiwavelet on the interval $[0, 1]$

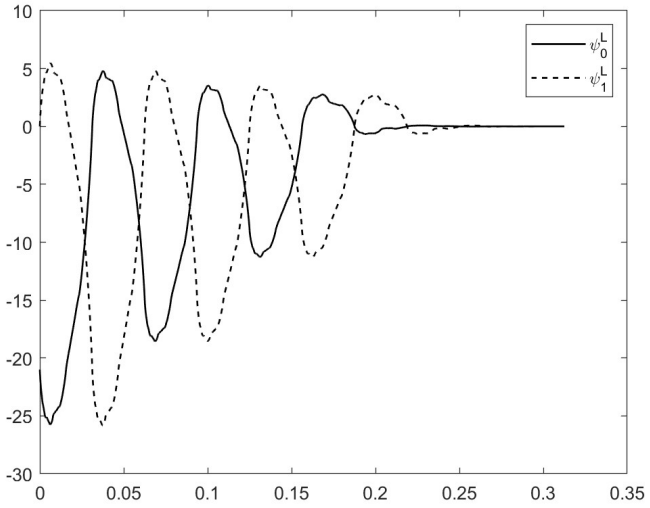

Figure 4.7: Left multiwavelet on the interval $[0, 1]$

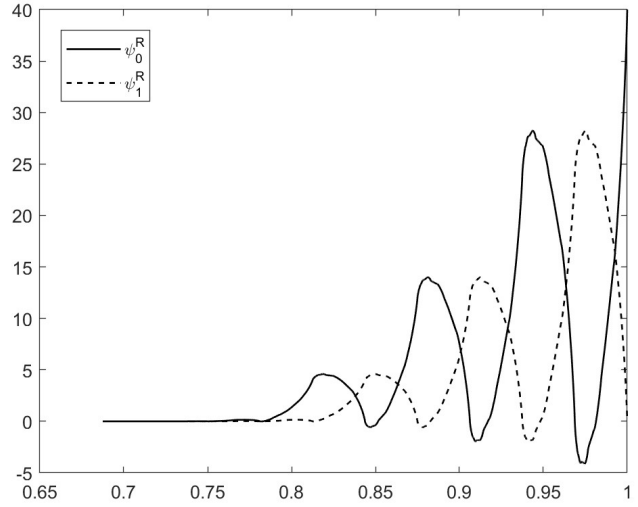

Figure 4.8: Right multiwavelet on the interval $[0, 1]$

Chapter 5

Orthogonal Scaling Vectors and Multiwavelets on the Interval

This chapter is concerned with the construction of the orthogonal boundary vectors and multiwavelets on the interval $[0, 1]$. So far such constructions have been studied for the univariate wavelets, see [18,21,58]. The orthogonal wavelets are very useful in some applications such as signal/image processing and numerical solutions of differential equations. However some properties such as orthogonality, compact support, symmetry and high order of vanishing moments are necessary in many applications and a scalar wavelet can not posses all of them simultaneously. To bypass these problems, we will utilize again the orthogonal construction from Karsten Koch, cf. [44], on the real line and adapt it to the interval. In Chapter 4, we have constructed new families of interpolating scaling vectors and multiwavelets on the interval but unfortunately they can not be orthogonal on the interval. Madych in [50] constructed a finite orthogonal transform based on the multiresolution analysis of Mallat and Meyer in [52,54] for the scalar wavelets. Moreover, Keinert in [2] and [3] has modified it for the multiwavelets. Here, we will utilize this approach to construct the orthogonal boundary vectors and multiwavelets based on the orthogonal multiresolution analysis in [44], which have desirable properties. First of all, we investigate the conditions for construction of orthogonal boundary scaling vectors. Particularity, we focus on the refinability and orthogonality conditions. Then in Section 5.2 we construct the Discrete Multiwavelet Transform on the Interval. In Section 5.3 we discuss about the polynomials reproduction and approximation order of scaling functions. Afterwards, we explain an algorithm for constructing boundary scaling vectors which are orthogonal. In the end, we construct the orthogonal multiwavelets and present some examples.

5.1 Definitions and Conditions

In this section, we will determine the necessary and sufficient conditions to construct an orthogonal multiresolution analysis. We suppose that the boundary scaling functions are linear combinations of the scaling functions on the line that cross the boundaries. First of all, we provide the following basic assumptions concerning the scaling functions on the line, which were constructed by Karsten Koch in [44].

- Let $\Phi = (\phi_0, \phi_1)^\top$ be the interpolating 2-scaling vector of $L_2(\mathbb{R})$-functions such that it satisfies a matrix refinement equation (3.7) and is supported on $[-N, N+1]$ for

$N \in \mathbb{N}$. Thus, we can write (3.7) as

$$\Phi(x) = \sum_{k=-N}^{N+1} A_k \Phi(2x-k). \tag{5.1}$$

Moreover, the scaling vector Φ is orthogonal and provides approximation order $m \geq 1$.

- Let $\Psi = (\psi_0, \psi_1)^\top$ be the 2-multiwavelet corresponding to the scaling vector Φ with the same support and the masks $B_{-N}, \ldots, B_{N+1}$ for $N \in \mathbb{N}$. Therefore we have

$$\Psi(x) = \sum_{k=-N}^{N+1} B_k \Phi(2x-k). \tag{5.2}$$

Now we intend to show the following for the boundary vectors:

- There exists a left boundary scaling vector $\Phi^L = (\phi_0^L, \phi_1^L, \ldots, \phi_{l-1}^L)^\top,\ l > 0$, and also a right boundary scaling vector $\Phi^R = (\phi_0^R, \phi_1^R, \ldots, \phi_{r-1}^R)^\top,\ r > 0$, which both of left and right boundary functions are linear combinations of scaling functions that cross the boundaries. The construction of boundary vectors in this way has the benefit that the boundary functions automatically inherit continuity. In addition, we suppose that the number of boundary functions is the same at both edges but it is not necessarily a multiple of 2.
- The left and right boundary functions are refinable, orthogonal, continuous, and provide approximation order≥ 1. Therefore they are regular which is very important for application purposes.

To construct the orthogonal left boundary vector on the interval $[0,1]$, we need that the masks A_k start with zero. Therefore we shift the scaling vector and corresponding multiwavelet in order to be supported on $[0, M]$. Hence, (5.1) turns into

$$\Phi(x) = \sum_{k=0}^{M} A_k \Phi(2x-k). \tag{5.3}$$

If the left boundary functions are linear combinations of boundary-crossing functions, then for $x \geq 0$, we define

$$\Phi^L(x) = \sum_{k=-M+1}^{-1} C_k \Phi(x-k), \tag{5.4}$$

where C_k is a matrix of size $l \times 2$. Consequently, for $0 \leq x \leq 1$, one can define

$$\Phi_j^L(x) = \sum_{k=-M+1}^{-1} C_k \Phi_{j,k}(x), \tag{5.5}$$

with j large enough for non-interacting the boundaries on the left and right side. Here $\Phi_j^L(x) := 2^{\frac{j}{2}} \Phi^L(2^j x)$ and $\Phi_{j,k}(x) := 2^{\frac{j}{2}} \Phi(2^j x - k)$.

For the right boundary vector we are working on the interval $[-M, 0]$. Thus, without loss of generality, we construct the right boundary functions for $x \leq 0$ and then shift them to be in the interval $[-M+1, 1]$. Therefore for $x \leq 0$ we have

$$\Phi(x) = \sum_{k=-M}^{0} A_k \Phi(2x-k), \tag{5.6}$$

and similar to the left side, we define

$$\Phi^R(x) = \sum_{k=1}^{M-1} D_k \Phi(x-k). \tag{5.7}$$

Here D_k is a matrix of size $r \times 2$. Now for $-1 \leq x \leq 0$ we have

$$\Phi_j^R(x) = \sum_{k=1}^{M-1} D_k \Phi_{j,k}(x), \tag{5.8}$$

where $\Phi_j^R(x) = 2^{j/2}\Phi^R(2^j x)$. Hence, the construction of orthogonal boundary vectors reduces to find the matrices C_k and D_k.

5.1.1 Refinement Equation on the Interval

As we have seen in Chapter 3, the scaling vectors on the line satisfy the refinement equation (3.7). The boundary vectors Φ^L and Φ^R are refinable if they satisfy

$$\begin{aligned} \Phi_j^L(x) &= 2^{-\frac{1}{2}} E \Phi_{j+1}^L(x) + 2^{-\frac{1}{2}} \sum_{t=0}^{M-2} F_t \Phi_{j+1,t}(x), \qquad x \geq 0, \\ \Phi_j^R(x) &= 2^{-\frac{1}{2}} \sum_{t=-M+2}^{0} \widetilde{F}_t \Phi_{j+1,t}(x) + 2^{-\frac{1}{2}} \widetilde{E} \Phi_{j+1}^R(x), \quad x \leq 0, \end{aligned} \tag{5.9}$$

where $E = \langle \Phi_j^L, \Phi_{j+1}^L \rangle$, $F_t = \langle \Phi_j^L, \Phi_{j+1,t} \rangle$, $\widetilde{E} = \langle \Phi_j^R, \Phi_{j+1}^R \rangle$ and $\widetilde{F}_t = \langle \Phi_j^R, \Phi_{j+1,t} \rangle$. The matrices E and $\widetilde{E}$ are of size $l \times l$ and $r \times r$ respectively. F_t is a $l \times 2$ matrix and $\widetilde{F}_t$ is a $r \times 2$ matrix. Our aim is to find the matrices E, $\widetilde{E}$, F_t and $\widetilde{F}_t$ such that the equations (5.9) are possible.
We will call Φ^L, Φ^R *refinable*, if they satisfy the equations (5.9). Using the definition of the left scaling vector $\Phi_j^L(x)$ and (5.3), we see that

$$\begin{aligned} \Phi_j^L(x) &= \sum_{k=-M+1}^{-1} C_k \Phi_{j,k}(x) \\ &= \sum_{k=-M+1}^{-1} C_k \left[2^{-\frac{1}{2}} \sum_{t=2k}^{M+2k} A_{t-2k} \Phi_{j+1,t}(x) \right] \\ &= 2^{-\frac{1}{2}} \sum_{t=-M+1}^{M-2} \left[\sum_{k=-M+1}^{-1} C_k A_{t-2k} \right] \Phi_{j+1,t}(x), \end{aligned} \tag{5.10}$$

where the lower limit in the last t-summation is obtained by taking the restriction $x \geq 0$ into consideration. If we substitute (5.5) into (5.9) for the left boundary vector, we get

$$\Phi_j^L(x) = 2^{-\frac{1}{2}} E \sum_{t=-M+1}^{-1} C_t \Phi_{j+1,t}(x) + 2^{-\frac{1}{2}} \sum_{t=0}^{M-2} F_t \Phi_{j+1,t}(x). \tag{5.11}$$

By comparing (5.10) and (5.11), we obtain the following equations:

$$\sum_{k=-M+1}^{-1} C_k A_{t-2k} = E C_t, \qquad t = -M+1, \ldots, -1,$$
$$\sum_{k=-M+1}^{-1} C_k A_{t-2k} = F_t, \qquad t = 0, \ldots, M-2.$$

If $\Phi^L(x)$ is a refinable vector, the coefficients have to satisfy

$$\begin{aligned} CV &= EC, \\ CW &= F, \end{aligned} \tag{5.12}$$

where $C = (C_{-M+1}, C_{-M+2}, \cdots, C_{-1})$, $F = (F_0, \cdots, F_{M-2})$, $V = (A_{t-2k})_{k,t}$, $k, t = -M+1, \ldots, -1$ and $W = (A_{t-2k})_{k,t}$ for $k = -M+1, \ldots, -1$, $t = 0, \ldots, M-2$. Moreover, both of matrices V and W are of size $2(M-1) \times 2(M-1)$. The equation $CV = EC$ is a type of eigenvalue problem and plays an important role for constructing the left boundary vector. In Section 5.4.1, we will describe an algorithm to find the matrices C, E and F using (5.12).

For the right boundary vector we proceed analogously. By (5.6), we have

$$\begin{aligned} \Phi_j^R(x) &= \sum_{k=1}^{M-1} D_k \Phi_{j,k}(x) \\ &= \sum_{k=1}^{M-1} D_k \left[2^{-\frac{1}{2}} \sum_{t=-M+2k}^{2k} A_{t-2k} \Phi_{j+1,t}(x) \right] \\ &= 2^{-\frac{1}{2}} \sum_{t=-M+2}^{M-1} \left[\sum_{k=1}^{M-1} D_k A_{t-2k} \right] \Phi_{j+1,t}(x), \end{aligned} \tag{5.13}$$

for $x \leq 0$. By substituting (5.8) into (5.9) for the right boundary vectors, we get

$$\Phi_j^R(x) = 2^{-\frac{1}{2}} \sum_{t=-M+2}^{0} \widetilde{F}_t \Phi_{j+1,t}(x) + 2^{-\frac{1}{2}} \widetilde{E} \sum_{t=1}^{M-1} D_t \Phi_{j+1,t}(x). \tag{5.14}$$

By comparing (5.13) and (5.14), we obtain the following identities:

$$\sum_{k=1}^{M-1} D_k A_{t-2k} = \widetilde{F}_t, \qquad t = -M+2, \ldots, 0,$$
$$\sum_{k=1}^{M-1} D_k A_{t-2k} = \widetilde{E} D_t, \qquad t = 1, \ldots, M-1.$$

Therefore for the refinability of $\Phi^R(x)$, the coefficients have to satisfy

$$\begin{aligned} D\widetilde{W} &= \widetilde{F}, \\ D\widetilde{V} &= \widetilde{E}D, \end{aligned} \tag{5.15}$$

where $D = (D_1, D_2, \cdots, D_{M-1})$, $\widetilde{F} = (\widetilde{F}_{-M+2}, \cdots, \widetilde{F}_0)$, $\widetilde{V} = (A_{t-2k})_{k,t}$, $k, t = 1, \ldots, M-1$ and $\widetilde{W} = (A_{t-2k})_{k,t}$ for $k = 1, \ldots, M-1$, $t = -M+2, \ldots, 0$. Furthermore, the matrices $\widetilde{V}$ and $\widetilde{W}$ are of size $2(M-1) \times 2(M-1)$. In the similar manner to the left boundaries, we can calculate the matrices D, $\widetilde{E}$ and $\widetilde{F}$ from solving the eigenvalue problem in (5.15).

5.1.2 Orthogonality Conditions for Boundary Scaling Vectors

The central aim of this chapter is to construct the boundary vectors which are orthogonal. As we have already seen in Subsection 3.2.2, the orthogonal scaling vectors on the real line have to satisfy the condition (3.16). For the left boundary scaling functions we have almost the same conditions:

$$\begin{aligned} &\langle \phi_\rho^L, \phi_\mu^L \rangle = \delta_{\rho,\mu}, \quad 0 \le \rho, \mu \le l-1, \\ &\langle \phi_\rho^L, \phi_\mu(\cdot - k) \rangle = 0, \quad 0 \le \rho \le l-1,\ 0 \le \mu \le 1,\ k \ge 0, \\ &\langle \phi_\rho^L, \psi_\mu(\cdot - k) \rangle = 0, \quad 0 \le \rho \le l-1,\ 0 \le \mu \le 1,\ k \ge 0, \end{aligned}$$

or simply the following vector form:

$$\begin{aligned} &\langle \Phi^L(x), \Phi^L(x) \rangle = I_l, \\ &\langle \Phi^L(x), \Phi(x-k) \rangle = 0, \quad k \ge 0, \\ &\langle \Phi^L(x), \Psi(x-k) \rangle = 0, \quad k \ge 0. \end{aligned} \tag{5.16}$$

Now we want to find a more applicable version of conditions (5.16). The first relation of (5.16) and the equation (5.9) for $j = 0$ lead to

$$\begin{aligned} I_l &= \langle \Phi^L(x), \Phi^L(x) \rangle \\ &= \langle E\Phi^L(2x) + \sum_{t=0}^{M-2} F_t \Phi(2x-t), E\Phi^L(2x) + \sum_{t=0}^{M-2} F_t \Phi(2x-t) \rangle \\ &= EE^\top \langle \Phi^L(2x), \Phi^L(2x) \rangle + \sum_{t=0}^{M-2} F_t F_t^\top \langle \Phi(2x-t), \Phi(2x-t) \rangle \\ &= \frac{1}{2} EE^\top + \frac{1}{2} \sum_{t=0}^{M-2} F_t F_t^\top = \frac{1}{2}(EE^\top + FF^\top). \end{aligned}$$

Therefore, the first condition in (5.16) reduces to

$$\frac{1}{2}(EE^\top + FF^\top) = I_l. \tag{5.17}$$

Moreover, using the second condition in (5.16), the equations (5.9) and (5.3) we obtain

$$\begin{aligned}
&\langle \Phi^L(x), \Phi(x-k)\rangle \\
&= \langle E\Phi^L(2x) + \sum_{t=0}^{M-2} F_t \Phi(2x-t), \sum_{t=2k}^{M+2k} A_{t-2k}\Phi(2x-t)\rangle \\
&= \sum_{t=0}^{M-2} F_t A_{t-2k}^\top,
\end{aligned}$$

where $k \geq 0$. Hence, we have

$$\sum_{t=0}^{M-2} F_t A_{t-2k}^\top = 0, \qquad k \geq 0. \tag{5.18}$$

In the same manner, from third condition we obtain

$$\sum_{t=0}^{M-2} F_t B_{t-2k}^\top = 0, \qquad k \geq 0. \tag{5.19}$$

Similarly orthogonality for the right boundary functions means

$$\begin{aligned}
&\langle \Phi^R(x), \Phi^R(x)\rangle = I_r, \\
&\langle \Phi^R(x), \Phi(x-k)\rangle = 0, \qquad k \geq 0, \\
&\langle \Phi^R(x), \Psi(x-k)\rangle = 0, \qquad k \geq 0.
\end{aligned} \tag{5.20}$$

In the same way as the left side, the conditions (5.20) transform to

$$\frac{1}{2}(\widetilde{E}\widetilde{E}^\top + \widetilde{F}\widetilde{F}^\top) = I_r, \tag{5.21}$$

$$\begin{aligned}
\sum_{t=-M+2}^{0} \widetilde{F}_t A_{t-2k}^\top = 0, \qquad k \geq 0, \\
\sum_{t=-M+2}^{0} \widetilde{F}_t B_{t-2k}^\top = 0, \qquad k \geq 0.
\end{aligned} \tag{5.22}$$

Since the boundary functions are linear combinations of boundary-crossing functions, they are orthogonal to all interior functions. Therefore the conditions (5.18), (5.19) and (5.22) are automatically satisfied. The conditions (5.17)and (5.21) are the main conditions that are used to find the suitable matrices E, $\widetilde{E}$, F and $\widetilde{F}$. Moreover, using the cascade algorithm, we can prove the sufficiency of these conditions. The cascade algorithm for the left boundary vector is given by

$$\Phi^{L(n)}(x) = E\Phi^{L(n-1)}(2x) + \sum_{t=0}^{M-2} F_t \Phi(2x-t). \tag{5.23}$$

The idea is that we start with an orthogonal initial vector $\Phi^{L(0)}$ and then we have

$$\begin{aligned}
&\langle \Phi^{L(1)}(x), \Phi^{L(1)}(x)\rangle \\
&= \langle E\Phi^{L(0)}(2x) + \sum_{t=0}^{M-2} F_t\Phi(2x-t), E\Phi^{L(0)}(2x) + \sum_{t=0}^{M-2} F_t\Phi(2x-t)\rangle \\
&= EE^\top \langle \Phi^{L(0)}(2x), \Phi^{L(0)}(2x)\rangle + \sum_{t=0}^{M-2} F_tF_t^\top \langle \Phi(2x-t), \Phi(2x-t)\rangle \\
&= \frac{1}{2}EE^\top + \frac{1}{2}\sum_{t=0}^{M-2} F_tF_t^\top = \frac{1}{2}(EE^\top + FF^\top) = I_l.
\end{aligned}$$

Therefore, the condition (5.17) ensures that each $\Phi^{L(n)}$ will be orthogonal. If the iteration converges, the limit will also be orthogonal. This will be shown in Section 5.3.

5.2 Discrete Multiwavelet Transform on the Interval

In Subsection 3.2.4, we have already seen that the Discrete Multiwavelet Transform leads to an orthogonal decomposition in terms of scaling vectors Φ and multiwavelets Ψ. Consequently, we obtained the decomposition matrix in (3.21) which is infinite and orthogonal. In this section, we want to modify the DMWT and decomposition matrix on the interval. Moreover, we compute the number of boundary scaling vectors at the endpoints.

To define the DMWT on the interval, we need the boundary multiwavelets denoted by $\Psi^L = (\psi_0^L, \psi_1^L, \ldots, \psi_{l-1}^L)^\top,\ l > 0$, and $\Psi^R = (\psi_0^R, \psi_1^R, \ldots, \psi_{r-1}^R)^\top,\ r > 0$, which have to satisfy the recursion equations

$$\begin{aligned}
\Psi_j^L(x) &= 2^{-\frac{1}{2}} G\Phi_{j+1}^L(x) + 2^{-\frac{1}{2}} \sum_{t=0}^{M-2} H_t\Phi_{j+1,t}(x), \quad x \geq 0, \\
\Psi_j^R(x) &= 2^{-\frac{1}{2}} \sum_{t=-M+2}^{0} \widetilde{H}_t\Phi_{j+1,t}(x) + 2^{-\frac{1}{2}} \widetilde{G}\Phi_{j+1}^R(x), \quad x \leq 0,
\end{aligned} \tag{5.24}$$

where $G = \langle \Psi_j^L, \Phi_{j+1}^L\rangle$, $H_t = \langle \Psi_j^L, \Phi_{j+1,t}\rangle$, $\widetilde{G} = \langle \Psi_j^R, \Phi_{j+1}^R\rangle$ and $\widetilde{H}_t = \langle \Psi_j^R, \Phi_{j+1,t}\rangle$. Matrices G and $\widetilde{G}$ are of size $l \times l$ and $r \times r$ respectively. H_t is of size $l \times 2$ and $\widetilde{H}_t$ is of size $r \times 2$.

For adapting the infinite matrix in (3.21), we need some modifications at the endpoint. From the results in [2, 3, 50], we define the finite decomposition matrix as

$$\mathcal{S}_M = \begin{pmatrix}
X_0 & X_1 & \ldots & X_k & 0 & \ldots & \ldots & 0 & 0 \\
0 & S_0 & S_1 & \ldots & S_k & 0 & \ldots & 0 & 0 \\
\vdots & 0 & S_0 & S_1 & \ddots & S_k & 0 & \vdots & \vdots \\
\vdots & \vdots & \ddots & \ddots & \ddots & \ddots & \ddots & \vdots & \vdots \\
0 & 0 & \ldots & 0 & S_0 & S_1 & \ldots & S_k & 0 \\
0 & 0 & \ldots & \ldots & 0 & Y_0 & Y_1 & \ldots & Y_k
\end{pmatrix}, \tag{5.25}$$

where S_k is defined as in (3.20) and the matrices X_k and Y_k, $k = \left\lceil \frac{M-1}{2} \right\rceil$, are unknown boundary matrices.

Now suppose that we only have two block matrices S_0 and S_1 as

$$S_0 = \begin{pmatrix} A_0 & A_1 \\ B_0 & B_1 \end{pmatrix}, \quad S_1 = \begin{pmatrix} A_2 & A_3 \\ B_2 & B_3 \end{pmatrix}. \tag{5.26}$$

Here we assume that M is odd. Otherwise, we can introduce extra masks $A_M = 0$ and $B_M = 0$ to form the block matrices S_k. Consequently, the matrix in (5.25) can be written as

$$\mathcal{S}_3 = \begin{pmatrix} X_0 & X_1 & 0 & 0 \\ 0 & S_0 & S_1 & 0 \\ 0 & 0 & Y_0 & Y_1 \end{pmatrix}, \tag{5.27}$$

and similar to the matrices S_0 and S_1, we define

$$X_0 = \begin{pmatrix} E \\ G \end{pmatrix}, \quad X_1 = \begin{pmatrix} F \\ H \end{pmatrix},$$

for the left side and

$$Y_0 = \begin{pmatrix} \widetilde{F} \\ \widetilde{H} \end{pmatrix}, \quad Y_1 = \begin{pmatrix} \widetilde{E} \\ \widetilde{G} \end{pmatrix},$$

for the right side. Since the infinite matrix S in (3.21) is orthogonal, their coefficients satisfy

$$\begin{aligned} &\frac{1}{2}\left(S_0\ S_0^\top + S_1\ S_1^\top\right) = I \\ &S_0\ S_1^\top = 0. \end{aligned} \tag{5.28}$$

Moreover, the orthogonality conditions in Subsection 5.1.2 lead to the orthogonality of matrix $\mathcal{S}_3$.

Regarding relations (5.28) and Singular Value Decomposition (SVD) of S_0 and S_1, one can prove the following lemma and theorem stated in [2,3].

Lemma 5.1. *Suppose that S_0, S_1 are square matrices of size $4k \times 4k$ for $k = \left\lceil \frac{M-1}{2} \right\rceil$ which satisfy relations (5.28). Then there exist orthogonal matrices U, V such that*

$$S_0 = U \begin{pmatrix} \sqrt{2} I_{\mu_0} & 0 \\ 0 & 0_{\mu_1} \end{pmatrix} V^\top, \quad S_1 = U \begin{pmatrix} 0_{\mu_0} & 0 \\ 0 & \sqrt{2} I_{\mu_1} \end{pmatrix} V^\top, \tag{5.29}$$

where $\mu_0 = rank(S_0)$, $\mu_1 = rank(S_1)$ and $\mu_0 + \mu_1 = 4k$. Here I_μ denotes the identity matrix of size $\mu \times \mu$.

Theorem 5.2. *If $\mathcal{S}_3$ is orthogonal and has the structure given in (5.27), then $X_0,\ X_1,\ Y_0,\ Y_1$ must have sizes $2\mu_1 \times \mu_1$, $2\mu_1 \times 4k$, $2\mu_0 \times 4k$ and $2\mu_0 \times \mu_0$, respectively.*

As a result of this theorem, we can determine the number of scaling functions at the boundaries with $l = \mu_1$ and $r = \mu_0$.

In the case of more than two matrices S_k, we reduce the DMWT decomposition matrix in (3.21) to the case of only two matrices S_0 and S_1 with forming the block matrices. For example if we have $A_0, \ldots, A_7$, (3.21) yields three matrices $S_0, \ldots, S_3$. We define

$$\hat{S}_0 = \begin{pmatrix} S_0 & S_1 & S_2 \\ 0 & S_0 & S_1 \\ 0 & 0 & S_0 \end{pmatrix}, \quad \hat{S}_1 = \begin{pmatrix} S_3 & 0 & 0 \\ S_2 & S_3 & 0 \\ S_1 & S_2 & S_3 \end{pmatrix}.$$

The new matrices $\hat{S}_0$ and $\hat{S}_1$ still satisfy the relations in (5.28). For more details, see [50].

5.3 Approximation Order of Scaling Vectors on the Interval

This section is concerned with the approximation order conditions for boundary scaling vectors. As we have already discussed in Section 3.2.6, the interior scaling vectors have approximation order m and satisfy the equation (3.25). Therefore for the interpolating 2-scaling vector Φ, we obtain

$$x^n = \sum_{k\in\mathbb{Z}} p_{nk}\Phi(x-k), \tag{5.30}$$

where $p_{nk} = (k^n, (k+\frac{1}{2})^n)$ and $|n| < m$.

In the following theorem, we want to investigate the necessary and sufficient conditions for the approximation order of orthogonal scaling vectors on the interval. The results derived originally from [3], but for our case, it was necessary to do some modifications.

Theorem 5.3. *Suppose that $\Phi = (\phi_0, \phi_1)^\top$ is a compactly supported orthogonal 2-scaling vector and provides approximation order m. Moreover, the left and right boundary vectors defined by (5.5) and (5.8) are refinable and satisfy equations (5.9). Then the left boundary vector Φ^L has approximation order m, if and only if there exist row vectors υ_n, $n = 0, \cdots, m-1$, such that for $x \geq 0$:*

$$\begin{aligned} &\upsilon_n E = 2^{-n}\upsilon_n, \\ &\upsilon_n F_t = \zeta_{nt}, \quad t = 0, \cdots, M-2, \end{aligned} \tag{5.31}$$

where

$$\zeta_{nt} = 2^{-n}p_{nt} - \sum_{k=0}^{\lfloor \frac{t}{2} \rfloor} p_{nk}A_{t-2k},$$

with p_{nk} defined in (5.30). Similarly, the necessary and sufficient conditions for approximation order m at the right boundary are the existence of vectors $\widetilde{\upsilon}_n$, $n = 0, \cdots, m-1$, such that for $x \leq 0$:

$$\begin{aligned} &\widetilde{\upsilon}_n \widetilde{E} = 2^{-n}\widetilde{\upsilon}_n, \\ &\widetilde{\upsilon}_n \widetilde{F}_t = \widetilde{\zeta}_{nt}, \quad t = -M+2, \cdots, 0, \end{aligned}$$

with

$$\widetilde{\zeta} = 2^{-n}p_{nt} - \sum_{k=\lceil \frac{t}{2} \rceil}^{0} p_{nk}A_{t-2k}.$$

Proof. First af all, we start with the left side. It has been already mentioned that the approximation order of scaling vector is connected with its ability to reproduce polynomials. Consequently, the boundary vector Φ^L has approximation order m if there exist row vectors υ_n, $n = 0, \cdots, m-1$, such that for $x \geq 0$:

$$x^n = \upsilon_n\Phi^L(x) + \sum_{k=0}^{\infty} p_{nk}\Phi(x-k). \tag{5.32}$$

If we replace x by $2^j x$, we have

$$(2^j x)^n = \upsilon_n \Phi^L(2^j x) + \sum_{k=0}^{\infty} p_{nk} \Phi(2^j x - k),$$

or

$$(2^j x)^n = 2^{-\frac{j}{2}} \upsilon_n \Phi_j^L(x) + 2^{-\frac{j}{2}} \sum_{k=0}^{\infty} p_{nk} \Phi_{j,k}(x). \tag{5.33}$$

By combining the equations (5.9), (5.3) and (5.33), we obtain

$$\begin{aligned}(2^j x)^n &= 2^{-\frac{j}{2}} \upsilon_n \left(2^{-\frac{1}{2}} E \Phi_{j+1}^L(x) + 2^{-\frac{1}{2}} \sum_{t=0}^{M-2} F_t \Phi_{j+1,t}(x) \right) \\ &\quad + 2^{-\frac{j}{2}} \sum_{k=0}^{\infty} p_{nk} \left(2^{-\frac{1}{2}} \sum_{t=2k}^{M+2k} A_{t-2k} \Phi_{j+1,t}(x) \right) \\ &= 2^{-\frac{j}{2}} \upsilon_n(\ldots) + 2^{-\frac{j+1}{2}} \left(\sum_{t=0}^{M-2} \sum_{k=0}^{\lfloor \frac{t}{2} \rfloor} p_{nk} A_{t-2k} \Phi_{j+1,t}(x) + \sum_{t=M-1}^{\infty} \sum_{k=\lceil \frac{t-M}{2} \rceil}^{\lfloor \frac{t}{2} \rfloor} p_{nk} A_{t-2k} \Phi_{j+1,t}(x) \right) \quad x \geq 0.\end{aligned}$$

Consequently, we get

$$\begin{aligned}(2^j x)^n &= 2^{-\frac{j+1}{2}} \upsilon_n E \Phi_{j+1}^L(x) + 2^{-\frac{j+1}{2}} \sum_{t=0}^{M-2} \left(\upsilon_n F_t + \sum_{k=0}^{\lfloor \frac{t}{2} \rfloor} p_{nk} A_{t-2k} \right) \Phi_{j+1,t}(x) \\ &\quad + 2^{-\frac{j+1}{2}} \sum_{t=M-1}^{\infty} \sum_{k=\lceil \frac{t-M}{2} \rceil}^{\lfloor \frac{t}{2} \rfloor} p_{nk} A_{t-2k} \Phi_{j+1,t}(x).\end{aligned} \tag{5.34}$$

On the other hand replacing j by $j+1$ in (5.33) yields

$$(2^{j+1} x)^n = 2^{-\frac{j+1}{2}} \upsilon_n \Phi_{j+1}^L(x) + 2^{-\frac{j+1}{2}} \sum_{t=0}^{\infty} p_{nt} \Phi_{j+1,t}(x),$$

or

$$(2^j x)^n = 2^{-\frac{j+1}{2}}\ 2^{-n} \upsilon_n \Phi_{j+1}^L(x) + 2^{-\frac{j+1}{2}}\ 2^{-n} \sum_{t=0}^{\infty} p_{nt} \Phi_{j+1,t}(x).$$

If we compare this equation and (5.34), we see that

$$\begin{aligned} 2^{-n} \upsilon_n &= \upsilon_n E, \\ 2^{-n} p_{nt} &= \upsilon_n F_t + \sum_{k=0}^{\lfloor \frac{t}{2} \rfloor} p_{nk} A_{t-2k}, \quad t = 0, \cdots, M-2, \\ 2^{-n} p_{nt} &= \sum_{k=\lceil \frac{t-M}{2} \rceil}^{\lfloor \frac{t}{2} \rfloor} p_{nk} A_{t-2k}, \quad t = M-1, \cdots, \infty, \end{aligned} \tag{5.35}$$

where $n = 0, \cdots, m-1$.
We have an analogous result for the right endpoints. The boundary vector Φ^R has approximation order m if there exist row vectors $\widetilde{\upsilon}_n, \quad n = 0, \cdots, m-1$, such that for $x \leq 0$ we have

$$(2^j x)^n = \sum_{k=-\infty}^{0} p_{nk} \Phi(2^j x - k) + \widetilde{\upsilon}_n \Phi^R(2^j x),$$

or

$$(2^j x)^n = 2^{-\frac{j}{2}} \sum_{k=-\infty}^{0} p_{nk} \Phi_{j,k}(x) + 2^{-\frac{j}{2}} \widetilde{\upsilon}_n \Phi_j^R(x). \tag{5.36}$$

By combining the equations (5.9), (5.6) and (5.36), we obtain

$$\begin{aligned}(2^j x)^n = 2^{-\frac{j}{2}} \sum_{k=-\infty}^{0} p_{nk} \left(2^{-\frac{1}{2}} \sum_{t=-M+2k}^{2k} A_{t-2k} \Phi_{j+1,t}(x) \right) \\ + 2^{-\frac{j}{2}} \widetilde{\upsilon}_n \left(2^{-\frac{1}{2}} \sum_{t=-M+2}^{0} \widetilde{F}_t \Phi_{j+1,t}(x) + 2^{-\frac{1}{2}} \widetilde{E} \Phi_{j+1}^R(x) \right), \quad x \leq 0,\end{aligned}$$

Consequently, we have

$$\begin{aligned}(2^j x)^n = 2^{-\frac{j+1}{2}} \sum_{t=-\infty}^{-M+1} \sum_{k=\lceil \frac{t}{2} \rceil}^{\lfloor \frac{t+M}{2} \rfloor} p_{nk} A_{t-2k} \Phi_{j+1,t}(x) \\ + 2^{-\frac{j+1}{2}} \sum_{t=-M+2}^{0} \left(\widetilde{\upsilon}_n \widetilde{F}_t + \sum_{k=\lceil \frac{t}{2} \rceil}^{0} p_{nk} A_{t-2k} \right) \Phi_{j+1,t}(x) + 2^{-\frac{j+1}{2}} \widetilde{\upsilon}_n \widetilde{E} \Phi_{j+1}^R(x),\end{aligned} \tag{5.37}$$

On the other hand, similar to the left side, replacing j by $j+1$ in (5.36) yields

$$(2^j x)^n = 2^{-\frac{j+1}{2}} \; 2^{-n} \sum_{t=-\infty}^{0} p_{nt} \Phi_{j+1,t}(x) + 2^{-\frac{j+1}{2}} \; 2^{-n} \widetilde{\upsilon}_n \Phi_{j+1}^R(x).$$

By comparing this equation and (5.37), we have

$$\begin{aligned}2^{-n} p_{nt} &= \sum_{k=\lceil \frac{t}{2} \rceil}^{\lfloor \frac{t+M}{2} \rfloor} p_{nk} A_{t-2k}, \quad t = -\infty, \cdots, -M+1, \\ 2^{-n} p_{nt} &= \widetilde{\upsilon}_n \widetilde{F}_t + \sum_{k=\lceil \frac{t}{2} \rceil}^{0} p_{nk} A_{t-2k}, \quad t = -M+2, \cdots, 0, \\ 2^{-n} \widetilde{\upsilon}_n &= \widetilde{\upsilon}_n \widetilde{E},\end{aligned}$$

where $n = 0, \cdots, m-1$. The first of these conditions and the third condition in (5.35) are corresponding to interior approximation order and are automatically satisfied. Furthermore, conditions (5.31) are sufficient if the cascade algorithm for the left boundary

vector converges. We start with an initial vector $\Phi^{L(0)}$ in (5.23) which is supported on $[0, M-1]$. Then $\Phi^{L(1)}$ can be determined on $[(M-1)/2, M-1]$ by a linear combination of translates $\Phi(2x)$. Afterward, $\Phi^{L(2)}$ is given on $[(M-1)/4, (M-1)/2]$ as a linear combination of $\Phi(4x-t)$. With iterating this process, the cascade algorithm will be converge to a continuous function on $(0, M-1]$. Note that in every step, $\Phi^{L(n)}$ is a linear combination of continuous functions and therefore it will be continuous as well. Now, it remains to show the convergence for $x = 0$. Equivalently, we can prove that for a fixed x_0 in $(0, 1]$, the sequence $\Phi^L(2^{-n}x_0)$ converges to a continuous vector as follows. First of all, using the equation (5.3), we have

$$\Phi(\frac{x_0}{2}) = A_0\Phi(x_0) + A_1\Phi(x_0 - 1) + \ldots + A_M\Phi(x_0 - M).$$

Since that $x_0 \in (0, 1]$, we obtain

$$\begin{aligned}
\Phi(\frac{x_0}{2}) &= A_0\Phi(x_0),\\
\Phi(\frac{x_0}{4}) &= A_0^2\Phi(x_0),\\
&\vdots\\
\Phi(2^{-n}x_0) &= A_0^n\Phi(x_0).
\end{aligned}$$

Similarly, for the left boundary vector we have

$$\begin{aligned}
&\Phi^L(\frac{x_0}{2}) = E\Phi^L(x_0) + F_0\Phi(x_0) + F_1\Phi(x_0 - 1) + \ldots + +F_{M-2}\Phi(x_0 - M + 2)\\
&= E\Phi^L(x_0) + F_0\Phi(x_0),\\
&\Phi^L(\frac{x_0}{4}) = E^2\Phi^L(x_0) + (EF_0 + F_0A_0)\Phi(x_0),\\
&\vdots\\
&\Phi^L(2^{-n}x_0) = E^n\Phi^L(x_0) + \mathcal{R}_{n-1}\Phi(x_0).
\end{aligned}$$

where

$$\mathcal{R}_{n-1} = E^{n-1}F_0 + E^{n-2}F_0A_0 + \ldots + F_0A_0^{n-1}. \tag{5.38}$$

Now, we have to check the convergence of E^n and $\mathcal{R}_{n-1}$. First, we suppose that $\mathrm{spec}(E) = 1$. In this case, the eigenvalues of E are as

$$\lambda_0 = 1 \quad \text{and} \quad |\lambda_i| < 1 \text{ for } i = 1, \ldots, l-1,$$

and

$$EQ = Q\Lambda,$$

or

$$E = Q\Lambda Q^{-1}, \tag{5.39}$$

where Q is the square $l \times l$ matrix whose columns are the right eigenvectors q_i of E for $i = 0, \ldots, l-1$, and Λ is the diagonal matrix whose diagonal entries are the corresponding eigenvalues λ_i, $i = 0, \ldots, l-1$. Furthermore, we have

$$Q^{-1} = \begin{pmatrix} \upsilon_0 \\ \vdots \\ \upsilon_{l-1} \end{pmatrix},$$

where υ_i, $i = 0, \ldots, l-1$, are the corresponding left eigenvectors of E. Then

$$E = (q_0, \ldots, q_{l-1}) \begin{pmatrix} 1 & 0 & 0 & \ldots & 0 \\ 0 & \lambda_1 & 0 & \ldots & 0 \\ \vdots & \ddots & \ddots & \ddots & \vdots \\ 0 & \ldots & 0 & \lambda_{l-2} & 0 \\ 0 & \ldots & 0 & 0 & \lambda_{l-1} \end{pmatrix} \begin{pmatrix} \upsilon_0 \\ \vdots \\ \upsilon_{l-1} \end{pmatrix},$$

and thus

$$E^n \longrightarrow (q_0, \ldots, q_{l-1}) \begin{pmatrix} 1 & 0 & \ldots & 0 \\ 0 & 0 & \ldots & 0 \\ \vdots & \ddots & \ddots & \vdots \\ 0 & \ldots & 0 & 0 \end{pmatrix} \begin{pmatrix} \upsilon_0 \\ \vdots \\ \upsilon_{l-1} \end{pmatrix} = q_0 \upsilon_0$$

as $n \longrightarrow \infty$.

Moreover, the equation (5.39) leads to

$$Q^{-1}E = \Lambda Q^{-1}.$$

Consequently, for $i = 0$, we obtain

$$\begin{aligned} &\upsilon_0 E = \upsilon_0, \\ &\vdots \\ &\upsilon_0 E^n = \upsilon_0, \end{aligned}$$

Therefore, for $\mathcal{R}_{n-1}$ in (5.38), we get

$$\begin{aligned} \upsilon_0 \mathcal{R}_{n-1} &= \upsilon_0 \left(E^{n-1} F_0 + E^{n-2} F_0 A_0 + \ldots + F_0 A_0^{n-1} \right) \\ &= \upsilon_0 F_0 \left(I + A_0 + A_0^2 + \ldots + A_0^{n-1} \right) \\ &\longrightarrow \upsilon_0 F_0 (I - A_0)^{-1}, \quad \text{as} \quad n \longrightarrow \infty. \end{aligned} \tag{5.40}$$

Furthermore, for the interior scaling vector, we have

$$A_0^n \Phi(x_0) \longrightarrow \Phi(0) = 0, \quad \text{as} \quad n \longrightarrow \infty,$$

for any x_0. This implies that $\text{spec}(A_0) < 1$ and therefore, $(I - A_0)^{-1}$ exists.

Afterward, for $i = 1, \ldots, l-1$, we get

$$\upsilon_i E^n = \lambda_i^n \upsilon_i,$$

and then

$$\upsilon_i \mathcal{R}_{n-1} = \upsilon_i F_0 \left(\lambda_i^{n-1} + \lambda_i^{n-2} A_0 + \ldots + A_0^{n-1} \right). \tag{5.41}$$

It was shown in [36], that for a matrix A and given $\epsilon > 0$, there is a matrix norm such that

$$\|A\| \leq \text{spec}(A) + \epsilon.$$

As stated, $\text{spec}(A_0) < 1$ and therefore, there is a norm such that $\|A_0\| < 1$. Let

$$h = \max(\|A_0\|, |\lambda_1|, \ldots, |\lambda_{l-1}|) < 1.$$

Then, the norm of equation (5.41) will be as

$$\begin{aligned}\|\upsilon_i \mathcal{R}_{n-1}\| &\leq \|\upsilon_i\|\|F_0\| \sum_{k=0}^{n-1} |\lambda_i|^k \|A_0\|^{n-k-1} \\ &\leq \|\upsilon_i\|\|F_0\| n h^{n-1},\end{aligned}$$

which converges to zero as $n \longrightarrow \infty$. This, together with (5.40) implies that $Q^{-1}\mathcal{R}_{n-1}$ converges to

$$\begin{pmatrix} \upsilon_0 \\ 0 \\ \vdots \\ 0 \end{pmatrix} F_0 (I - A_0)^{-1},$$

and then

$$\mathcal{R}_{n-1} = QQ^{-1}\mathcal{R}_{n-1} = (q_0, \ldots, q_{l-1}) \begin{pmatrix} \upsilon_0 \\ \vdots \\ \upsilon_{l-1} \end{pmatrix} \mathcal{R}_{n-1} \longrightarrow q_0 \upsilon_0 F_0 (I - A_0)^{-1}.$$

Thus, $\Phi^L(2^{-n}x_0)$ converges to

$$\Phi^L(0) = q_0 \upsilon_0 \left(\Phi^L(x_0) + F_0 (I - A_0)^{-1} \Phi(x_0) \right). \tag{5.42}$$

It is easy to show that $\Phi^L(2^{-n}x_0)$ converges to zero if $\mathrm{spec}(E) < 1$. Moreover, for $\mathrm{spec}(E) > 1$, it diverges for most starting functions. Therefore, it will not lead to nice solutions and we do not consider it here.

To complete the proof, we show that (5.42) is indipendent of x. By assumption, for $n = 0$ in (5.32), we have

$$1 = \upsilon_0 \Phi^L(x) + p_{00} \Phi(x), \tag{5.43}$$

and by conditions (5.35) for $t = 0$ and $n = 0$, we get

$$\begin{aligned}\upsilon_0 E &= \upsilon_0, \\ \upsilon_0 F_0 &= p_{00}(I - A_0).\end{aligned}$$

Therefore

$$p_{00} = \upsilon_0 F_0 (I - A_0)^{-1}.$$

By combining (5.43) and (5.42), we obtain

$$\begin{aligned}\Phi^L(0) &= q_0 \left(\upsilon_0 \Phi^L(x) + \upsilon_0 F_0 (I - A_0)^{-1} \Phi(x) \right) \\ &= q_0 \left(\upsilon_0 \Phi^L(x) + p_{00} \Phi(x) \right) \\ &= q_0.\end{aligned}$$

This proves the continuity of $\Phi^L(x)$ at $x = 0$.

Analogously, it can be proceeded for the right boundary vector.

□

5.4 Construction of Orthogonal Boundary Scaling Vectors

5.4.1 General Approach

In this subsection, we will describe an algorithm to find suitable matrices C, E and F in (5.12) for the left boundary vector and D, $\widetilde{E}$ and $\widetilde{F}$ in (5.15) for the right boundary vectors. Then we can construct the orthogonal scaling vectors on the interval.

It was stated in section 5.1.1, that the equation $CV = EC$ is an eigenvalue problem. The rows of C are the eigenvectors of matrix V and every row of EC is a linear combination of rows of C. This implies that rowspan$\{C\}$ is a left invariant subspace for the matrix V. That is, the rows of C must be a linear combination of no more than l left eigenvectors of V. The matrix E is a diagonal matrix with the l eigenvalues of V as entries.
Note that, to compute the desired solutions for the scaling vector Φ^L, we can choose an invertible matrix U and replace Φ^L by $U\Phi^L$. The new scaling vector still spans the same space. Furthermore the orthogonality and approximation order is preserved. Consequently, after replacing Φ^L in (5.4) by $U\Phi^L$, we have

$$U\Phi^L(x) = \sum_{k=-M+1}^{-1} UC_k\Phi(2x-k), \quad x \geq 0.$$

Therefore the matrix C turns into UC. If we substitute UC into (5.12), we get

$$\begin{aligned} UCV &= EUC, \\ UCW &= F. \end{aligned}$$

Replacing E and F by UEU^{-1} and UF, we have

$$\begin{aligned} UCV &= UEU^{-1}UC, \\ UCW &= UF, \end{aligned}$$

which corresponds to (5.12). Thus, the effect of U on the matrices E, F and C will be as UEU^{-1}, UF and UC respectively. For the right scaling vectors, we proceed in the same way.

Based on the past results, we suggest the following construction of the left and right scaling vectors on the interval:

1. Using Lemma 5.1, we compute μ_0 and μ_1, which are equal to the number of right and left boundary scaling vectors respectively.

2. Utilizing the equation $CV = EC$ and $D\widetilde{V} = \widetilde{E}D$, we calculate the eigenvalues and left eigenvectors of the matrices V and $\widetilde{V}$.

3. We choose l eigenvalues of V and r eigenvalues of $\widetilde{V}$ to construct the diagonal matrices E and $\widetilde{E}$ respectively. Note that there might exist more selections and we prefer those, which lead to regular solutions, that is they include the simple eigenvalue 1. Now we select the left eigenvectors corresponding to these eigenvalues and form the matrices C and D. Consequently, we can calculate the matrices F and $\widetilde{F}$, using the equations $F = CW$ and $\widetilde{F} = D\widetilde{W}$.

4. The last and important step is the orthonormalization of the boundary vectors. For that, we use the equation (5.17) for the left boundary vectors and intend to find an invertible matrix U such that

$$(UEU^{-1})(UEU^{-1})^\top + (UF)(UF)^\top = 2I_l. \tag{5.44}$$

We multiply (5.44) from the left by U^{-1} and from the right by $(U^\top)^{-1}$ and we have

$$EU^{-1}(U^{-1})^\top E^\top + FF^\top = 2U^{-1}(U^{-1})^\top,$$

where $(U^{-1})^\top = (U^\top)^{-1}$. Now let the vector $\mathbf{e} = (\mathbf{e}_1, \ldots, \mathbf{e}_l)^\top$ denotes the diagonal elements of E and we define $\widehat{E} = \mathbf{e}.\mathbf{e}^\top$. Then we obtain

$$\begin{aligned}
&\widehat{E} \odot (U^{-1}(U^{-1})^\top) + FF^\top = 2U^{-1}(U^{-1})^\top, \\
&FF^\top = (\mathbf{2} - \widehat{E}) \odot U^{-1}(U^{-1})^\top,
\end{aligned}$$

which leads to

$$U^{-1}(U^{-1})^\top = FF^\top \oslash (\mathbf{2} - \widehat{E}), \tag{5.45}$$

where $\odot$ and $\oslash$ indicate element-wise multiplication and division of matrices and $\mathbf{2}$ is a matrix with the entries 2. Consequently, we can find U^{-1} as a cholesky factor of the right-hand side of (5.45).

5. Finally, we set $C = UC$ and apply the first equation in (5.5) to obtain the left scaling vector on the interval $[0, 1]$.

Analogously, we proceed the steps 4 and 5 for the right boundary vector.

5.4.2 Examples

In this subsection we present some examples based on the results in the preceding sections. As stated above, the solutions obtained by our construction are not unique. Therefore, we select those solutions which are regular.

Example 5.4. As in the interpolation case, we start with the orthonormal scaling vector in Example 3.16 which has approximation order 1. First of all, we shift this vector to be in the interval $[0, 3]$. The masks A_k are

$$\begin{aligned}
A_0 &= \begin{pmatrix} 0 & 0.2208 \\ 0 & 0.0514 \end{pmatrix}, \quad A_1 = \begin{pmatrix} 1 & 0.9486 \\ 0 & 0.2208 \end{pmatrix}, \\
A_2 &= \begin{pmatrix} 0 & -0.2208 \\ 1 & 0.9486 \end{pmatrix}, \quad A_3 = \begin{pmatrix} 0 & 0.0514 \\ 0 & -0.2208 \end{pmatrix},
\end{aligned}$$

and their corresponding multiwavelet coefficients are

$$\begin{aligned}
B_0 &= \begin{pmatrix} 0 & -0.2208 \\ 0 & -0.0514 \end{pmatrix}, \quad B_1 = \begin{pmatrix} 1 & -0.9486 \\ 0 & -0.2208 \end{pmatrix}, \\
B_2 &= \begin{pmatrix} 0 & 0.2208 \\ 1 & -0.9486 \end{pmatrix}, \quad B_3 = \begin{pmatrix} 0 & -0.0514 \\ 0 & 0.2208 \end{pmatrix}.
\end{aligned}$$

Now we can form the matrices S_0 and S_1 in (5.26) and compute their ranks $\mu_0 = \mu_1 = 2$. That means there are two left and right boundary functions. Furthermore, for the left boundary vector, the matrices V and W are

$$V = \begin{pmatrix} A_2 & A_3 \\ A_0 & A_1 \end{pmatrix}, \qquad W = \begin{pmatrix} 0 & 0 \\ A_2 & A_3 \end{pmatrix}.$$

Consequently, we have the following left eigenvectors and their corresponding eigenvalues of matrix V:

$$\begin{aligned} &\lambda_1 = 1, \quad v_1 = (0.5, 0.5, 0.5, 0.5), \\ &\lambda_2 = 0.2227, \quad v_2 = (0.6491, 0.1446, 0, 0.7468), \\ &\lambda_3 = 0.4733, \quad v_3 = (0.8855, 0.4191, 0, -0.1871). \end{aligned}$$

First we choose the eigenvalues λ_1 and λ_2 and then we form the matrices E and C:

$$E = \begin{pmatrix} 1 & 0 \\ 0 & 0.2227 \end{pmatrix}, \quad C = \begin{pmatrix} 0.5 & 0.5 & 0.5 & 0.5 \\ 0.6491 & 0.1446 & 0 & 0.7468 \end{pmatrix}.$$

Consequently to find an orthogonal solution, we compute the matrix U:

$$U = \begin{pmatrix} 1.6021 & 0 \\ -1.9912 & 2.1370 \end{pmatrix}.$$

Then using the transformation matrix U, we obtain new matrices E, F and C:

$$\begin{aligned} E &= \begin{pmatrix} 1 & 0 \\ -0.9660 & 0.2227 \end{pmatrix}, \\ F &= \begin{pmatrix} 0.8011 & 0.5830 & 0 & -0.1357 \\ 0.6003 & 0.7893 & 0 & -0.1837 \end{pmatrix}, \\ C &= \begin{pmatrix} 0.8011 & 0.8011 & 0.8011 & 0.8011 \\ 0.3916 & -0.6866 & -0.9956 & 0.6003 \end{pmatrix}, \end{aligned}$$

which lead to a regular solution. That is the orthogonal left boundary vector Φ^L showing in Figure 5.1.

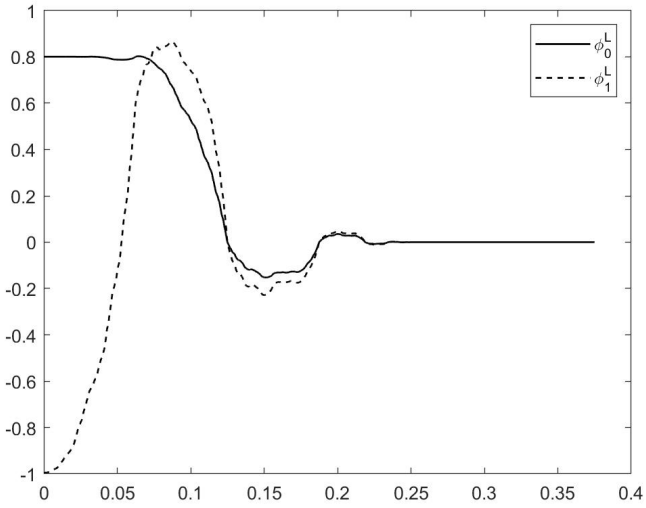

Figure 5.1: Orthogonal left scaling vector on the interval $[0, 1]$, solution 1

For the second regular solution, we choose the eigenvalues λ_1 and λ_3 and we have

$$E = \begin{pmatrix} 1 & 0 \\ 0 & 0.4733 \end{pmatrix}, \quad C = \begin{pmatrix} 0.5 & 0.5 & 0.5 & 0.5 \\ 0.8855 & 0.4191 & 0 & -0.1871 \end{pmatrix},$$

and the matrix U:

$$U = \begin{pmatrix} 1.6021 & 0 \\ 2.7682 & 10.1841 \end{pmatrix}.$$

Then using the transformation matrix U, we obtain

$$E = \begin{pmatrix} 1 & 0 \\ 0.9100 & 0.4733 \end{pmatrix},$$
$$F = \begin{pmatrix} 0.8011 & 0.5830 & 0 & -0.1357 \\ -0.5218 & -0.8006 & 0 & 0.1864 \end{pmatrix},$$
$$C = \begin{pmatrix} 0.8011 & 0.8011 & 0.8011 & 0.8011 \\ 10.4018 & 5.6525 & 1.3841 & -0.5218 \end{pmatrix}.$$

Figure 5.2 shows the second solution for the left boundary.

There are as well other orthogonal solutions which are not regular. For example, by choosing the eigenvalues λ_2 and λ_3, we obtain the left boundary scaling vector in Figure 5.3.

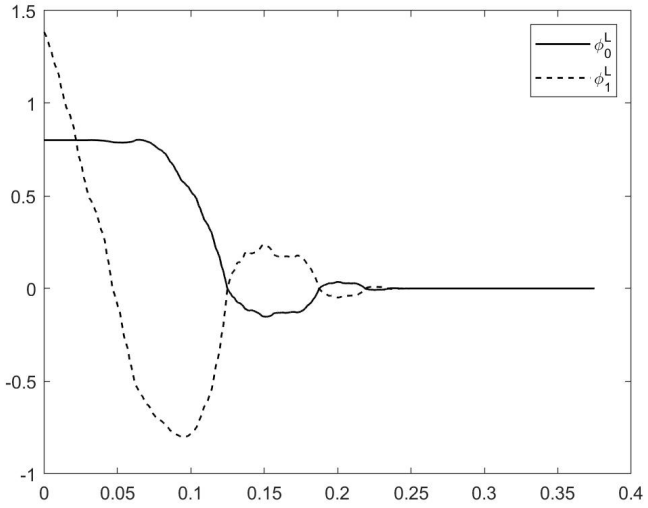

Figure 5.2: Orthogonal left scaling vector on the interval $[0, 1]$, solution 2

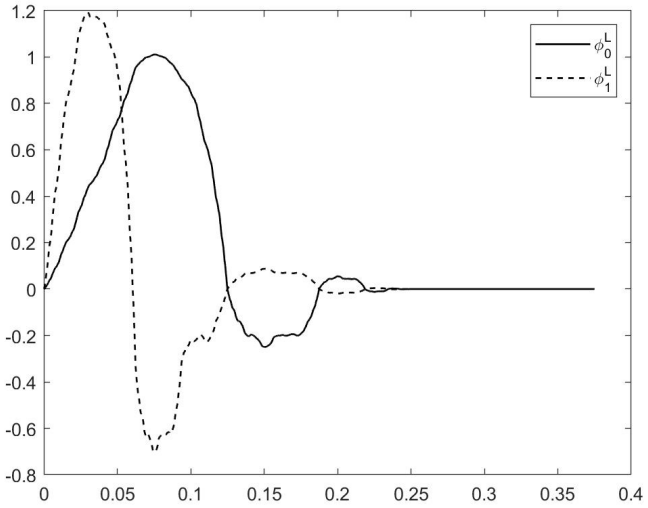

Figure 5.3: Orthogonal left scaling vector on the interval $[0, 1]$, solution 3

Similar to the left edge, we can plot the orthogonal scaling vector for the right side. First of all, we compute matrices $\widetilde{W}$ and $\widetilde{V}$:

$$\widetilde{W} = \begin{pmatrix} A_0 & A_1 \\ 0 & 0 \end{pmatrix}, \qquad \widetilde{V} = \begin{pmatrix} A_2 & A_3 \\ A_0 & A_1 \end{pmatrix},$$

and then we have the following left eigenvectors and their corresponding eigenvalues of matrix $\widetilde{V}$:

$$\begin{aligned} &\lambda_1 = 1, \quad && v_1 = (0.5, 0.5, 0.5, 0.5), \\ &\lambda_2 = 0.2227, \quad && v_2 = (0.6491, 0.1446, 0, 0.7468), \\ &\lambda_3 = 0.4733, \quad && v_3 = (0.8855, 0.4191, 0, -0.1871). \end{aligned}$$

Now as in the left edge, we choose the eigenvalues λ_1 and λ_2 and then we form matrices $\widetilde{E}$ and D:

$$\widetilde{E} = \begin{pmatrix} 1 & 0 \\ 0 & 0.2227 \end{pmatrix}, \quad D = \begin{pmatrix} 0.5 & 0.5 & 0.5 & 0.5 \\ 0.6491 & 0.1446 & 0 & 0.7468 \end{pmatrix}.$$

Then to find an orthogonal solution, we compute matrix U:

$$U = \begin{pmatrix} 1.2799 & 0 \\ -1.6131 & 2.4177 \end{pmatrix},$$

and we obtain new matrices $\widetilde{E}$, $\widetilde{F}$ and D:

$$\widetilde{E} = \begin{pmatrix} 1 & 0 \\ -0.9796 & 0.2227 \end{pmatrix},$$
$$\widetilde{F} = \begin{pmatrix} 0 & 0.1742 & 0.6400 & 0.7484 \\ 0 & 0.1450 & 0.7629 & 0.6228 \end{pmatrix},$$
$$D = \begin{pmatrix} 0.6400 & 0.6400 & 0.6400 & 0.6400 \\ 0.7629 & -0.4570 & -0.8065 & 0.9991 \end{pmatrix}.$$

Consequently we can plot the orthogonal right boundary vector Φ^R as in Figure 5.4.

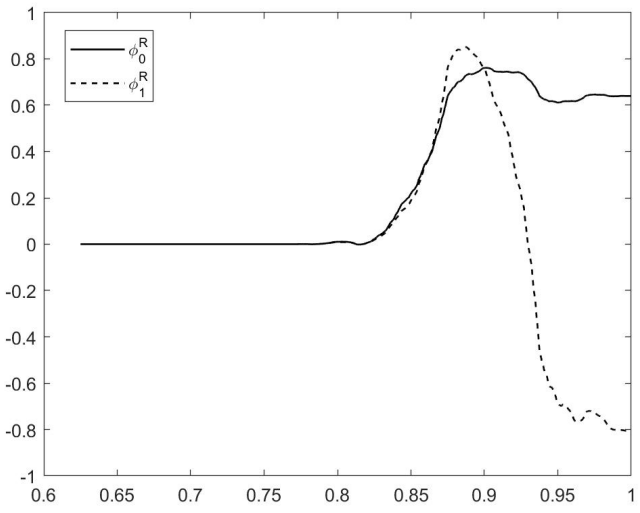

Figure 5.4: Orthogonal right scaling vector on the interval $[0, 1]$, solution 1

To find the second regular solution, we choose the eigenvalues λ_1 and λ_3 and we have

$$\widetilde{E} = \begin{pmatrix} 1 & 0 \\ 0 & 0.4733 \end{pmatrix}, \quad D = \begin{pmatrix} 0.5 & 0.5 & 0.5 & 0.5 \\ 0.8855 & 0.4191 & 0 & -0.1871 \end{pmatrix}.$$

Consequently, we compute the matrix U:

$$U = \begin{pmatrix} 1.2799 & 0 \\ -2.2772 & 2.0856 \end{pmatrix}.$$

Then using the transformation matrix U, we obtain

$$\widetilde{E} = \begin{pmatrix} 1 & 0 \\ -0.9370 & 0.4733 \end{pmatrix},$$
$$\widetilde{F} = \begin{pmatrix} 0 & 0.1742 & 0.6400 & 0.7484 \\ 0 & 0.1428 & 0.7081 & 0.6133 \end{pmatrix},$$
$$D = \begin{pmatrix} 0.6400 & 0.6400 & 0.6400 & 0.6400 \\ 0.7081 & -0.2645 & -1.1386 & -1.5289 \end{pmatrix}.$$

Figure 5.5 shows the second regular solution for the right boundary.

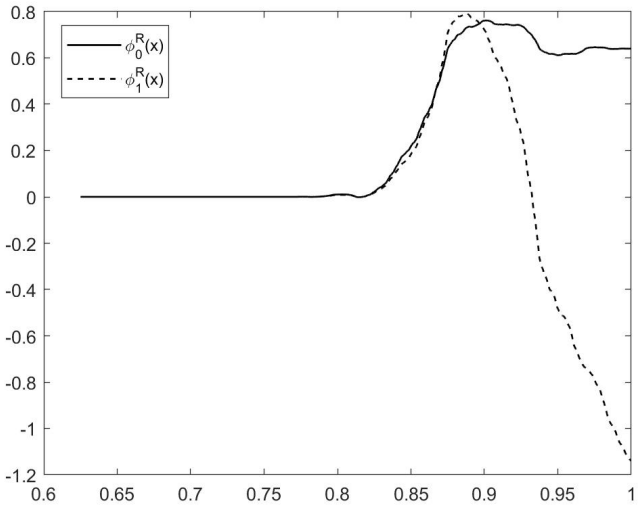

Figure 5.5: Orthogonal right scaling vector on the interval $[0, 1]$, solution 2

For the non-regular solution, we might choose the eigenvalues λ_2 and λ_3 and obtain the right boundary scaling vector in Figure 5.6.

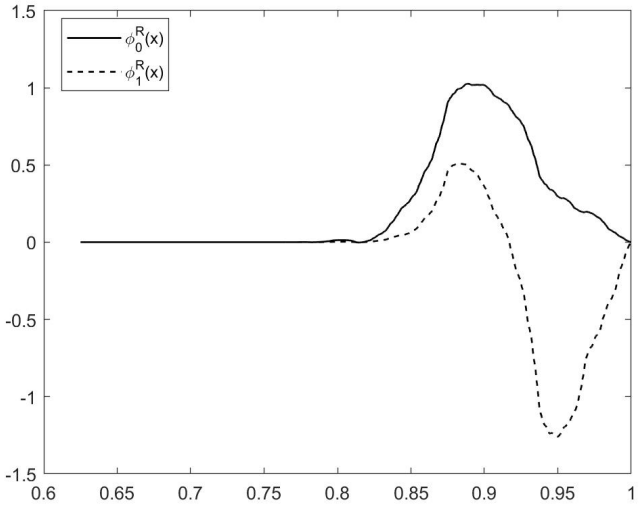

Figure 5.6: Orthogonal right scaling vector on the interval $[0, 1]$, solution 3

Example 5.5. Considering the orthonormal scaling vectors in Example 3.17 with approximation order 2, we want to construct the boundary scaling vectors. Again, we shift these vectors to be in the interval $[0, 5]$. The masks A_k are

$$A_0 = \begin{pmatrix} 0 & 0.0313 \\ 0 & 0.0040 \end{pmatrix}, \quad A_1 = \begin{pmatrix} 0 & 0.2460 \\ 0 & 0.0313 \end{pmatrix}, \quad A_2 = \begin{pmatrix} 1 & 0.9375 \\ 0 & 0.2421 \end{pmatrix},$$
$$A_3 = \begin{pmatrix} 0 & -0.2421 \\ 1 & 0.9375 \end{pmatrix}, \quad A_4 = \begin{pmatrix} 0 & 0.0313 \\ 0 & -0.2460 \end{pmatrix}, \quad A_5 = \begin{pmatrix} 0 & -0.0040 \\ 0 & 0.0313 \end{pmatrix},$$

and their corresponding multiwavelets coefficients are

$$B_0 = \begin{pmatrix} 0 & -0.0313 \\ 0 & -0.0040 \end{pmatrix}, \quad B_1 = \begin{pmatrix} 0 & -0.2460 \\ 0 & -0.0313 \end{pmatrix}, \quad B_2 = \begin{pmatrix} 1 & -0.9375 \\ 0 & -0.2421 \end{pmatrix},$$
$$B_3 = \begin{pmatrix} 0 & 0.2421 \\ 1 & -0.9375 \end{pmatrix}, \quad B_4 = \begin{pmatrix} 0 & -0.0313 \\ 0 & 0.2460 \end{pmatrix}, \quad B_5 = \begin{pmatrix} 0 & 0.0040 \\ 0 & -0.0313 \end{pmatrix}.$$

Now we define matrices S_0, S_1 and S_2 by

$$S_0 = \begin{pmatrix} A_0 & A_1 \\ B_0 & B_1 \end{pmatrix}, \quad S_1 = \begin{pmatrix} A_2 & A_3 \\ B_2 & B_3 \end{pmatrix}, \quad S_2 = \begin{pmatrix} A_4 & A_5 \\ B_4 & B_5 \end{pmatrix}.$$

Since there are more than four masks, we form the block matrices $\hat{S}_0$ and $\hat{S}_1$:

$$\hat{S}_0 = \begin{pmatrix} S_0 & S_1 \\ 0 & S_0 \end{pmatrix}, \quad \hat{S}_1 = \begin{pmatrix} S_2 & 0 \\ S_1 & S_2 \end{pmatrix}.$$

After computing the ranks of these matrices, we obtain $\mu_0 = \mu_1 = 4$.

Now, for the left boundary vector, we compute the matrices V and W:

$$V = \begin{pmatrix} A_4 & A_5 & 0 & 0 \\ A_2 & A_3 & A_4 & A_5 \\ A_0 & A_1 & A_2 & A_3 \\ 0 & 0 & A_0 & A_1 \end{pmatrix}, \quad W = \begin{pmatrix} 0 & 0 & 0 & 0 \\ 0 & 0 & 0 & 0 \\ A_4 & A_5 & 0 & 0 \\ A_2 & A_3 & A_4 & A_5 \end{pmatrix},$$

and we find the following left eigenvectors and their corresponding eigenvalues of matrix V:

$$\begin{aligned}
&\lambda_1 = 1, \quad v_1 = (0.3536, 0.3536, 0.3536, 0.3536, 0.3536, 0.3536, 0.3536, 0.3536),\\
&\lambda_2 = 0.5, \quad v_2 = (0.6030, 0.4523, 0.3015, 0.1508, 0, -0.1508, -0.3015, -0.4523),\\
&\lambda_3 = 0.4672, \quad v_3 = (-0.5770, -0.4215, -0.2695, -0.1259, 0, 0.1555, 0.3329, 0.5157),\\
&\lambda_4 = 0.2689, \quad v_4 = (0.7284, 0.4260, 0.1959, 0.0527, 0, 0.0568, 0.2111, 0.4460),\\
&\lambda_5 = -0.1956, \quad v_5 = (-0.3308, 0.9364, 0.0647, -0.0127, 0, -0.0182, 0.0928, -0.0227),\\
&\lambda_6 = -0.0757, \quad v_6 = (0.0956, -0.0224, -0.0072, 0.0005, 0, -0.0392, 0.5182, -0.8487),\\
&\lambda_7 = 0, \quad v_7 = (0.7015, 0.0891, 0, 0, 0, 0, -0.0891, 0.7014).
\end{aligned}$$

In this case, we have more solutions but we would select some of these and orthonormalize them. First we choose the eigenvalues λ_1, λ_2, λ_3 and λ_4 and then we form the matrices E and C:

$$E = \begin{pmatrix} 1 & 0 & 0 & 0 \\ 0 & 0.5 & 0 & 0 \\ 0 & 0 & 0.4672 & 0 \\ 0 & 0 & 0 & 0.2689 \end{pmatrix},$$

$$C = \begin{pmatrix} 0.3536 & 0.3536 & 0.3536 & 0.3536 & 0.3536 & 0.3536 & 0.3536 & 0.3536 \\ 0.6030 & 0.4523 & 0.3015 & 0.1508 & 0 & -0.1508 & -0.3015 & -0.4523 \\ -0.5770 & -0.4215 & -0.2695 & -0.1259 & 0 & 0.1555 & 0.3329 & 0.5157 \\ 0.7284 & 0.4260 & 0.1959 & 0.0527 & 0 & 0.0568 & 0.2111 & 0.4460 \end{pmatrix}.$$

Consequently to find an orthogonal solution, we compute the matrix U:

$$U = \begin{pmatrix} 1.5119 & 0 & 0 & 0 \\ 2.6386 & 3.5602 & 0 & 0 \\ 5.2870 & 126.1328 & 107.6904 & 0 \\ -4.5705 & -345.1550 & -340.2733 & 47.8640 \end{pmatrix}.$$

Then using the transformation matrix U, we obtain the new matrices E, F and C:

$$E = \begin{pmatrix} 1 & 0 & 0 & 0 \\ 0.8726 & 0.5 & 0 & 0 \\ -0.1665 & 1.1631 & 0.4672 & 0 \\ 0.3466 & -0.2099 & -0.6263 & 0.2689 \end{pmatrix},$$

$$F = \begin{pmatrix} 0.5345 & 0.5157 & 0.5345 & 0.3863 & 0 & -0.1148 & 0 & 0.0146 \\ -0.1406 & -0.3640 & -0.6773 & -0.5923 & 0 & 0.1622 & 0 & -0.0206 \\ -0.3137 & -0.0494 & 0.3641 & 0.3973 & 0 & -0.0994 & 0 & 0.0126 \\ -0.7135 & -0.6906 & 0.3420 & 0.5066 & 0 & -0.1064 & 0 & 0.0135 \end{pmatrix},$$

$$C = \begin{pmatrix} 0.5345 & 0.5345 & 0.5345 & 0.5345 & 0.5345 & 0.5345 & 0.5345 & 0.5345 \\ 3.0798 & 2.5430 & 2.0063 & 1.4696 & 0.9329 & 0.3962 & -0.1406 & -0.6773 \\ 15.7971 & 13.5277 & 10.8729 & 7.3240 & 1.8692 & -0.3991 & -0.3137 & 0.3641 \\ 21.4371 & 6.0859 & -4.5902 & -8.2806 & -1.6159 & 0.2194 & -0.7135 & 0.3420 \end{pmatrix},$$

which lead to a regular solution and the orthogonal left boundary vector corresponding to this solution can be seen in Figure 5.7.

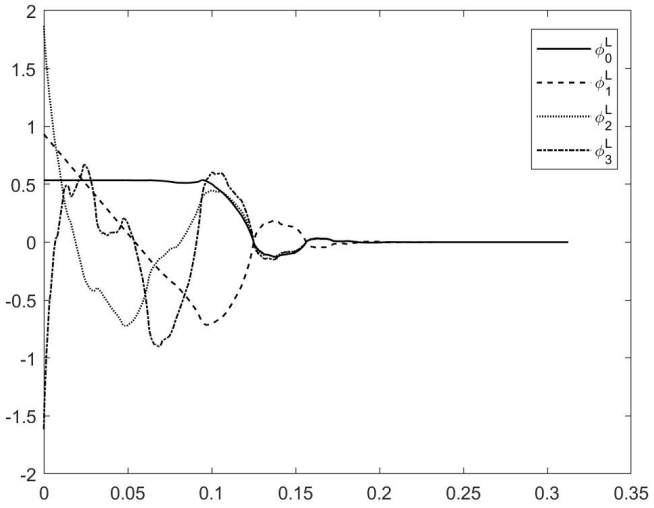

Figure 5.7: Orthogonal left scaling vector on the interval $[0, 1]$, solution 1

For another regular solution, we choose the eigenvalues λ_1, λ_4, λ_5 and λ_6 and we have

$$E = \begin{pmatrix} 1 & 0 & 0 & 0 \\ 0 & 0.2689 & 0 & 0 \\ 0 & 0 & -0.1956 & 0 \\ 0 & 0 & 0 & -0.0757 \end{pmatrix},$$

$$C = \begin{pmatrix} 0.3536 & 0.3536 & 0.3536 & 0.3536 & 0.3536 & 0.3536 & 0.3536 & 0.3536 \\ 0.7284 & 0.4260 & 0.1959 & 0.0527 & 0 & 0.0568 & 0.2111 & 0.4460 \\ -0.3308 & 0.9364 & 0.0647 & -0.0127 & 0 & -0.0182 & 0.0928 & -0.0227 \\ 0.0956 & -0.0224 & -0.0072 & 0.0005 & 0 & -0.0392 & 0.5182 & -0.8487 \end{pmatrix},$$

$$U = \begin{pmatrix} 1.5119 & 0 & 0 & 0 \\ -1.7863 & 3.1164 & 0 & 0 \\ -0.6285 & 0.2697 & 10.8109 & 0 \\ -2.2480 & 11.7180 & -55.2470 & 6.8603 \end{pmatrix}.$$

Then using the transformation matrix U, we obtain

$$E = \begin{pmatrix} 1 & 0 & 0 & 0 \\ -0.8638 & 0.2689 & 0 & 0 \\ -0.4495 & 0.0402 & -0.1956 & 0 \\ 0.1238 & 1.2428 & 0.6129 & -0.0757 \end{pmatrix},$$

$$F = \begin{pmatrix} 0.5345 & 0.5157 & 0.5345 & 0.3863 & 0 & -0.1148 & 0 & 0.0146 \\ 0.0263 & 0.3003 & 0.7585 & 0.6930 & 0 & -0.1858 & 0 & 0.0236 \\ 0.8380 & 0.7937 & -0.3477 & -0.5406 & 0 & 0.1117 & 0 & -0.0142 \\ 0.1064 & -0.1062 & -0.1341 & -0.1294 & 0 & 0.0363 & 0 & -0.0046 \end{pmatrix},$$

$$C = \begin{pmatrix} 0.5345 & 0.5345 & 0.5345 & 0.5345 & 0.5345 & 0.5345 & 0.5345 & 0.5345 \\ 1.6385 & 0.6962 & -0.0210 & -0.4674 & -0.6316 & -0.4546 & 0.0263 & 0.7585 \\ -3.6016 & 10.0157 & 0.5302 & -0.3448 & -0.2222 & -0.4032 & 0.8380 & -0.3477 \\ 26.6700 & -47.6878 & -2.1237 & 0.5257 & -0.7948 & 0.6044 & 0.1064 & -0.1341 \end{pmatrix}.$$

Figure 5.8 shows the second solution for the left boundary.

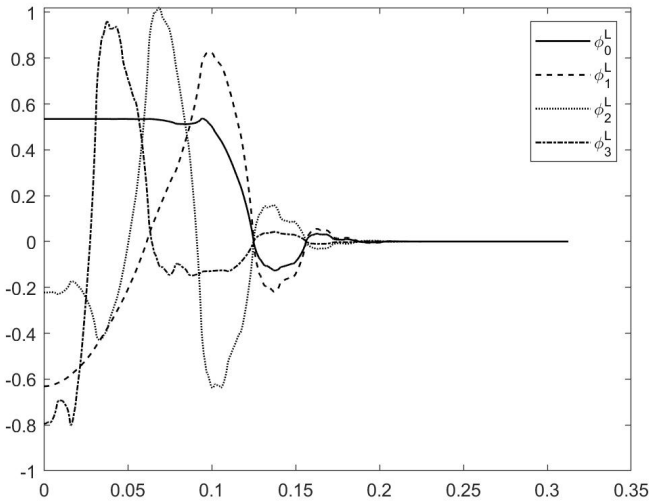

Figure 5.8: Orthogonal left scaling vector on the interval $[0, 1]$, solution 2

There exist other possible combinations as well. For example, the choice of eigenvalues λ_1, λ_2, λ_4 and λ_5 leads to the left boundary scaling vector in Figure 5.9.

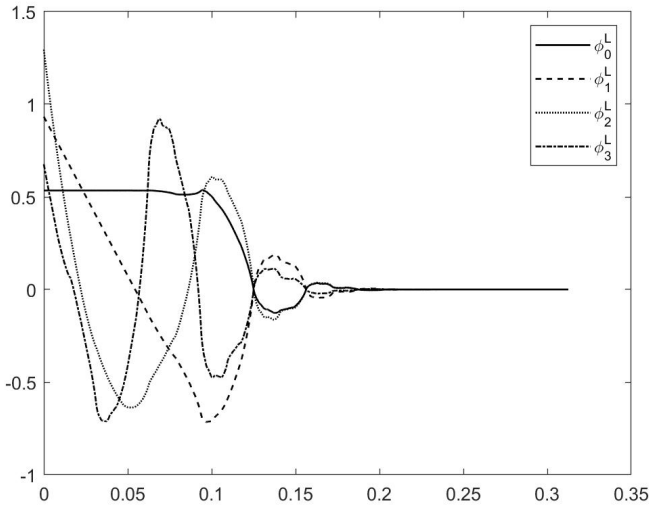

Figure 5.9: Orthogonal left scaling vector on the interval $[0, 1]$, solution 3

Two other regular solutions based on $(1, 3, 5, 6)$ and $(1, 2, 3, 7)$ are shown in Figure 5.10 and 5.11 respectively.

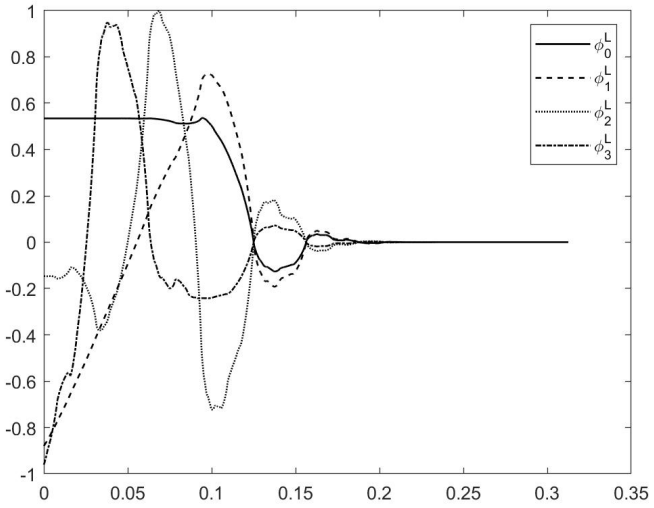

Figure 5.10: Orthogonal left scaling vector on the interval $[0, 1]$, solution 4

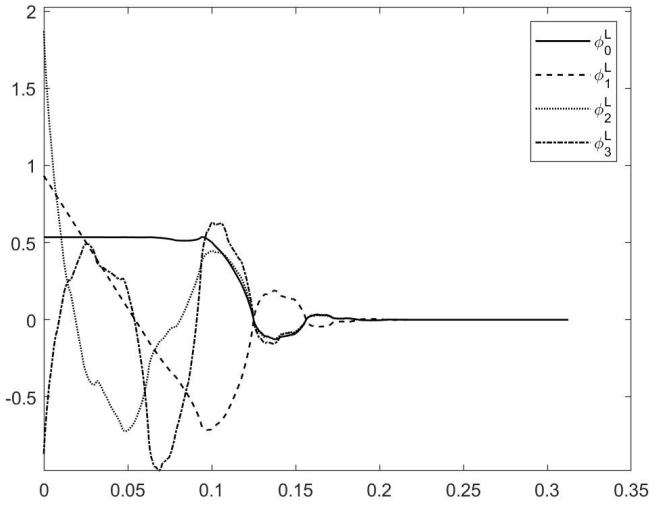

Figure 5.11: Orthogonal left scaling vector on the interval $[0, 1]$, solution 5

The choices of $(2, 3, 6, 7)$ and $(2, 3, 4, 5)$ lead to non-regular solutions which can be seen in Figure 5.12 and 5.13.

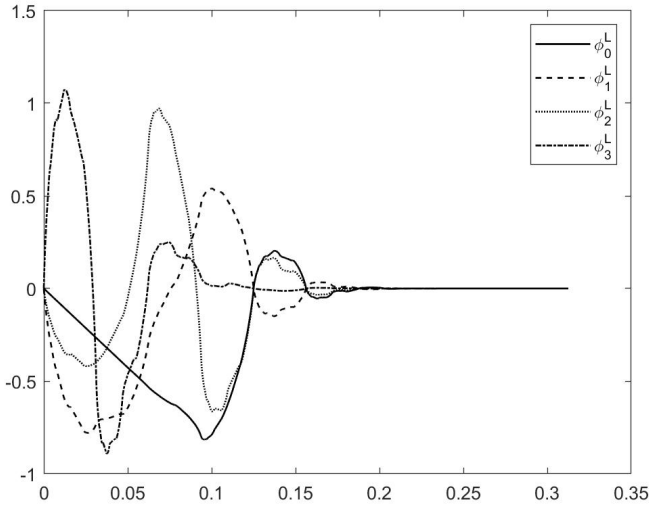

Figure 5.12: Orthogonal left scaling vector on the interval $[0, 1]$, solution 6

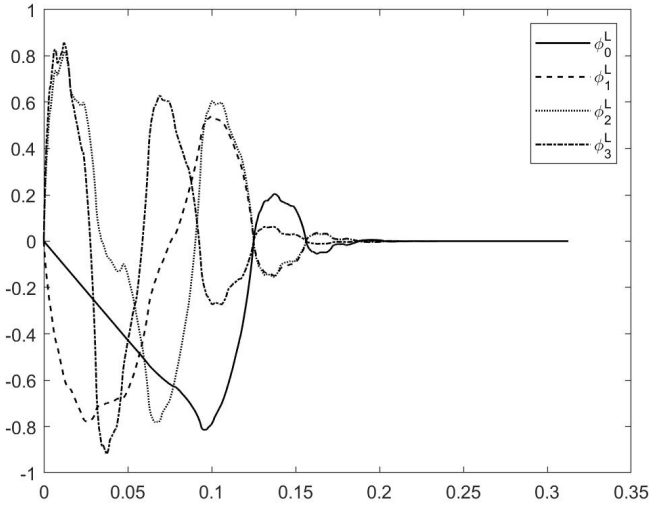

Figure 5.13: Orthogonal left scaling vector on the interval $[0, 1]$, solution 7

Finally, we want to plot the orthogonal scaling vector for the right side. Similar to the left edge, we compute matrices $\widetilde{W}$ and $\widetilde{V}$:

$$\widetilde{W} = \begin{pmatrix} A_0 & A_1 & A_2 & A_3 \\ 0 & 0 & A_0 & A_1 \\ 0 & 0 & 0 & 0 \\ 0 & 0 & 0 & 0 \end{pmatrix}, \quad \widetilde{V} = \begin{pmatrix} A_4 & A_5 & 0 & 0 \\ A_2 & A_3 & A_4 & A_5 \\ A_0 & A_1 & A_2 & A_3 \\ 0 & 0 & A_0 & A_1 \end{pmatrix},$$

and then we have following left eigenvectors and their corresponding eigenvalues of matrix $\widetilde{V}$:

$$\begin{aligned}
&\lambda_1 = 1, \quad v_1 = (0.3536, 0.3536, 0.3536, 0.3536, 0.3536, 0.3536, 0.3536, 0.3536),\\
&\lambda_2 = 0.5, \quad v_2 = (0.6030, 0.4523, 0.3015, 0.1508, 0, -0.1508, -0.3015, -0.4523),\\
&\lambda_3 = 0.4672, \quad v_3 = (-0.5770, -0.4215, -0.2695, -0.1259, 0, 0.1555, 0.3329, 0.5157),\\
&\lambda_4 = 0.2689, \quad v_4 = (0.7284, 0.4260, 0.1959, 0.0527, 0, 0.0568, 0.2111, 0.4460),\\
&\lambda_5 = -0.1956, \quad v_5 = (-0.3308, 0.9364, 0.0647, -0.0127, 0, -0.0182, 0.0928, -0.0227),\\
&\lambda_6 = -0.0757, \quad v_6 = (0.0956, -0.0224, -0.0072, 0.0005, 0, -0.0392, 0.5182, -0.8487),\\
&\lambda_7 = 0, \quad v_7 = (0.7015, 0.0891, 0, 0, 0, 0, -0.0891, 0.7014).
\end{aligned}$$

As in the left boundary, we have many choices and here we present some of them. By selecting the eigenvalues λ_1, λ_2, λ_3 and λ_4, we obtain matrices $\widetilde{E}$ and D:

$$\widetilde{E} = \begin{pmatrix} 1 & 0 & 0 & 0 \\ 0 & 0.5 & 0 & 0 \\ 0 & 0 & 0.4672 & 0 \\ 0 & 0 & 0 & 0.2689 \end{pmatrix},$$

$$D = \begin{pmatrix} 0.3536 & 0.3536 & 0.3536 & 0.3536 & 0.3536 & 0.3536 & 0.3536 & 0.3536 \\ 0.6030 & 0.4523 & 0.3015 & 0.1508 & 0 & -0.1508 & -0.3015 & -0.4523 \\ -0.5770 & -0.4215 & -0.2695 & -0.1259 & 0 & 0.1555 & 0.3329 & 0.5157 \\ 0.7284 & 0.4260 & 0.1959 & 0.0527 & 0 & 0.0568 & 0.2111 & 0.4460 \end{pmatrix}.$$

Consequently to find an orthogonal solution, we compute matrix U:

$$U = \begin{pmatrix} 1.3333 & 0 & 0 & 0 \\ -2.3360 & 2.4449 & 0 & 0 \\ -4.5136 & 81.6236 & 83.3098 & 0 \\ -5.7884 & 333.2705 & 394.4857 & 39.8692 \end{pmatrix}.$$

Then we obtain new matrices $\widetilde{E}$, $\widetilde{F}$ and D:

$$\widetilde{E} = \begin{pmatrix} 1 & 0 & 0 & 0 \\ -0.8760 & 0.5 & 0 & 0 \\ 0.1164 & 1.0960 & 0.4672 & 0 \\ 0.2825 & 0.1591 & 0.9386 & 0.2689 \end{pmatrix},$$

$$\widetilde{F} = \begin{pmatrix} 0 & 0.0166 & 0 & 0.1307 & 0.4714 & 0.5727 & 0.4714 & 0.4585 \\ 0 & 0.0214 & 0 & 0.1683 & 0.6484 & 0.6710 & 0.2798 & 0.0693 \\ 0 & -0.0130 & 0 & -0.1021 & -0.4413 & -0.3450 & 0.2081 & 0.4464 \\ 0 & 0.0090 & 0 & 0.0706 & 0.3623 & 0.1960 & -0.5932 & -0.6441 \end{pmatrix},$$

$$D = \begin{pmatrix} 0.4714 & 0.4714 & 0.4714 & 0.4714 & 0.4714 & 0.4714 & 0.47140.4714 \\ 0.6484 & 0.2798 & -0.0887 & -0.4573 & -0.8259 & -1.1945 & -1.5630 - 1.9316 \\ -0.4413 & 0.2081 & 0.5594 & 0.2190 & -1.5958 & -0.9455 & 1.52564.4550 \\ 0.3623 & -0.5932 & -0.0804 & 0.6225 & -2.0465 & 11.3210 & 37.199168.4627 \end{pmatrix}.$$

Now we can plot the orthogonal right boundary vector $\Phi^R = (\phi_0^R, \phi_1^R, \phi_2^R, \phi_3^R)$ as in Figure 5.14.

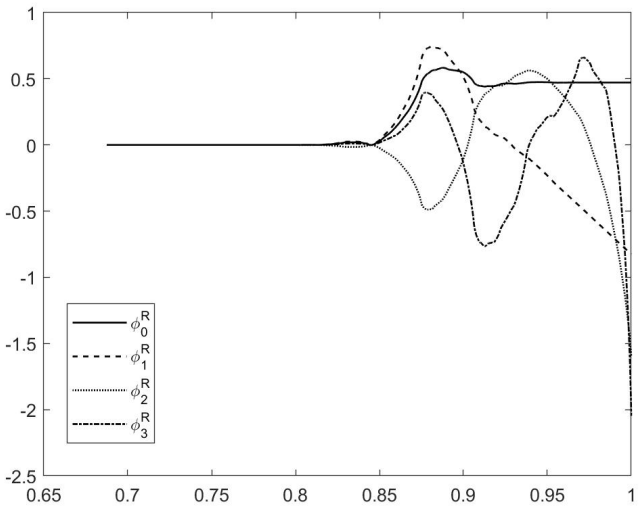

Figure 5.14: Orthogonal right scaling vector on the interval $[0, 1]$, solution 1

Furthermore, the choice of $(1, 4, 5, 6)$ leads to a regular solution which can be seen in Figure 5.15.

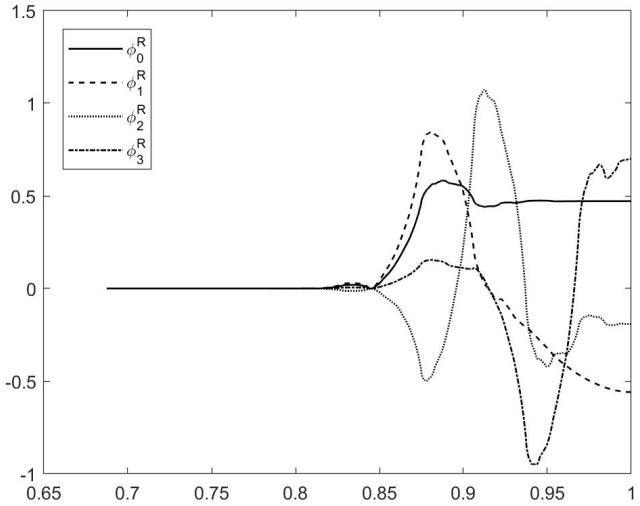

Figure 5.15: Orthogonal right scaling vector on the interval $[0, 1]$, solution 2

Two other regular solutions have been shown in Figures 5.16 and 5.17.

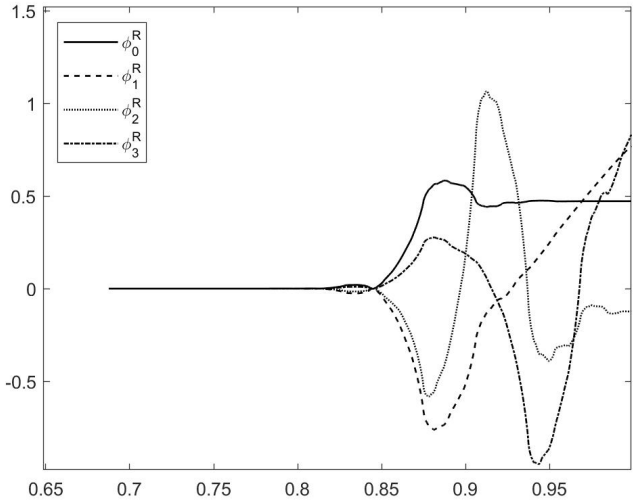

Figure 5.16: Orthogonal right scaling vector on the interval $[0, 1]$, solution 3, (1,3,5,6)

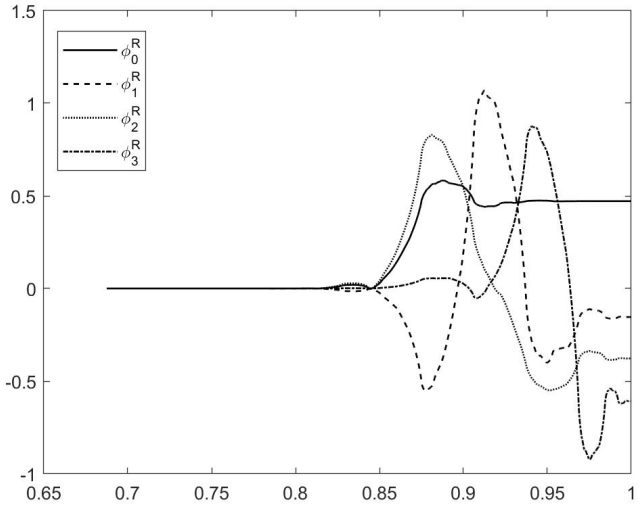

Figure 5.17: Orthogonal right scaling vector on the interval $[0, 1]$, solution 4, (1,5,6,7)

For the non-regular solution, we might choose the eigenvalues $(2, 3, 4, 5)$ and obtain the right boundary scaling vector in Figure 5.18.

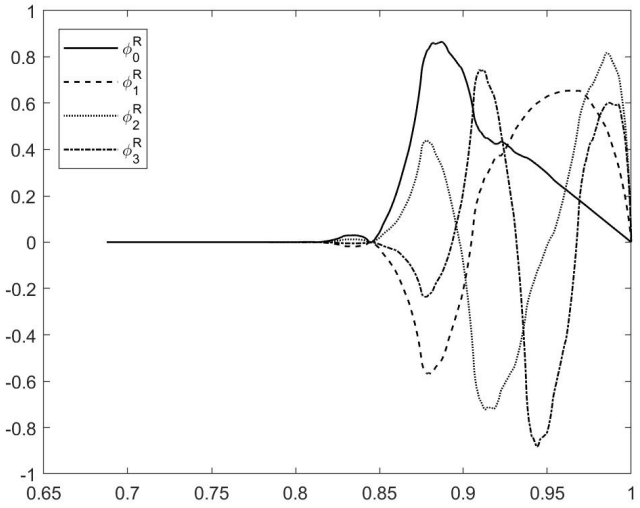

Figure 5.18: Orthogonal right scaling vector on the interval $[0, 1]$, solution 5

5.5 Construction of Orthogonal Multiwavelets on the Interval

Given the orthogonal multigenerators on the interval $[0, 1]$, our purpose is now to determine the corresponding multiwavelets. In this section, by applying the orthogonal conditions for the multiwavelets, we intend to find the boundary multiwavelets and their

recursion coefficients. Therefore, we may compute the matrices G and H_t, $\widetilde{G}$ and $\widetilde{H}_t$ in (5.24) to determine the boundary multiwavelets and then visualize them.

Since our boundary scaling vectors are orthogonal, we may consider the boundary multiwavelets Ψ^L and Ψ^R to be orthogonal as well, i.e.,

$$\begin{aligned}
&\langle \Psi^L(x), \Psi^L(x)\rangle = I_l,\\
&\langle \Psi^L(x), \Phi^L(x)\rangle = 0,\\
&\langle \Psi^L(x), \Psi(x-k)\rangle = 0, \qquad k \geq 0,\\
&\langle \Psi^L(x), \Phi(x-k)\rangle = 0, \qquad k \geq 0,
\end{aligned} \tag{5.46}$$

for the left side and

$$\begin{aligned}
&\langle \Psi^R(x), \Psi^R(x)\rangle = I_r,\\
&\langle \Psi^R(x), \Phi^R(x)\rangle = 0,\\
&\langle \Psi^R(x), \Psi(x-k)\rangle = 0, \qquad k \geq 0,\\
&\langle \Psi^R(x), \Phi(x-k)\rangle = 0, \qquad k \geq 0,
\end{aligned}$$

for the right boundary multiwavelet. Consequently, the first relation of (5.46) and the equation (5.24) for $j = 0$ lead to

$$\begin{aligned}
&\langle \Psi^L(x), \Psi^L(x)\rangle\\
&= \langle G\Phi^L(2x) + \sum_{t=0}^{M-2} H_t\Phi(2x-t), G\Phi^L(2x) + \sum_{t=0}^{M-2} H_t\Phi(2x-t)\rangle\\
&= \frac{1}{2}GG^\top + \frac{1}{2}\sum_{t=0}^{M-2} H_tH_t^\top = \frac{1}{2}(GG^\top + HH^\top),
\end{aligned}$$

where $H = (H_0, \cdots, H_{M-2})$. Thus, the first condition in (5.46) reduces to

$$\frac{1}{2}(GG^\top + HH^\top) = I_l. \tag{5.47}$$

Moreover, for the second condition in (5.46), we get

$$\begin{aligned}
&\langle \Psi^L(x), \Phi^L(x)\rangle\\
&= \langle G\Phi^L(2x) + \sum_{t=0}^{M-2} H_t\Phi(2x-t), E\Phi^L(2x) + \sum_{t=0}^{M-2} F_t\Phi(2x-t)\rangle\\
&= \frac{1}{2}GE^\top + \frac{1}{2}\sum_{t=0}^{M-2} H_tF_t^\top = \frac{1}{2}(GE^\top + HF^\top).
\end{aligned}$$

Therefore we obtain

$$GE^\top + HF^\top = 0. \tag{5.48}$$

For the other orthogonal conditions in (5.46), we have

$$\sum_{t=0}^{M-2} H_tB_{t-2k}^\top = 0, \qquad \sum_{t=0}^{M-2} H_tA_{t-2k}^\top = 0, \tag{5.49}$$

where $k \geq 0$.

The conditions (5.49) lead to a trivial solution and is automatically satisfied. Therefore, for finding the matrices G and H_t, we apply the conditions (5.47) and (5.48) and it yields a system of equations. However, it is clear that this system may be underdetermined and there exist several solutions anyway.
Similarly, for the construction of right boundary multiwavelet, we apply the following orthogonal conditions

$$\begin{aligned} &\frac{1}{2}(\widetilde{G}\widetilde{G}^\top + \widetilde{H}\widetilde{H}^\top) = I_r, \\ &\widetilde{G}\widetilde{E}^\top + \widetilde{H}\widetilde{F}^\top = 0, \end{aligned} \tag{5.50}$$

where $\widetilde{H} = (\widetilde{H}_{-M+2}, \cdots, \widetilde{H}_0)$.

As stated above, the solutions obtained by our construction are not unique. In the sequel, we present a couple of these solutions.

Example 5.6. For the left boundary multiwavelet corresponding to the scaling vector in Example 5.4, we have to compute the matrices G and H in (5.47). Suppose that $G = (g_{ij})$, $1 \leq i, j \leq 2$, and $H = (h_{ij})$, $1 \leq i \leq 2$, $1 \leq j \leq 4$. After applying the conditions (5.47) and (5.48) for matrices E and F in solution 1, we get a system of equations with 5 degrees of freedom. For $g_{12} = 0$, $h_{11} = -0.6$, $h_{21} = -0.55$ and $h_{13} = h_{23} = 0$, we have

$$G = \begin{pmatrix} 0.1252 & 0 \\ 0.2224 & 1.1206 \end{pmatrix},$$
$$H = \begin{pmatrix} -0.6000 & 0.8339 & 0 & 0.9638 \\ -0.5500 & 0.2396 & 0 & -0.5786 \end{pmatrix}.$$

Consequently, we obtain the orthogonal left boundary multiwavelet depicted in Figure 5.19.

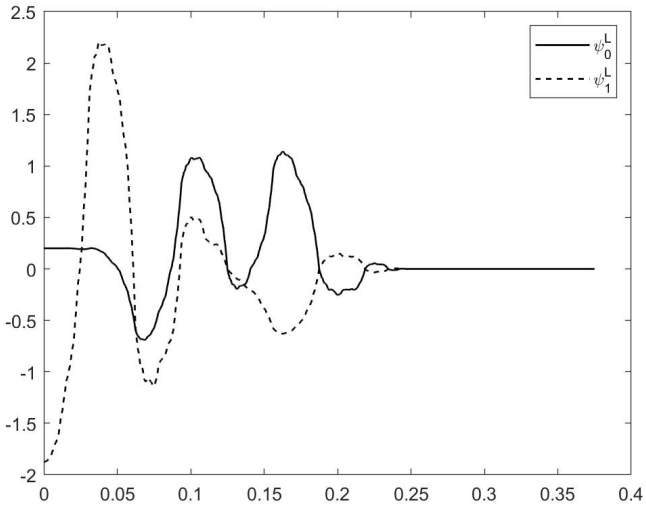

Figure 5.19: Orthogonal left multiwavelet on the interval $[0, 1]$, solution 1

The left boundary multiwavelet corresponding to solution 2 in Example 5.4 has been shown in Figure 5.20. Here we set $g_{12} = 0$, $h_{11} = -0.65$, $h_{21} = -0.55$ and $h_{13} = h_{23} = 0$. Then we obtain

$$G = \begin{pmatrix} 0.1646 & 0 \\ -0.0167 & 0.7525 \end{pmatrix},$$
$$H = \begin{pmatrix} -0.6500 & 0.8274 & 0 & 0.9305 \\ -0.5500 & 0.5763 & 0 & -0.8937 \end{pmatrix}.$$

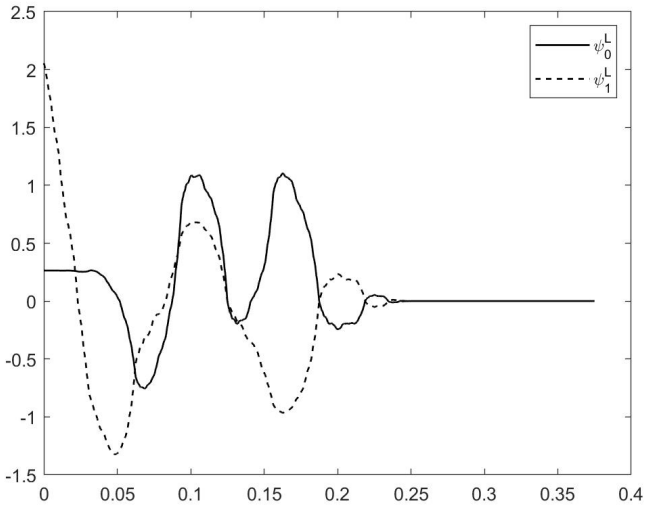

Figure 5.20: Orthogonal left multiwavelet on the interval $[0, 1]$, solution 2

Similar to the left boundary multiwavelet, we find the matrices $\widetilde{G}$ and $\widetilde{H}$ using the conditions (5.50). First of all, we compute the solution corresponding to the solution 1 for the right boundary scaling vector in Example 5.4. Let $\widetilde{G} = (\widetilde{g}_{ij})$, $1 \le i, j \le 2$, and $\widetilde{H} = (\widetilde{h}_{ij})$, $1 \le i \le 2$, $1 \le j \le 4$. We set $\widetilde{g}_{12} = 0$, $\widetilde{h}_{13} = 0.55$, $\widetilde{h}_{21} = 0.45$ and $\widetilde{h}_{11} = \widetilde{h}_{21} = 0$ and obtain

$$\widetilde{G} = \begin{pmatrix} 0.0699 & 0 \\ -0.0996 & -1.2752 \end{pmatrix},$$
$$\widetilde{H} = \begin{pmatrix} 0 & 1.0243 & 0.5500 & -0.8022 \\ 0 & -0.3654 & 0.4500 & -0.1667 \end{pmatrix}.$$

Then we get the orthogonal right boundary multiwavelet depicted in Figure 5.21.

Moreover, for the right boundary multiwavelet corresponding to solution 2 in Example 5.4, we set $\widetilde{g}_{12} = 0$, $\widetilde{h}_{13} = 0.55$, $\widetilde{h}_{23} = 0.45$ and $\widetilde{h}_{11} = \widetilde{h}_{21} = 0$ and obtain

$$\widetilde{G} = \begin{pmatrix} 0.0575 & 0 \\ 0.2921 & 0.9095 \end{pmatrix},$$
$$\widetilde{H} = \begin{pmatrix} 0 & -1.2774 & 0.5500 & -0.2498 \\ 0 & 0.3756 & 0.4500 & -0.8626 \end{pmatrix}.$$

These matrices lead to the solution 2 showing in Figure 5.22.

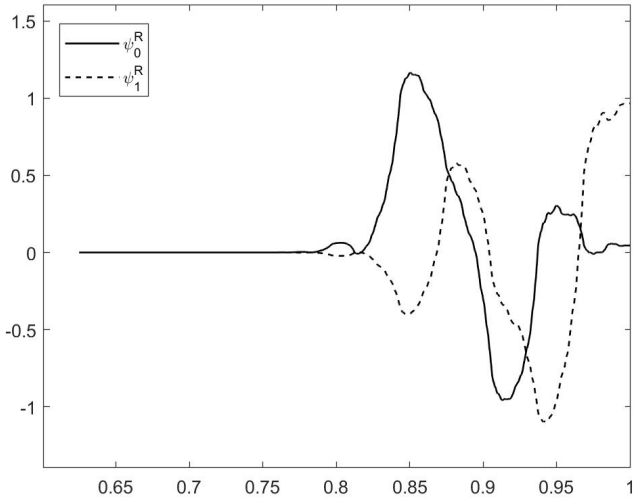

Figure 5.21: Orthogonal right multiwavelet on the interval $[0, 1]$, solution 1

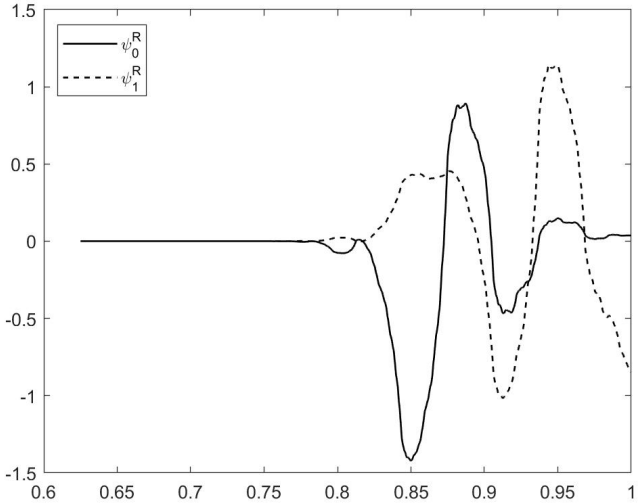

Figure 5.22: Orthogonal right multiwavelet on the interval $[0, 1]$, solution 2

Chapter 6

Conclusion and Perspectives

In this thesis, we have discussed the construction of boundary scaling vectors and multiwavelets, which are either orthonormal or interpolating. We introduced two different approaches, to find appropriate boundary vectors. In the following, we want to summarize our results and discuss the future prospects.

The first approach given in chapter 4 leads to interpolating scaling vector on the interval. By using the Lagrange polynomials, we defined an interpolation operator and then boundary interpolating functions which still satisfy the interpolation property and have the same approximation order as those on the line. Therefore, we expect our approach to be useful in application purposes, especially for solving the boundary value problems. The only disadvantage of this approach is that the boundary scaling vectors can not be orthonormal anymore. Consequently, we proved the error estimate of interpolation operator in $L_2(\mathbb{R})$ as well as $L_2[0,1]$ which plays a significant role in our construction. Moreover, the refinability of boundary scaling vectors was verified which is important to construct a multiresolution analysis on the interval. In addition, we constructed the boundary multiwavelates corresponding to interpolating scaling vectors. Finally, we provided some examples which are the first ones of their kind throughout the known literature.

In chapter 5, we presented a second approach, base on orthonormal scaling vectors in [42]. Applying the orthogonality and refinability conditions, we tried to construct new edge functions, which are orthonormal and keep the approximation order. As states before, this new boundary functions can be put to good use in signal processing when the signal is finite. In contrast to the results in [2], which are only for the case of four masks and provide the approximation order 1 or 2, our construction justifies for an arbitrary number of masks and better approximation order. Consequently, we constructed corresponding orthogonal multiwavelets and the Discrete Multiwavelet Transform on the interval which is a very useful tool in applications.

In the following, we want to present some future researches:

- In this thesis we discuss more theoretical aspects. The implementation of new bases and numerical experiments will be one of the possible future works.

- We introduced an approach to construct the interpolating multiwavelets on the interval. The next challenge is to generalize the approach to higher-dimensional domains. We will start with simple geometries such as cubes. Our aim will be to construct generalized, highly anisotropic tensor wavelets as, e.g., introduced in [26]

for the single generator case. The approximation properties of these new bases will be carefully studied, and similar to the single generator setting we expect dimension-independent convergence rates. We expect that these new bases will be extremely well-suited for the treatment of high-dimensional problems.

- The next step will be the generalization to more complicated domains. We will restrict ourselves to polygonal and polyhedral domains. For these kinds of domains, a first construction of generalized tensor wavelets has been performed in [10]. There, by the application of extension operators, bases on domains have been constructed from corresponding bases on subdomains that form a non-overlapping decomposition. As subdomains, hypercubes (or smooth parametric images of those), equipped with tensor product wavelet bases have been used. Of course, for our purposes, this construction has to be generalized to the multiwavelet case. Once again, we will study the approximation properties, and similar to the construction in [10], we expect dimension-independent convergence rates.

Zusammenfassung

In den letzten Jahren haben sich Wavelets zu einem hochwertigen Hilfsmittel in der angewandten Mathematik entwickelt. Eine Waveletbasis ist im Allgemeinen ein System von Funktionen, das durch die Skalierung, Translation und Dilatation einer endlichen Menge von Funktionen, den sogenannten Mutterwavelets, entsteht. Wavelets wurden sehr erfolgreich in der digitalen Signal- und Bildanalyse, z. B. zur Datenkompression verwendet. Ein weiteres wichtiges Anwendungsfeld ist die Analyse und die numerische Behandlung von Operatorgleichungen. Insbesondere ist es gelungen, adaptive numerische Algorithmen basierend auf Wavelets für eine riesige Klasse von Operatorgleichungen, einschließlich Operatoren mit negativer Ordnung, zu entwickeln, siehe [15, 16]. Der Erfolg der Wavelet-Algorithmen ergibt sich als Konsequenz der folgenden Fakten:

- Gewichtete Folgennormen von Wavelet-Expansionskoeffizienten sind in einem bestimmten Bereich (abhängig von der Regularität der Wavelets) äquivalent zu Glättungsnormen wie Besov- oder Sobolev-Normen.
- Für eine breite Klasse von Operatoren ist ihre Darstellung in Wavelet-Koordinaten nahezu diagonal.
- Die verschwindenden Momente von Wavelets entfernen den glatten Teil einer Funktion und führen zu sehr effizienten Komprimierungsstrategien.

Diese Fakten können z. B. verwendet werden, um adaptive numerische Strategien mit optimaler Konvergenzgeschwindigkeit zu konstruieren, in dem Sinne, dass diese Algorithmen die Konvergenzordnung der besten N-Term-Approximationsschemata realisieren. Die maßgeblichen Ergebnisse lassen sich für lineare, symmetrische, elliptische Operatorgleichungen erzielen. Es existiert auch eine Verallgemeinerung für nichtlineare elliptische Gleichungen [17]. Hier verbirgt sich jedoch eine ernste Schwierigkeit: Jeder numerische Algorithmus für diese Gleichungen erfordert die Auswertung eines nichtlinearen Funktionals, welches auf eine Wavelet-Reihe angewendet wird. Obwohl einige sehr ausgefeilte Algorithmen existieren [22], erweisen sie sich als ziemlich langsam in der Praxis. In neueren Studien wurde gezeigt, dass dieses Problem durch sogenannte Interpolanten verbessert werden kann [61]. Dabei stellt sich heraus, dass die meisten bekannten Basen der Interpolanten keine stabilen Basen in $L_2[a, b]$ bilden.

In der vorliegenden Arbeit leisten wir einen wesentlichen Beitrag zu diesem Problem und konstruieren neue Familien von Interpolanten auf beschränkten Gebieten, die nicht nur interpolierend, sondern auch stabil in $L_2[a, b]$ sind. Da dies mit nur einem Generator schwer (oder vielleicht sogar unmöglich) zu erreichen ist, werden wir mit Multigeneratoren und Multiwavelets arbeiten. Es wurde in den Artikeln [42, 43, 45] gezeigt, dass es im Rahmen von Multiwavelets möglich ist, orthogonale und biorthogonale Basen zu konstruieren,

die zumindest auf der reellen Linie interpolierend sind. Das Ziel dieses Projektes ist es, die Konstruktionen in [42] auf einem Intervall anzupassen. Zunächst beschränken wir uns auf die Interpolationseigenschaft. Innerhalb des Intervalls verwenden wir ausschließlich die interpolierenden Wavelets aus [42]. Um jedoch die Approximationseigenschaften der Multiskalenanalyse zu bewahren, sind einige Modifikationen am Rand erforderlich, in dem Sinne, dass die polynomiale Genauigkeit beibehalten wird. Diese Modifikationen müssen so durchgeführt werden, dass die Interpolationseigenschaft nicht zerstört wird. Wir folgen teilweise dem Ansatz in [4, 5]. Die Analyse in diesen Artikeln wurde nur für einen einzelnen Generator durchgeführt und muss daher für mehrere Generatoren verallgemeinert werden. Daher werden wir Multigeneratoren konstruieren, die einen kleinen Träger haben und deren interpolierende Natur zu einem praktischen Weg führt, um die Multiskalenanalyse auf komplexeren Geometrien zu erzielen.

Der nächste Schritt ist die Konstruktion von den Skalierungsvektoren, um die Orthogonalität zu bewahren. Für den Fall eines Generators existieren bereits mehrere Ansätze zur Konstruktion von biorthogonalen und orthonormalen Basen auf Intervallen [18,21,58]. Jedoch können skalare orthogonale Wavelets vorteilhafte Eigenschaften wie kompakter Träger, Approximationsordnung und Glätte nicht gleichzeitig aufweisen. Darüber hinaus betrachten die bisher veröffentlichten Arbeiten einen speziellen Fall orthogonaler Wavelets auf dem Intervall. Um diese Einschränkungen zu überwinden, konstruieren wir orthogonale Multigeneratoren und Multiwavelets, die alle vorteilhaften Eigenschaften bewahren. Motiviert durch die Ergebnisse in [2, 3, 41] entwickeln wir einen Ansatz, um die Diskrete Multiwavelet-Transformation (DMWT) auf das Intervall anzupassen. Der DMWT wird zum Entrauschen und Komprimieren von unendlichen Signalen und Bildern verwendet. In vielen Anwendungen haben wir es mit endlichen Signalen zu tun und müssen die DMWT nahe der Grenzen modifizieren. Wir benutzen wieder die Konstruktion von Karsten Koch in [42] und versuchen, die passenden Randfunktionen an den Kanten zu finden.

Diese Arbeit ist wie folgt gegliedert. In Kapitel 2 führen wir die notwendigen Notationen und Definitionen ein. Unter anderem definieren wir in Unterkapitel 2.1.1 Sobolev-Räume. Im Anschluss stellen wir einige Definitionen vor, die in dieser Arbeit benötigt werden. Kapitel 3 ist der Wavelet- und Multiwavelet-Einführung gewidmet. In Abschnitt 3.1 wiederholen wir kurz einige Grundkonzepte von Wavelets. Außerdem betrachten wir die Skalierungsvektoren und ihre Eigenschaften in Abschnitt 3.2. Hier erfolgt zunächst die Einführung der Diskreten Multiwavelet-Transformation und Multiwavelets. Insbesondere konzentrieren wir uns auf die Konstruktion von Karsten Koch in [42]. In Kapitel 4 passen wir diese Konstruktion an einen beschränkten Definitionsbereich an. In Abschnitt 4.1 entwickeln wir eine Methode zur Konstruktion der interpolierenden Skalierungsvektoren auf dem Intervall $[0, 1]$. Im nächsten Abschnitt werden wir überprüfen, ob diese auch verfeinerbar sind. Dies ist besonders wichtig, um eine neue Multiskalenanalyse für das Intervall zu konstruieren. Abschnitt 4.3 widmet sich der Approximationsordnung der neuen Skalierungsvektoren. Zuerst untersuchen wir die Fähigkeit der Randskalierungsvektoren, die Polynome zu reproduzieren. Im Mittelpunkt dieses Abschnitts steht die Überprüfung, ob der Interpolationsoperator die Fehlerabschätzungen in $L_2(\mathbb{R})$ und dann in $L_2[0, 1]$ erfüllt. Nachfolgend visualisieren wir unsere Konstruktion und geben einige Beispiele an. Schließlich konstruieren wir, aufbauend auf den neuen, interpolierenden Skalierungsvektoren, Multiwavelets. In Kapitel 5 entwickeln wir einen Ansatz zur Konstruktion orthogonaler Randskalierungsvektoren, die einen kleinen Träger und die gleiche Regularität wie

die Skalierungsvektoren auf der reellen Linie haben. Zunächst betrachten wir die notwendigen und hinreichenden Bedingungen für unsere Konstruktion. Dann modifizieren wir in Abschnitt 5.2 die DMWT, um geeignete Funktionen an den Grenzen zu finden. Außerdem berechnen wir die notwendige Anzahl von Randskalierungsfunktionen an jeder Kante. Der nächste Abschnitt beschäftigt sich mit den notwendigen und hinreichenden Bedingungen für die Approximationsordnung orthogonaler Randvektoren. In Abschnitt 5.4.1 leiten wir den allgemeinen Algorithmus unserer Konstruktion her und stellen dann einige Beispiele vor. Der letzte Abschnitt ist der Konstruktion orthogonaler Multiwavelets gewidmet, die orthogonalen Randvektoren entsprechen, sowie deren Visualisierung. Abschließend fassen wir in Kapitel 6 unsere Ergebnisse zusammen und diskutieren die zukünftige Forschung. Außerdem befindet sich ab Seite 97 eine Liste zur Erklärung der, in dieser Arbeit verwendeten, Notation.

Notation

We list here all used notations in this thesis. The number in the right column refers to the page where the symbol is introduced or where it appears first.

$\mathbb{N}$	Set of natural numbers	
$\mathbb{N}_0$	Set of non-negative integers	
$\mathbb{Z}$	Set of integers	
$\mathbb{R}$	Set of real numbers	
$\mathbb{C}$	Set of complex numbers	
$\mathbb{R}^n$	n-dimensional Euclidian space	
$\lvert\cdot\rvert$	Absolute value, Euclidian norm on $\mathbb{R}^n$	
$\langle\cdot,\cdot\rangle$	Standard scalar product on $\mathbb{R}^n$	40
$\lVert\cdot\rVert_2$	norm $\sqrt{\langle\cdot,\cdot\rangle}$ on $\mathbb{R}^n$	40
$A \subseteq B$	A is a subset of B	
$A \subset B$	A is a proper (or strict) subset of B, i.e., $A \subset B$ and $A \neq B$	
$\hookrightarrow$	Continuously linearly embedded	9
$\operatorname{supp} f$	Support of a function f	5
$\operatorname{ess\,sup}$	Essential supremum of a function f	6
$\operatorname{span}(S)$	Set of all finite linear combinations of elements (vectors) of S	20
$\operatorname{range}(A)$	Set of all possible linear combinations of column vectors of matrix A	12
$\operatorname{null}(A)$	Set of solutions to the equation $Ax = 0$	12
$\operatorname{rank}(A)$	Dimension of the vector space generated (or spanned) by columns of A	62
$\operatorname{spec}(A)$	Spectrum of an operator or a matrix A	21
$\lfloor x \rfloor$	greatest integer $\leq x$	63
$\lceil x \rceil$	smallest integer $\geq x$	61
$\delta_{i,j}$	Kronecker delta	
$\chi_A(x)$	Characteristic function for a given subset A	13
Ω	Domain, i.e., an open subset in $\mathbb{R}^n$	5
$\partial\Omega$	Boundary of a domain $\Omega \subseteq \mathbb{R}^n$	7
$D^\alpha f$, $\alpha \in \mathbb{N}_0^n$	generalized/weak/distributional derivative	5
$L_p(\Omega)$	Lebesgue space	6
$\ell_p(\mathbb{Z})$	Sequence space	6
$L_1^{loc}(\Omega)$	Space of local integrable functions	7
$C^m(\Omega)$	Space of m times continuously differentiable functions	5
$C^{m,k}(\Omega)$	Space of Hölder continuous functions	6
$C_0^\infty(\Omega)$	Space of test functions	6
$W_p^m(\Omega)$	Sobolev space with integer smoothness	7

$W_p^s(\Omega)$	Sobolev space with non-negative smoothness	7
$H^s(\Omega)$	Sobolev space with non-negative smoothness and parameter $p = 2$	8
$\langle f, g \rangle$	Inner product for two functions or two vectors f and g	6
$\hat{\varphi}$	Fourier transform of a function φ	9
$\mathcal{S}(\mathbb{R}^n)$	Schwartz space of rapidly decreasing real-valued functions on $\mathbb{R}^n$	9
$\mathcal{S}'(\mathbb{R}^n)$	Space of real-valued tempered distributions	9
$\{V_j\}_{j\in\mathbb{Z}}$	Multiresolution analysis (MRA)	13
$\{\widetilde{V}_j\}_{j\in\mathbb{Z}}$	Dual multiresolution analysis	24
W_j	Wavelet/Multiwavelet space	15
$(a_k)_{k\in\mathbb{Z}}$	Masks of a refinable function	14
$(b_k)_{k\in\mathbb{Z}}$	wavelet coefficients	15
$\phi_{j,k}$	Dyadic shifts and dilations of the scaling function	14
$\widetilde{\phi}$	Dual of scaling function ϕ	17
$\psi_{j,k}$	Mother wavelet corresponding to $\phi_{j,k}$	13
Φ	Multigenerator/Scaling vector	17
$\widehat{\Phi}$	Fourier transform of the scaling vector Φ	18
$\widetilde{\Phi}$	Dual of scaling vector Φ	24
Ψ	Multiwavelet	22
$\widehat{\Psi}$	Fourier transform of the multiwavelet Ψ	22
$(A_k)_{k\in\mathbb{Z}}$	Masks of refinable scaling vector	18
$\mathbf{A}(z)$	Symbol matrix of a refinable scaling vector	18
$\widetilde{\mathbf{A}}$	Symbol matrix of $\widetilde{\Phi}$	24
$\mathbf{A}_i(z)$	ith subsymbol of $\mathbf{A}(z)$	19
$(B_k)_{k\in\mathbb{Z}}$	Multiwavelet coefficients	22
$\mathbf{B}(z)$	Symbol matrix of a multiwavelet	22
$\overline{A}^\top$	Conjugate transpose of a matrix A	24
ϕ^L	Left boundary scaling function	34
ϕ^R	Right boundary scaling function	34
Φ^L	Left boundary scaling vector	34
Φ^R	Right boundary scaling vector	34
$\Phi^{[\,]}$	Scaling vector on the interval	38
$A^{[\,]}$	Mask of refinable scaling vector on the interval	38
ψ^L	Left boundary wavelet	49
ψ^R	Right boundary wavelet	50
Ψ^L	Left boundary multiwavelet	49
Ψ^R	Right boundary multiwavelet	50
$\Psi^{[\,]}$	Multiwavelet on the interval	49

$\|f\|_{C^m(\Omega)}$, $m \in \mathbb{N}_0$	5
$\|f\|_{C^{m,k}(\Omega)}$, $m \in \mathbb{N}_0$, $0 < k < 1$	6
$\|f\|_{L_p(\Omega)}$, $1 \le p \le \infty$	6
$\|c\|_{\ell_p}$, $1 \le p \le \infty$	6
$\|f\|_{W_p^m(\Omega)}$, $m \in \mathbb{N}_0$, $1 \le p \le \infty$	7

Bibliography

[1] R. A. Adams, *Sobolev Spaces*, Academic Press, New York, 1975.

[2] A. Altürk and F. Keinert, *Construction of Multiwavelets on an Interval*, Axioms **2** (2013), 122–141.

[3] ———, *Regularity of Boundary Wavelets*, J. Applied and Computational Harmonic Analysis **32** (2012), 65–85.

[4] S. Bertoluzza and G. Naldi, *A Wavelet Collocation Method for the Numerical Solution of Partial Differential Equations*, J. Applied and Computational Harmonic Analysis **3** (1996), 1–9.

[5] S. Bertoluzza, G. Naldi and J. C. Ravel, *Wavelet Methods for the Numerical Solution of Boundary Value Problems on the Interval*, Wavelet Analysis and Its Applications **5** (1994), 425–448.

[6] G. Beylkin, R. Coifman and V. Rokhlin, *Fast wavelet transforms and numerical algorithms I*, Comm. Pure Appl. Math. XLIV, no. 2 (1991).

[7] S. Brenner and R. L. Scott, *The Mathematical Theory of Finite Element Methods*, Springer, New York, 1994.

[8] C. Cabrelli, C. Heil, and U. Molter, *Accuracy of Lattice Translates of Several Multidimensional Refinable Functions*, J. Approx. Theory **95** (1998),5–52.

[9] ———, *Accuracy of Several Multidimensional Refinable Distributions*, J. Fourier Anal. Appl. **6** (2000), no. 5, 483–502.

[10] N. Chegini, S. Dahlke, U. Friedrich and R. Stevenson, *Piecewise Tensor Product Wavelet Bases by Extensions and Approximation*, Mathematics of computation **82** (2013), 2157–2190.

[11] O. Christensen, *An Introduction to Frames and Riesz Bases*, Birkhäuser, 2003.

[12] C. K. Chui and Q. T. Jiang, *Multivariate Balanced Vector–Valued Refinable Functions*, Modern developments in multivariate approximation. Proceedings of the 5th international conference, Witten–Bommerholz, Germany, September 22–27 (W. Haussmann, K. Jetter, M. Reimer, and J. Stöckler, eds.), Int. Ser. Numer. Math., vol. 145, Birkhäuser (2003), 71–102.

[13] ———, *Balanced Multi-Wavelets in* $\mathbf{R}^s$, Math. Comput. **74** (2005), 1323–1344.

[14] C. K. Chui and C. Li, *A General Framework of Multivariate Wavelets with Duals*, Appl. Comput. Harmon. Anal. **1** (1994), no. 4, 368–390.

[15] A. Cohen, W. Dahmen and R. DeVore, *Adaptive Wavelet Methods II–Beyond the Elliptic Case*, Found. Comput. Math. **2** (2002), no. 3, 203–245.

[16] _____, *Adaptive Wavelet Methods for Elliptic Operator Equations:Convergence rates*, Math. Comp. **70** (2001), no. 233, 27–75.

[17] _____, *Adaptive Wavelet Schemes for Nonlinear Variational Problems*, SIAM J. Numer. Anal. **41** (2003), no. 5, 1785–1823.

[18] A. Cohen, I. Daubechies and P. Vial, *Wavelets on the Interval and Fast Wavelet Transforms*, J. Applied and Computational Harmonic Analysis **1** (1993), 54–81.

[19] S. Dahlke, *Wavelets: Construction Principles and Applications to the Numerical Treatment of Operator Equations*, Habilitation thesis, RWTH Aachen, Berichte aus der Mathematik, Shaker, Aachen, 1997.

[20] S. Dahlke and A. Kunoth, *A Biorthogonal Wavelet Approach for Solving Boundary Value Problems*, Preprint, 1993.

[21] W. Dahmen, A. Kunoth and K. Urban, *Biorthogonal Spline Wavelets on the Interval- Stability and Moment Conditions*, Applied and Computational Harmonic Analysis **6** (1999), 132–196.

[22] W. Dahmen, R. Schneider and Y. Xu, *Nonlinear Functionals of Wavelet Expansions–Adaptive Reconstruction and Fast Evaluation*, Numer. Math. **86** (2000), no. 1, 49–101.

[23] I. Daubechies, *Orthonormal Bases of Compactly Supported Wavelets*, Commun. Pure Appl. Math. **41** (1988), no. 7, 909–996.

[24] _____, *Ten Lectures on Wavelets*, CBMS–NSF Regional Conference Series in Applied Math., vol. 61, SIAM, Philadelphia, 1992.

[25] C. de Boor, R. DeVore, and A. Ron, *On the Construction of Multivariate (pre–) Wavelets*, Constr. Approx. **9** (1993), no. 2, 123–166.

[26] T. J. Dijkema, C. Schwab and R. Stevenson, *An Adaptive Wavelet Method for Solving High-Dimensional Elliptic PDEs*, Constr. Approx. **30** (2009), 423–455.

[27] M. Dobrowolski, *Applied Functional Analysis. Functional Analysis, Sobolev Spaces and Elliptic Differential Equations (Angewandte Funktionalanalysis. Funktionalanalysis, Sobolev-Räume und elliptische Differentialgleichungen)*, 2nd revised and extended ed., Springer-Lehrbuch Masterclass, Berlin, 2010.

[28] D. Donoho, *Interpolating Wavelet Transform*, Preprint, 1992.

[29] J. Geronimo, D. Hardin, and P. R. Massopust, *Fractal Functions and Wavelet Expansions Based on Several Functions*, J. Approximation Theory **78** (1994), 373–401.

[30] G. H. Golub and C. F. Van Loan, *Matrix Computations*, 2nd ed. Baltimore: Johns University Press, 1989.

[31] T. N. T. Goodman and S. L. Lee, *Wavelets of Multiplicity r*, Trans. Amer. Math. Soc. **342** (1994), no. 1, 307–324.

[32] T. N. T. Goodman, S. L. Lee and W. S. Tang, *Wavelets in Wandering Subspaces*, Trans. Amer. Math. Soc. **338** (1993), no. 2, 639–654.

[33] A. Haar, *Zur Theorie der Orthogonalen Funktionensysteme*, Math. Annalen **69** (1910), 331–371.

[34] C. Heil, G. Strang, and V. Strela, *Approximation by Translates of Refinable Functions*, Numer. Math. **73** (1996), 75–94.

[35] L. Hervé, *Multi-resolution Analysis of Multiplicity d: Applications to Dyadic Interpolation*, Appl. Comput. Harmon. Anal. **1** (1994), no. 4, 299–315.

[36] R. A. Horn and C. R. Johnson, *Matrix Analysis*, Cambridge University Press, Cambridge, 1990.

[37] A. Hussen and A. Zeyani, *Fejer-Riesz Theorem and Its Generalization*, International Journal of Scientific and Research Publications, vol. 11 (2021), Issue 6, 2250–3153.

[38] R. Q. Jia, *Shift–Invariant Spaces and linear Operator Equations*, Isr. J. Math. **103** (1998), 259–288.

[39] R. Q. Jia and Z. Shen, *Multiresolution and Wavelets*, Proc. Edinb. Math. Soc. **37** (1994), 271–300.

[40] Q. T. Jiang, *Multivariate Matrix Refinable Functions with Arbitrary Matrix Dilation*, Trans. Amer. Math. Soc. **351** (1999), 2407–2438.

[41] F. Keinert, *Wavelets and Multiwavelets*, Stud. Adv. Math., Chapman & Hall/CRC, Boca Raton, FL, 2004.

[42] K. Koch, *A New Family of Interpolating Scaling Vectors*, Preprint **22**, Preprint Series DFG-SPP **1114** (2003).

[43] ———, *Interpolating Scaling Vectors*, IJWMIP, vol. 3, no. 3 (2005).

[44] ———, *Interpolating Scaling Vectors and Multiwavelets in* $\mathbb{R}^d$, Logos Verlag, Berlin, 2007.

[45] ———, *Interpolating Scaling Vectors: Application to Signal and Image Denoising*, Preprint **50**, Preprint Series DFG-SPP **1114** (2004).

[46] ———, *Multivariate Orthonormal Interpolating Scaling Vectors*, Appl. Comput. Harmon. Anal. **22** (2007), 198–216.

[47] ———, *Multivariate Symmetric Interpolating Scaling Vectors with Duals*, J. Fourier. Anal. Appl. **15** (2009), 1–30.

[48] ———, *Nonseparable Orthonormal Interpolating Scaling Vectors*, Appl. Comput. Harmon. Anal., vol. 22, no. 2 (2007).

[49] J. V. Lambers, A. C. Sumner *Explorations in Numerical Analysis*, World Scientific, 2017.

[50] W. R. Madych, *Finite Orthogonal Transforms and Multiresolution Analyses on Intervals*, J. Fourier. Anal. Appl. **3** (1997), 257–294.

[51] S. Mallat, *A Wavelet Tour of Signal Processing*, Academic Press, San Diege, Edition **2** (1999).

[52] ———, *Multiresolution Approximation and Wavelet Orthonormal Bases of* $L_2(\mathbb{R}^d)$, Trans. Amer. Math. Soc. **315** (1989), 69–87.

[53] W. McLean, *Strongly Elliptic Systems and Boundary Integral Equations*, Cambridge University Press, 2000.

[54] Y. Meyer, *Wavelets and Operators. Translated by D.H. Salinger*, Cambridge Stud. Adv. Math., vol. 37, Cambridge Univ. Press, Cambridge, 1992.

[55] G. Plonka, *Approximation Order Provided by Refinable Function Vectors*, Constr. Approx. **13** (1997), 221–244.

[56] G. Plonka, *Necessary and Sufficient Conditions for Orthonormality of Scaling Vectors*, Multivariate Approximation and Splines (Basel) (G. Nürnberger, J. W. Schmitd, and G. Walz, eds.), ISNM, vol. 125, Birkhäuser, (1997), 205–218.

[57] G. Plonka and V. Strela, *From Wavelets to Multiwavelets*, Mathematical Methods of Curves and Surfaces II (Nashville) (M. Daehlen, T. Lyche, and L. L. Schumaker, eds.), Vanderbilt University Press, (1998), 1–25.

[58] M. Primbs, *New Stable Biorthogonal Spline–Wavelets on the Interval*, Results. Math. **57** (2010), 121–162.

[59] I. W. Selesnick, *Interpolating Multiwavelet Bases and the Sampling Theorem*, IEEE Trans. on Signal Processing **47** (1999), no. 6, 1615–1621.

[60] O. Steinbach, *Numerical Approximation Methods for Elliptic Boundary Value Problems. Finite and Boundary Elements*, Springer, New York, 2008.

[61] R. Stevenson and C. Schwab, *Fast Evaluation of Nonlinear Functionals of Tensor Product Wavelet Expansions*, Numer. Math. **119** (2011), 765–786.

Index